Electrohydrodynamic spraying techniques for food ingredient component nanocapsulation

A thesis submitted in partial fulfilment of the requirements for the degree of

Doctor of Philosophy

By

Megdi Eltayeb

April 2015

Department of Mechanical Engineering

University College London

Torrington Place, London WC1E 7JE, UK

Declaration

I, Megdi Eltayeb, confirm that the work presented in this thesis is my own. Where information has been derived from other sources, I confirm that this has been indicated in the thesis.

……..

Megdi Eltayeb

Abstract

Nanoparticles are being widely investigated for food purposes and are beginning to see application in food production. There are numerous techniques to produce such nanoparticles, including emulsion-based techniques and spray drying, each with their advantages. Electrohydrodynamic spraying provides an alternative technique for preparing food component loaded particles in the nano-scale with a good control of important particle characteristics, such as size. In this work, Electrohydrodynamic spraying was used to investigate its potential for producing nanoparticles intended for nanoencapsulation of low solubility food components. Different processing parameters including flow rate, solute concentration, food component loading and their influence on nanoparticle characteristics and food component release were studied using food flavour as a model food component and ethylcellulose and stearic acid as a carrier materials.

This work, EHD spraying was used to investigate its potential for producing nanoparticles intended for food delivery. Different processing parameters including flow rate, solution concentration, food component loading and their effect on nanoparticle characteristics and food flavour release rate were investigated. Polymeric and lipid nanoparticles were studied in detail with respect to nanoparticle characteristics and food component release kinetics and additional studies were performed for nanoparticles prepared with ethylcellulose as a model hydrophilic polymer to form the polymeric core; and stearic acid as a model lipid to form the lipid monolayer. EHD sprayed nanooparticles were prepared with diameters between 10-100 nm and a near-monodisperse size distribution was obtained in most cases. The flavour release rates were found that the release rate was a function of both the nanoparticle size and structure, and hence of the processing conditions. EHD sprayed nanoparticles generally had a slower flavour release rate compared with conventional techniques. The results indicated that EHD spraying is an attractive nanotechnology for generating food component loaded nanoparticles that can be tailored towards an intended food delivery application. Compared with the conventional techniques it provides better control of nanoparticle and demonstrated its suitability for producing nanoparticle formulations in which the food component and is released rate in a sustained manner to potentially improve bioavailability of low solubility food component such as flavour.

Publications and Conference Presentations

Peer-reviewed Journal Articles

1. Eltayeb, M., et al., Preparation of solid lipid nanoparticles containing active compound by electrohydrodynamic spraying. Food Research International, 2013. 53(1): p. 88-95.
2. Eltayeb, M., E. Stride, and M. Edirisinghe, Electrosprayed core–shell polymer–lipid nanoparticles for active component delivery. Nanotechnology, 2013. 24(46): p. 465604
3. Eltayeb, M., Stride, E., & Edirisinghe, M. (2015). Preparation, characterisation and release kinetics of ethylcellulose nanoparticles encapsulating ethylvanillin as a model functional component. Journal of Functional Foods, 14, 726-735.
4. Eltayeb, Megdi, Stride, Eleanor, & Edirisinghe, Mohan. Electrohydrodynamic sprayed Nanoparticle Delivery System for Controlled Release of Food Flavouring, in preparation.

Conference Proceedings papers

1. Megdi Eltayeb, Eleanor Stride, and Mohan Edirisinghe. Hybrid nanoparticles for controlled food component loading and release, 4th International Conference on Nanotek and Expo December 1-3, 2014 San Francisco, USA.

Conference Presentations

1. Megdi Eltayeb, Eleanor Stride, and Mohan Edirisinghe. Oral presentation: Hybrid nanoparticles for controlled food component loading and release, 4th International Conference on Nanotek and Expo December 1-3, 2014 San Francisco, USA.
2. Megdi Eltayeb. Oral presentation and poster nanoparticle in health care engineering. Mechanical Engineering Conference, London, UK, 14th June 2012.

3. Megdi Eltayeb. Oral presentation nanoparticle in health care engineering. Mechanical Engineering Conference, London, UK, 14th June 2013.

Conference Posters

1. Megdi Eltayeb, Eleanor Stride, and Mohan Edirisinghe. Poster presentation: Hybrid nanoparticles for controlled food component loading and release, 4th International Conference on Nanotek and Expo December 1-3, 2014 San Francisco, USA.
2. Megdi Eltayeb, Eleanor Stride, and Mohan Edirisinghe. Poster presentation: Encapsulation of Vanillin in solid lipid nanoparticles using Electrohydrodynamic technology. UCL Annual Research Poster Competition 2012, London, UK, on 27 February 2012.
3. Megdi Eltayeb, Eleanor Stride, and Mohan Edirisinghe. Poster presentation: Encapsulation and release of flavour from solid lipid nanoparticle. UCL Annual Research Poster Competition 2013, London, UK, 25 February 2013.
4. Megdi Eltayeb, Eleanor Stride, and Mohan Edirisinghe. Poster presentation: nanoparticle in health care engineering. Mechanical Engineering Conference, London, UK, 14th June 2013.
5. Megdi Eltayeb, Eleanor Stride, and Mohan Edirisinghe. Poster presentation: Nanotechnology offers small food for thought. UCL Annual Research Poster Competition 2013, London, UK, 3 March 2014.

Participating in symposia

1. 4th Bubble & Encapsulation Symposium Biomaterials, Particles, Bubbles, Capsules & Fibres for Healthcare at UCL, London, UK on 18th April 2012.

Acknowledgements

At the very outset my wholehearted thanks goes to my supervisor Professor Mohan Edirisinghe for his continuous guidance, constructive criticism, confidence building and valuable support during the period of my study. My thanks are equally due to my second supervisor Professor Eleanor Stride for her trust, guidance, advice and great support throughout this research work. I feel extremely privileged to be jointly supervised by Professor Edirisinghe and Professor Eleanor Stride

Continuous and invaluable support provided by my colleagues, is unforgettable and many thanks to them. The lovely memories I have with these peoples will always be cherished. My dream of doing this research study wouldn't have been possible if not for the unparalleled understanding.

Last but not least, I would like to give a special thanks to my family and friends for their love, belief, support and help in the past years, without which I would not be brave enough to face this challenge in my life.

Without these important people in my life, I cannot have these achievements.

Thank you all.

Dedication

All of my work is dedicated to YOU!!!

Table of Contents

List of Figures

List of Tables

Glossary of Abbreviations

Abbreviation	Definition
AI	Active ingredient
AV	Applied voltage
DSC	Differential scanning calorimetry
EC	Ethylcellulose
EE	Encapsulation efficiency
EHD	Electrohydrodynamic
EM	Ethymaltol
EV	Ethylvanillin
FDA	Food and drug administration
FDPS	Food delivery particulate systems
FR	Flow rate
FTIR	Fourier transform infrared
LC	Loading capacity
MA	Maltol
MW	Molecular weight
MWD	Molecular weight distribution
SA	Stearic acid
SEM	Scanning electron microscopy
TTC	Tip-to-collector
UV	Ultraviolet
VA	Vanillin
w/o	Water-in-oil
w/o/w	Water-in-oil-in-water
w/w	Weight/weight
WPI	Whey protein isolate
wt%	Weight total
XRD	X-ray diffractometry
SLN	Solid lipid nanoparticles

Chapter 1 Introduction and Background

1.1 Background

Nanotechnology is the understanding and control of matter at dimensions of ~ 1-100 nm. There is a huge demand for nanotechnology in the food industry (Fathi & Mohebbi, 2010; Neethirajan & Jayas, 2011; Rizvi et al., 2010; Sanguansri & Augustin, 2006). However, many nanotechnological applications in the food industry may be difficult to adopt commercially, owing to high cost and/or scale requirements.

Nanotechnology has been used to deliver food ingredients (Chen et al., 2006a; Shimoni et al., 2009) and nanoencapsulation has been exploited in pharmaceutics, cosmetics and food science (Celebioglu & Uyar, 2012; Ezhilarasi et al., 2013; Farokhzad & Langer, 2009; Fathi et al., 2012; Müller et al., 2007; Risch & Reineccius, 1995; Sagalowicz et al., 2006; Shah et al., 2007; Shimoni et al., 2009) with a variety of polymeric based materials being used, such as ethyl cellulose and lipids based materials, such as fatty acid stearic acid.

The designed nanocarriers systems for accomplishing accurate delivery to food components are expected to be nontoxic, high encapsulation efficiently and load capacity of the food ingredient component, to improve the bioavailability, controlled release, enable precision targeting and promising process and to enhance their functionality and stability (McClements et al., 2009; Mozafari et al., 2006).

Polymeric and lipid nanoparticles represent the main classes of carrier system capable of efficiently encapsulating a variety of food ingredient components to protect them from unfavourable environmental conditions by restricting the transfer of gases and maintaining the pH (Fang & Bhandari, 2010; Zimet & Livney, 2009). This enables increased storage

periods, and improves bioavailability by releasing food ingredient components at a sustained rate.

Lipid based delivery nanocarrier systems now under serious research can be divided into main classes, such as solid lipid nanoparticles, liposome, emulsions, microemulsions, nanoemulsions, multiple emulsions and filled hydrogel particles (Flanagan & Singh, 2006; Matalanis et al., 2011; McClements & Li, 2010; Velikov & Pelan, 2008; Weiss et al., 2008).

Lipid based colloidal delivery carrier systems have wide spectrum of applications as encapsulation and delivery carrier in pharmaceutical, food, and cosmetic areas, for example flavour, nutraceuticals, vitamins, and preservatives (Given, 2009; Sagalowicz & Leser, 2010; Sanguansri & Augustin, 2006; Velikov & Pelan, 2008). With respect to food delivery applications, lipid nanoparticles and liposome are effective carriers for both lipophilic and hydrophilic food ingredient component used in nutraceuticals, to increase oral bioavailability, efficiency and solubility (Fathi & Varshosaz, 2013; Lacatusu et al., 2013; Stratulat et al., 2014; Ting et al., 2014).

Polymer nanoparticles have emerged as a highly promising area of scientific research and have been utilised in a wide spectrum of application areas in recent decades due to their unique properties, which include their ability to encapsulate and deliver food ingredient components (Chen et al., 2006b; Shimoni, 2009). The characteristics of polymer nanoparticles have to be adjusted according to the particular application.

The technique of nanoparticle production thus plays a vital role, as it is this that will largely determine the ability to predict and control the desired properties. Conventional processes for preparing polymer nanoparticles are frequently complex, commonly requiring multiple step processing, such as emulsification, drying, removal of surfactants (Ezhilarasi et al., 2013; Fathi & Mohebbi, 2010; Neethirajan & Jayas, 2011; Rizvi et al., 2010; Sanguansri &

Augustin, 2006; Silva et al., 2012). This is not only time consuming but may reduce the degree of control over nanoparticle physicochemical properties and reduce product recovery; all of which increases the cost of production and uniformity of the final product. Further details on the different methods for polymer nanoparticle preparation can be found in the review by (Rao & Geckeler, 2011).

Recently, flavour encapsulation has become a popular technique in the food industry (Karathanos et al., 2007). Most flavour compounds are highly volatile and chemically unstable as a result of oxidation, chemical interactions and volatilisation. So, encapsulation of flavour compounds is essential to stabilise them and offer their release when required (Choi et al., 2009). The use of a combination of polymers and lipids results in the formation of nanoparticles with a hydrophilic core and a hydrophobic shell. Both water soluble and insoluble food ingredient components can be encapsulated, including poorly soluble substances such as fatty acids, carotenoids, and phytosterols (Humberstone & Charman, 1997).

The development of novel polymer-lipid nanoparticles for food ingredient component encapsulation with predictable and controlled properties is essential to meet the requirements of food applications. Furthermore, it is crucial to select the appropriate encapsulation technique based on the nature of the core-shell particles, physicochemical properties of the materials, and required size.

Conventional techniques for producing polymer-lipid nanoparticles are relatively complex, usually requiring a two or more step formulation process: firstly, development of nanoparticles of the core material (polymeric), and secondly, encapsulation of the core nanoparticles by the shell (lipid) (De Miguel et al., 2000; Thevenot et al., 2007). This often results in poor control over the final nanoparticle physicochemical structure. More details on

food ingredient component encapsulation can be found in the review by Ezhilarasi et al. (Ezhilarasi et al., 2013).

Electrohydrodynamic (EHD) processing is a method of generating fine droplets ranging from micro-nanometers in diameter from the breakup of a jet depending on the flow rate and large electrical potential difference. One of the emerging technologies in food formulations is the application of EHD technology for encapsulating food ingredients such as, emulsifiers, and flavours (Yoshii et al., 2001). EHD spray technology has advantages; particle size can be in the micrometer to nanometer size range according to the requirement of the food materials (Luo et al., 2012). The size distribution of the particles can be near-monodisperse leading to better flavour perception (Gañán-Calvo & Montanero, 2009). EHD spraying technology essentially generates droplets from which solid relics are deposited. Droplet generation and droplet size can be effectively controlled by optimising the parameters such as voltage at the capillary needle, the flow rate of the solution and distance between needle and collector, this in turn regulates relics.

1.2 Objectives of the research

The main goal of this project is to use EHD processing to prepare nanoparticles, ≤100 nm in diameter, encapsulating food ingredient component and to study their characteristics.

The **first** objective was to understand and get familiar with the fundamentals of the EHD processing technique and perform experiments to investigate the effect of key parameters of the EHD spraying process. Encapsulation of materials in nanoparticles with a well-controlled size distribution is an important application of the EHD spraying technique. Thus, food component-exchange phase loaded nanoparticles by EHD spraying were produced. The different physical and mechanical processing parameters such as solution flow rate, applied

voltage, liquid viscosity and surface tension affecting the produced nanoparticles diameter were investigated.

The **second** objective of this study was to produce EHD sprayed polymeric nanoparticles with entrapped food flavour, used ethylcellulose (EC) as a model hydrophobic polymer since it has been approved and accepted by both the United States Food and Drug Administration (FDA) and the European Union (EU) for food, cosmetic and pharmaceutical applications. I investigated the different polymer concentrations for which a stable cone-jet could be obtained during EHD processing; and by tuning the operating parameters (flow rate and applied voltage), food ingredient component encapsulating nanoparticle populations with varying mean size (≤100 nm) and size distributions were obtained.

Food ingredient component release was expected to occur through two different processes: "burst" release of EV encapsulated near the surface of the EC nanoparticle due to hydration; and slower release from the polymer matrix as it degrades. The release profiles can be influenced by the properties of the polymer, its concentration, the nature of the loaded food ingredient component, its concentration and distribution and the nanoparticle size distribution. These in turn may be controlled by the EHD operating parameters. Smaller particles typically give rise to higher release rates, due to the higher surface area to volume ratio and hence more rapid penetration by water.

The **third** objective of this study was to form stearic acid (SA) nanoparticles encapsulating ethylvanillin (EV). Both materials are widely used in the food industry and representative of typical hydrophobic coating and hydrophilic flavour components respectively. This objective utilises an EHD technique to prepare core-shell lipid nanoparticles with a tunable size and high food ingredient loading capacity, encapsulation efficiency and controlled release.

The **fouth** objective, EHD technology is used to encapsulate water soluble flavour within matrices of SA and EC and the process control parameters are optimised to control the particle size of nanoparticles produced. Based on the findings of this project EHD spraying carried out at the ambient temperature with the major process control parameter of applied voltage and flow rate and can be exploited as a potentially attractive method to prepare polymer-lipid nanoparticles containing a low solubility food ingredient such as flavour.

These nanoparticles comprise distinct functional components: polymeric (EC) core, which can encapsulate dosages of water soluble material and release them at a sustained rate and lipid (SA) in the shell, which can prevent the carried agents from freely diffusing out of the nanoparticles and reduce water penetration into the nanoparticles, thereby enhancing food ingredient component encapsulation efficiency, biocompatibility and decrease the rate of food ingredient component release from the nanoparticles (Phadke et al., 1994). Due to its hydrophobic nature, SA reduces food ingredient component (flavour) dissolution and release and slows the release kinetics at higher SA levels.

1.3 The structure of the thesis

Chapter 1 describes background, objectives of research and the structure of thesis.

Chapter 2 describes review the importance of the EHD spraying processing parameters that enable the nanoparticle size to be tuned in a reproducible manner whilst allowing a narrow size distribution to be achieved with high encapsulation efficiencies throughout the process.

Here present a comprehensive review of the current state of the art in EHD spraying technology for the encapsulation of food ingredient component. The various applications of EHD spraying technology, with an emphasis on encapsulation, are also reviewed, for a description of the latest techniques used to produce lipid or/ and polymer system in the diverse and interesting field of functional food.

Chapter 3 describes describes the experimental setups, materials used, the characterisation techniques carried out, and a detailed description of the experimental tools employed.

Chapter 4 describes nanoparticles of food emulsifier ethylcellulose encapsulating food flavouring agent ethylvanillin (food ingredient component) were prepared by EHD processing with a mean size less than 100nm and a relatively narrow size distribution. The loading capacity and encapsulation efficiency were also investigated.

Chapter 5 describes focus on the use of EHD technique to prepare lipid nanoparticles with a tunable size, high food ingredient component loading capacity and encapsulation efficiency, and sustained food ingredient component kinetic release.

Chapter 6 describes focus on the use of EHD spraying processing techniques to produce polymer-lipid nanoparticle structure with a narrow size distrubution in a single step process. Focus on effect of EHD parameters, polymer-lipid concentrations and food flavour concentration on nanoparticles formation and encapsulation efficiency and loading capacity. Also, focus on the effect of tip-to-collector, stearic acid and food flavour on chemical, crystallinity, physical structure, and encapsulation efficiency and loading capacity

Chapter 7 describes summarizes what has been achieved in those studies and describes the future experimental plans.

Chapter 2 Literature Review

2.1 Introduction

The need for controlled delivery of food component has prompted the study of nanoencapsulation or nanocarrier which are intended to protect and release at a determined rate, thus releasing their encapsulated sensitive food ingredient components for sustained and specific delivery (Fang & Bhandari, 2010; Ghosh et al., 2009; Zimet & Livney, 2009). This method could potentially overcome the limitations of delivery and has drawn much research attention in the recent years, mainly in fields of flavour, nutrients, nutraceuticals, enzymes, vitamins and food additives, for which tailored food ingredient delivery is needed to enhance the stability of sensitive compounds during production, storage and ingestion (Khayata et al., 2012; Sáiz-Abajo et al., 2013).

Several approaches exist for manufacturing these food ingredient component delivery carriers with nanoemulsion/evaporation approaches being the most widely used (Jaiswal et al., 2004; Mainardes & Evangelista, 2005; Varshosaz et al., 2010b; Varshosaz et al., 2009). Spray drying, coacervation, microfluidics and nanoprecipitation are additional methods each presenting their own specific benefits and they are generally described in the literature (Fathi & Mohebbi, 2010; Neethirajan & Jayas, 2011; Rizvi et al., 2010; Sanguansri & Augustin, 2006; Zúñiga & Aguilera, 2008).

However, to date, few of the food ingredient component delivery systems produced via these approaches have been successfully transformed to the food industry, with few products being commercialized every year. This absence of transformational research is mostly attributed to numerous shortfalls related with these fabrication techniques. Such as, the requirement of large amounts of solvent to produce emulsions and therefore the need of using costly equipment to eliminate solvent before consumption and volatility during the procedures. In

emulsion methods, the solvent and cost are the main disadvantage. Also, encapsulated food ingredients vary in terms of nanoparticles characteristics, demonstrating a different degree of stability.

In other methods, residual traces of solvents and prolonged exposure to solvents or other method parameters in the final food ingredient component delivery systems are of concern. For instance, parameters can affect the stability of the entrapped food component, limiting their performance, and thus reducing their food industry utility. Additionally, different food applications need different food ingredient component release rates matching the necessity of a specific application. For this to happen, it is important to have a thorough understanding of the complex interplay of fabrication factors which rule the resultant nanoparticle properties.

One method to overcome these limitations is the method of EHD spraying. Although EHD is a well-established method in the field of electro-spraying and spinning, it has only been applied to the loading of food ingredient component delivery in the last 20 years and understanding and optimisation are still in their relative infancy with respect to nanoencapsulation (Farokhzad & Langer, 2009; Liu et al., 2008; Müller et al., 2007; Sagalowicz et al., 2006; Shimoni, 2009).

Briefly, in EHD spraying, a high electrical potential difference source is applied to an EHD sprayed solution fed through a needle. The electric charge created on the droplet competes with the surface tension of the droplet, causing the droplet to break up in small droplets, which undergo solvent evaporation. The resulting dried nano/micro-particles can then be collected (Hartman et al., 2000).

Food ingredient component can be incorporated into the EHD spray (e.g. polymer, lipid) solution prior to EHD spraying resulting in loaded nano/micro particles. There are several possible benefits to EHD spraying including the following: emulsion is not required but

optional; high temperature not required; no additional drying step needed; and there is better control over the size distribution of particles with the possibility of producing quasi-monodisperse particles (Brandenberger et al., 1999).

The monodispersity is mostly needed in food ingredient component delivery since it offers better controlled, and hence reproducible release profiles, which may in turn be easily tailored for a required application (Gomez et al., 1998). Control of size is therefore of dominant significance when fabricating carriers and EHD spraying is a method which can offer such control over and above that achieved with traditional methods, when suitable factors are used (Amsden & Goosen, 1997).

EHD spraying also holds potential to reduce solvents in food and is highly flexible in terms of the selection of matrix materials, setup, and food ingredient component. To date, food ingredient component such as food additive, nutrients, and nutraceuticals have been loaded in EHD sprayed particles and these investigations will be reviewed hereafter.

Chapter describes the current state of the art in EHD spraying technique for the controlled release rate of food ingredient component from nanoparticles. It reviews the techniques utilised for generating EHD sprayed particles and encapsulating food ingredient component, including important considerations to allow both physical properties and release rate patterns of the particles to be optimised and tailored. The numerous applications of EHD spraying technology, with highlighting on nanoencapsulation, are also described, for a representation of the latest approaches utilised to generate nano-system in the various and attractive area of food functionality.

2.2 The technique of EHD spraying

2.2.1 EHD spraying principles

EHD spraying is a technique of solution atomization, also known as electrospray. The principle of EHD spraying is based on the theory of electric charged droplets; stating that an electric field applied to a liquid droplet exiting a capillary is able to deform the interface of the droplet (Jaworek, 2008).

The electric charge creates an electrostatic force inside the droplet which competes with the surface tension of the droplet, forming the single stable cone jet mode or Taylor cone, property of electric charged droplet. Finally, the electrostatic force, created by the use of high electric voltage on the needle, is able to overcome the surface tension of the droplet. The excess electric charge then needs to be dissipated and smaller charged droplets on the micro to nano size are ejected from the primary droplet, thus decreasing its electric charge without considerably decreasing its mass. Owing to Coulomb repulsion of the electric charges, the droplets disperse well and do not coalesce during their flight toward the collector (Brandenberger et al., 1999). Numerous spraying modes can occur through EHD spraying; the best desired being the cone-jet mode, due to its reproducibility and stability (Hartman et al., 2000).

The numerous theories of EHD spraying physics have been summarized elsewhere with literatures on the applications of the technique and latest improvements (Jaworek, 2008; Jaworek & Sobczyk, 2008) however, limited review exists relating to theoretical and practical presence of delivery food ingredient component in this method.

Briefly, the two main factors that characterise the EHD sprayed are the electric charge and size of droplets. The electric charge is difficult to determine, due to electrical discharge, although the maximum surface charge of a droplet, q, has been identified as a function of the

surface tension, γ, and radius of droplet, R, expressed in Equation 1 (Rayleigh, 1882). The electric charge limit at which a droplet exposed to an electric force is no longer stable called the Rayleigh limit and is given as:

$$q = 8\pi\sqrt{\varepsilon_0 \gamma R^3} \qquad \text{Equation 1}$$

With increasing flow rate, the current increases and the stress ratio of the jet increases, above a threshold value whereby the jet starts to whip, leading to the production of heterogeneous sized droplets. Ideally, a sufficient stress ratio value must be employed to allow for jet break-up, but still a minimal value must be obtained for production of monodisperse and homogeneous particles (Hartman et al., 2000).

2.2.1.1 EHD spraying method

EHD spraying technique is a process of generating fine droplets ranging from micro or nanometers in diameter size from the breakup of a jet depending on surface charge, large electrical potential difference and droplet charge, the flow rate (Chen et al., 1995; De Juan & De La Mora, 1997; Kim et al., 2006). EHD spraying technique produces droplets from which solid relics are deposited. Droplet production and droplet size can be effectively controlled by optimising the factors such as the flow rate of the solution, voltage at the capillary needle and distance between needle and collector, this in turn regulates relics. Among some of the techniques developed to produce particles with well-defined properties, EHD processing has emerged as a single step technique that offers excellent control over particle characteristics (Gañán-Calvo & Montanero, 2009). EHD processing has been used to produce nano and micrometers for a wide range of applications (Bottger et al., 2007; Luo et al., 2012; Prilutsky et al., 2008; Teo & Ramakrishna, 2006; Yu et al., 2011; Yu et al., 2009; Yu et al., 2012).

2.2.2 Fabrication techniques

The EHD spraying system can be cheap, simple and reproducible (Celebioglu & Uyar, 2010): solution is loaded into a syringe mounted with a conductive needle, and fed at a required flow rate commonly implemented by a mechanical pump. The conductive needle is connected to high electric voltage (kilovolts) and several varieties of collectors, often grounded or more rarely negatively charged, are placed at a distance ranging from a few centimeters to several tens of centimeters from the needle.

Once the droplets are ejected from the Taylor cone according to the theory of charged droplets, solvent evaporation leads to the progressive contraction, and solidification of droplets resulting in solid particles impacting onto the collector. While particles are generally assumed to be dry or proven to contain residual solvent falling within the limit of safety standards (Rezvanpour et al., 2010), many studies also use subsequent vacuum treatment to ensure all residual solvent is removed. In the context of loading, the food ingredient component is generally mixed into the matrix materials (e.g. polymer, lipid) solution before EHD spraying.

2.2.2.1 EHD spraying apparatus

EHD spraying and food ingredient component loading properties can be designed by alterations in the parameter of EHD spraying (Figure 1). One type of apparatus involves the use of needle which is connected to high voltage. An electrical potential difference is applied between the needle and a collector grounded electrode. Usually the high electric voltage is applied on the needle and the ground electrode on the collector, respectively.

The use of a ring stabilises the EHD spraying process (Ciach, 2006; Ding et al., 2005; Xie & Wang, 2007a; Xie et al., 2006d), enabling more control over the desired EHD spraying particle pattern. For instance, in the cone jet mode, better uniform particles are prepared (Xie et al., 2006b).

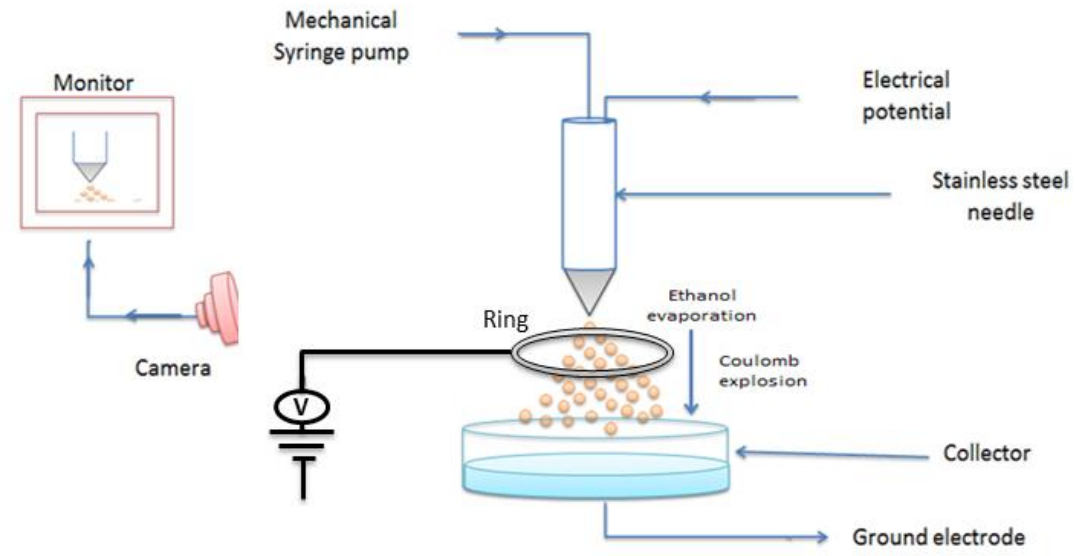

Figure 1: EHD spraying set-up

A corona discharge is prepared by a grounded conductive needle placed opposite the charged conductive needle in order to discharge the highly charged droplets. Particles can be obtained in a Petri dish (Xie & Wang, 2007a). The use of a chamber decreases solvent evaporation rate and smaller particles may be prepared, however, yield is reduced in this configuration due to deposition of particles in the chamber before collection. Additionally, the reduction of solvent evaporation rate obtained by using a varying collection distance can result in smoother particle surfaces due to improved particle matrix relaxation and therefore more organisation of particle matrix within the evaporating droplet, which, in turn, allow more homogenous particle degradation and release.

An alternative method for collection involves EHD spraying loaded particles into a liquid, within a container containing an immersed grounded collector (Pareta & Edirisinghe, 2006; Xu & Hanna, 2006, 2007) or a wire wrapped around the beaker (Valo et al., 2009). Collection media include distilled water (Xu & Hanna, 2007), or 70% ethanol supplemented with

surfactants (such as 0.01‑0.1% (v/v) Polysorbate 80 (Tween 80)), to lower the surface tension of the solution and prevent the aggregation or coalescence of particles (Peltonen et al., 2010).

Stronger solvents e.g. acetone may also be utilised, in order to neutralize residual solvent from the EHD spraying solution (Pareta & Edirisinghe, 2006). After particles have been obtained in the liquid, particles can be further filtered and dried. The main drawback of this collection method is the loss of surface adsorbed food ingredient component which may be desorbed into the collection media. There is, therefore, no burst release rate of food ingredient component (from the surface of EHD sprayed particles) is seen with these approaches, and a proportional amount of food ingredient component is lost, which again is a concern for cost and loading efficiency. Agglomeration in solution is a potential issue with hydrophobic polymers when EHD spraying in aqueous solutions. Coating is one method to enable more stabilisation of individual particles (Almería et al., 2011).

The most common collector for EHD spraying remains a grounded and conductive collector such as copper substrate and an aluminum (Arya et al., 2009; Hong et al., 2008; Ijsebaert et al., 2001; Wu et al., 2009b; Xie et al., 2008a). The advantage of a conductive substrate is that it restricts the deposition of particles to the charged area, lower losses and does not need any subsequent filtering or washing step.

In practice, despite EHD spraying enabling better control over morphology and size of particles compared to the traditional manufacturing techniques, it is not without associated disadvantages, including the low-throughput of the method and yields in the order of milligrams/hour (Jaworek, 2008). This can be overcome with multiple needle EHD spray apparatus. An extractor is essential in this type of setup to minimize interference between sources and to localize the electric field.

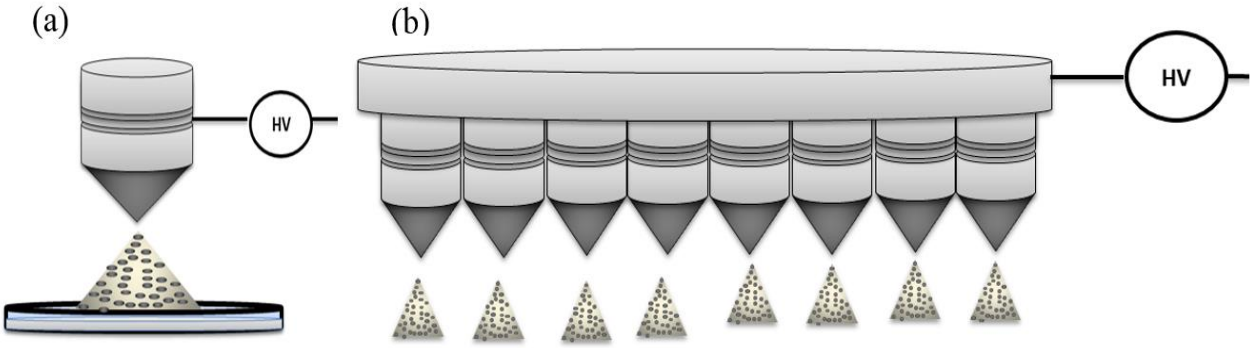

Figure 2: EHD spray setup (a) Single needle, and (b) Multiple needles.

Size and Morphology of particles were similar to that of the single setup (Figure 2a) and particle production could be scale-up by at least three orders of magnitude using 4 parallel multiple needles (Figure 2b) (Almería et al., 2010).

2.2.2.2 System and method of encapsulation

In recent years, the encapsulation of food ingredient component has become a dominant tool for delivery and controlled amount to targeted site specific delivery. Encapsulation can be obtained by the processing of materials (e.g. polymers or/ and lipids) which maintain integrity and relative long term storage of food ingredient components.

Nanocarrier system devices (e.g. polymer, lipid) can finally provide an exposure for extended periods ranging from minutes to hours allowing a specific release rate of food ingredient components. Numerous methods can be employed for the encapsulation of food ingredient component food ingredient component into EHD sprayed particles. The resultant particles may be classified into two categories:

- Particulate systems; food ingredient components is intimately distributed within the nanoparticles structure.
- Core-shell structure; shell is made of the lipid or/and polymer while the aqueous food ingredient component is located in the core.

In the course of EHD spraying the solvent evaporates from the droplet and the food ingredient component remains entrapped within the lipid or/and particle structure, randomly distributed. The food ingredient component can be mixed in its solid state, where it is directly dispersed in the solution and vortexed before EHD spraying. The food ingredient component may also be dissolved in an aqueous solution before mixing with the solution, by emulsification or nanoprecipitation.

Emulsions are broadly utilised in traditional encapsulation approaches with the water-in-oil-in-water (w/o/w) double emulsion being the most common used, since it offers access to a broad range of particle sizes by fine-tuning the parameters of the procedure process. For EHD spraying, a single water-in-oil emulsion (w/o) may be formed where hydrophilic food ingredient components are first dissolved in water before encapsulation.

Many surfactants (such as 0.01‑0.1% (v/v) Polysorbate 80 (Tween 80)) may be added to tailor the encapsulation efficiency and controlled release rates (Xie & Wang, 2007b). However, the interface between the aqueous and organic phases may cause food ingredient aggregation and denaturation, which is the major disadvantage of all emulsion-based approaches, shown in Figure 3.

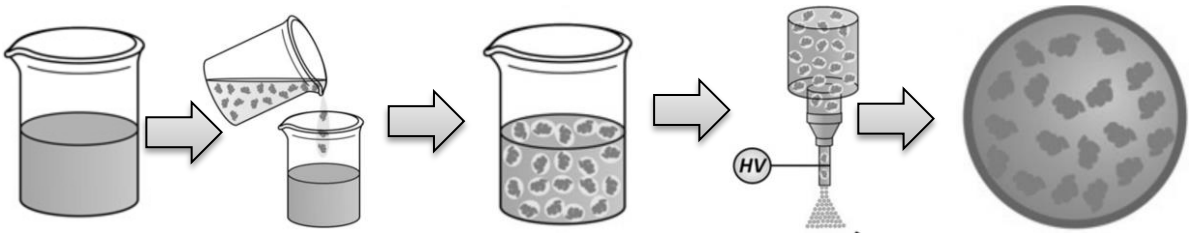

Figure 3: Emulsions method of food ingredient component incorporation within particles through EHD spraying.

Nanoprecipitation, on the other hand, avoids the denaturation problem since high shearing rates and interfaces are absent. However it can lead to agglomeration and is not suitable for

hydrophilic food ingredient component due to leakage in the aqueous phase (Lassalle & Ferreira, 2007), shown in Figure 4.

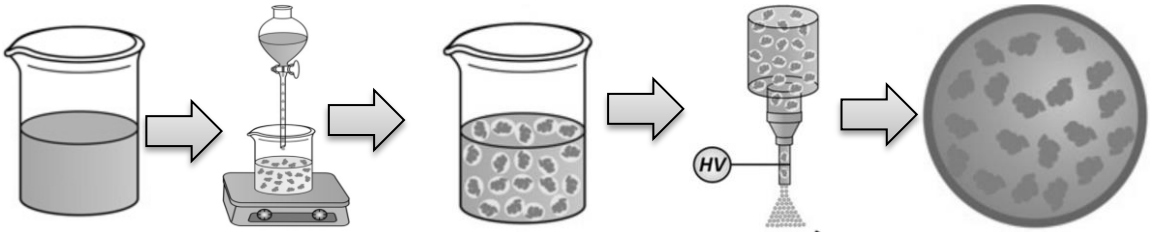

Figure 4: Nanoprecipitation method of food ingredient component incorporation within particles through EHD spraying.

Solid dispersion may thus remain the most attractive food ingredient option in EHD spraying, with no or limited denaturation and high flexibility of food ingredient components that may be incorporated (both hydrophobic and hydrophilic, food ingredient component types), shown in Figure 5.

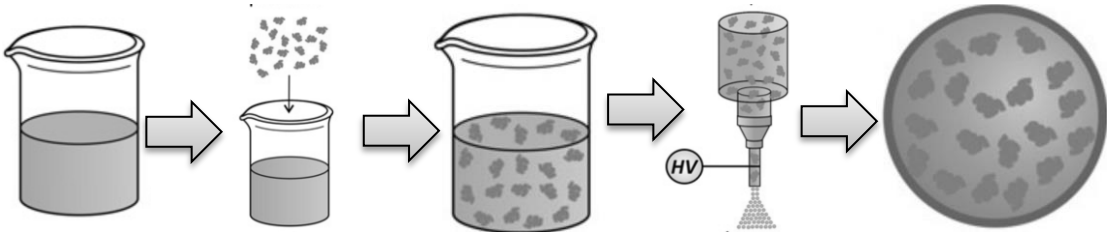

Figure 5: Solid dispersion method of food ingredient component incorporation within particles through EHD spraying.

Nevertheless, the food remains within the core-shell nanoparticle before delivery, which happens when the shell starts to degrade and channels open for release when required. This is an issue since the stability of some food in the aqueous state is known to be lower compared to its dry state, which may consequently result in loss of activity (Xie & Wang, 2007b). Nevertheless core-shell particle EHD spraying may supposedly allow more control over

release rates due to an increased number of factors (Chakraborty et al., 2009; Park et al., 2011; Yoon et al., 2008).

For instance, the particles size and shape are influenced by the rate of evaporation of ethanol from droplet, after the droplet shrinkage and the diffusion of the EC molecules in the droplets (Xie et al., 2006c). As EC is a relatively large molecule, its diffusion rate inside the droplets will be very slow; therefore, the presence of EC is confined to their surface. Loss of solvent through surface evaporation shrinks the droplet size and increases EC concentration close to the surface of the droplet, leading to the formation of a shell of solid EC and SA encapsulating food ingredient (Trotta et al., 2010).

Advantages of core-shell EHD spraying include high food ingredient encapsulation efficiencies within the carriers and the assurance that the food ingredient has minimum contact with the external environment.

2.3 Control of particle characteristics with EHD spraying parameters

2.3.1 Importance of EHD spraying parameters

Although EHD spraying is accepted as a method which can prepare particles with reproducible morphologies and monodisperse size distributions by controlling the EHD spraying parameters (Almería et al., 2010; Bock et al., 2011), preparing particles with very specific needs remains challenging due to the large number of variables involved in the EHD spray process.

The primary pre-requisite for reproducible EHD spraying and monodisperse size production is the stable cone-jet mode, for which the working window can be established by tailoring the flow rate, field strength and conductivity of the sprayed solution. Size and morphology can be

further controlled by optimising additional factors, such as the EHD spray solution concentration, the flow rate, the EHD spraying distance and chamber environment.

2.3.2 Processing parameters

2.3.2.1 Spraying modes

Several EHD spraying modes can take place in the course of EHD spraying and they vary according to the flow rate and electric field strength of the solution.

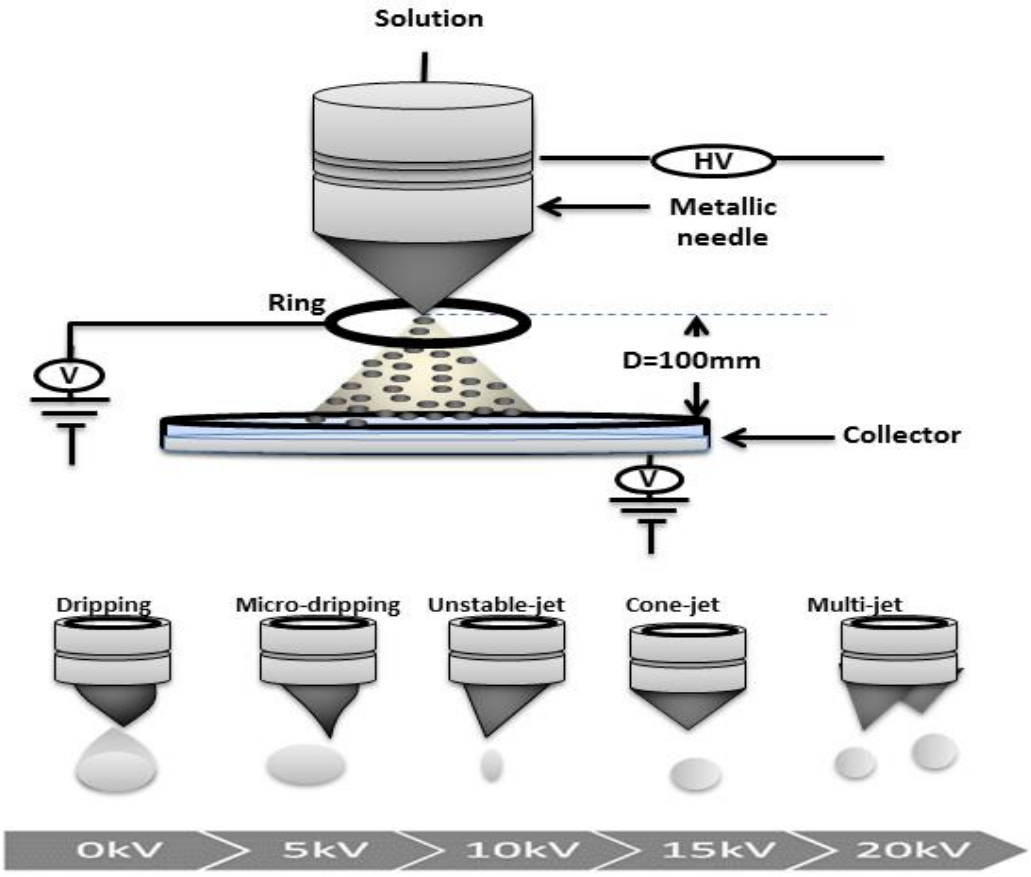

Figure 6: Typical EHD spraying modes.

The magnitude of the electric field strength is a key to reproducible spraying patterns (Ding et al., 2005) and its variation leads to several spraying modes, starting from the dripping

mode and moving to cone-jet mode with increasing applied electric voltage, shown in Figure 6 (Jaworek & Sobczyk, 2008).

When adequate electric voltage is applied to the droplet to form the Taylor cone (Figure 6), the ejection of highly charged and small droplets assumes the form of a cone which proportionally increases with an increase in the collection distance. This single cone-jet mode seen for moderate electric field strengths is fairly consistent and stable from one replicate to the next (Enayati et al., 2010).

Conversely, when increasing the voltage, multiple jets are produced, which are unpredictable, unstable and importantly can vary throughout the course of EHD spraying (Ding et al., 2005). Such modes can be create in all forms of EHD spraying apparatus and are also detected for the needle-ring apparatus when increasing the voltage between the ring and needle (Xie et al., 2006c). The multiple jet mode requires to be avoided so that only targeted areas are reached in order to ensure a high yield of particles. This is particularly essential when loading expensive food ingredient component, where minimal loss is required.

One approach to generate the single cone-jet mode is to lower the surface tension and electrical conductivity of the solution (Enayati et al., 2010). As a result, the stable single cone-jet mode region shifts and shrinks to a lower flow rate. On the other hand, increasing the viscosity of solutions (by increasing solution concentration for instance) results in a shift of the cone-jet mode to higher voltages. This is because of the lower conductivity of more viscous solutions: a stronger voltage should be applied to overcome the liquid viscosity and surface tension to form the cone jet (Enayati et al., 2010). It is essential to keep in mind that only in the stable cone-jet mode is the fabrication of monodisperse particles possible. Only then can the morphology and size of particles be controlled by carefully altering other parameters.

2.3.2.2 Electrical conductivity

Since EHD spraying depends on the electrical conductivity, *K*, of the EHD spray solution, the electrostatic attraction of charged particles to a grounded collector, and solvent is an important parameter when optimising the process. Along with flow rate, electrical conductivity provides a dominant means to control the EHD sprayed particle size, as revealed by the scaling laws from Gañan-Calvo, where an increase conductivity leads to a lower size (Ganan-Calvo et al., 1997). An increased conductivity of a solution implies that more charge is carried by the EHD spraying jet. Overall, a low electrical conductivity is preferred to obtain quasi-monodisperse particles (Meng et al., 2009) since a higher conductivity may favor elongated particles or even fibers if the solution concentration is high enough (Ramakrishna et al., 2005).

Correlating with viscosity, stable EHD spraying is known to be achieved only when viscosity is high or conductivity is low (Zhang & Kawakami, 2010). Changes in electrical conductivity can be obtained by changing the EHD spraying solvent or using co-solvents, although this latter case may be detrimental to size distribution and morphology of particles (Meng et al., 2009; Xu & Hanna, 2006).

Organic solvents are commonly less conductive than aqueous solvents and their conductivity can be improved by the addition of electrolytes, such didodecyltrimethylammonium bromide (Xie et al., 2006b) or ammonium hydroxide (Valo et al., 2009), which can increase conductivity by orders of magnitude. When the electrical conductivity is lower than 0.01 μS/m, it is expected that inadequate current can flow, and the liquid cannot be EHD sprayed, although too high conductivity value results in unstable EHD spraying (Ding et al., 2005).

The bending instability of the jet becomes more important when more charges are present due to increased conductivity, leading to a wider deposition of particles on the collector. With higher electrical conductivity, the Coulombic repulsion forces are higher and compete with the viscoelastic forces of the solution, disentangling more easily the polymer network which is being formed during EHD spraying.

In other words, increasing conductivity makes it easier for the solution to be broken up into smaller droplets. Therefore for the same materials (e.g. polymer) dissolved at the same concentration in a higher conductive solvent (or the same solvent but supplemented with organic salts), less chain entanglements take place during EHD spraying, in turn reducing the final particle size.

However, if the Coulombic repulsion forces are sufficiently high to overcome the entanglement forces, then Coulomb fission occurs before strong entanglements can form, and smaller off springs are ejected from the primary droplet. This will provide a bimodal size distribution, with particles presenting various types of morphologies, mostly unwanted and further discussed in Section 2.5. Low electrical conductivity may thus be more favorable for EHD spraying of quasi-monodisperse microparticles. When particles are required, increasing conductivity may be a good means of reducing particle size, although sufficient viscosity needs to be ensured so that entanglement forces remain higher than Coulomb forces, and the ejection of off spring droplets is avoided. Higher flow rates can also be used to produce particles if higher salt concentration is used to increase solution conductivity (Xie et al., 2006b). In the context of EHD spraying emulsions, the organic/aqueous volume ratio is another significant factor influencing the electrical conductivity whereby addition of water to the organic phase significantly increases the electrical conductivity of the resulting emulsions (Xu & Hanna, 2006).

2.3.2.3 Dielectric constant

The dielectric constant measures the polarisability of a material in an electric field. In turn, the polarization effectively reduces the magnitude of the external electric field. The electrical relaxation time (sec) is the time needed for a perturbation in the electric charge to be smoothed out and is given by Equation 2:

$$t_e = \varepsilon_r \varepsilon_o / K, \qquad \text{Equation 2}$$

where ε_r and ε_o (C V^{-1} m^{-1}) are the dielectric constants of the liquid and the vacuum, respectively, and K (S m^{-1}) is the electrical conductivity of the vacuum (Ganan-Calvo, 1997, 1999).

2.3.2.4 Flow rate

After the selection of solutions, flow rate is arguably the second most significant parameter in EHD spraying and together with the solution properties can control final product (Almería et al., 2010). Flow rate thus has consequences for both the size and morphology of particles and must be carefully selected since both these features will influence the food ingredient component dispersion within the particle matrix, eventually affecting food ingredient component release rate.

It is necessary to use a flow rate that allows for complete solvent evaporation, which is not possible with high flow rates. Particles are partially solvated when they impact the collector leading to a deformed and non-consistent morphology (Bock et al., 2011; Xie et al., 2006c). Furthermore, higher flow rates can trigger the formation of secondary and satellite droplets that confer a bimodal or polydisperse character to the size of EHD sprayed particles. This is described by the processes involved in solvent evaporation from the charged droplet, based on φ_{Ray}, the polymer volume fraction in a droplet at the Rayleigh limit, and expressed in

Equation 3. Q is the liquid flow rate ($m^3\ s^{-1}$), I the current, ε_{air} the permittivity of air, γ the surface tension of solution in ambient air, and d the initial droplet diameter, ε is the permittivity of the surrounding medium, φ is the polymer volume fraction. I/Q and d can be determined as a function of Q and the EHD spray solution properties:

$$\varphi_{Ray} = \varphi \frac{288\varepsilon_{air}\varepsilon\gamma}{(I/Q)^2 d^3} \quad \text{Equation 3}$$

According to Equation 3, flow rate has a major influence on φ_{Ray} and it was shown for the morphology of particles that larger flow rates lead to smaller φ_{Ray}, and thus non-spherical morphology and formation of satellite and primary droplets, while higher solution concentrations would preserve particle sphericity at higher flow rates (Almería et al., 2010).

In practice, the formation of satellite and primary droplets can be explained by the phenomena occurring when the droplets are ejected from the Taylor cone. Initially, a filament unites 2 droplets, but it is further broken up by the charge. Once broken from the farthest droplet, the filament flows back to the nearest droplet from the cone, and monodisperse particles can be achieved. This is seen for relatively low flow rates. At increased rates, φ_{Ray} becomes smaller, eventually falling in the case where entanglements are not strong enough to preserve the droplet integrity. Thus the filament cannot reach the former droplet anymore and instead it breaks, forming a secondary smaller droplet. At even higher flow rates, a filament between primary and secondary can form, which, being unable to reach back to the primary droplet, turns into a satellite droplet (even smaller than secondary droplets) (Hartman et al., 2000). If the solvent has a high evaporation rate, it is even possible that the filament remains frozen, leading not only to polydisperse sizes but also leading to elongated particles (Almería et al., 2010).

2.3.2.5 Effect of voltage

The main incidence of applied voltage is on EHD spraying modes as described previously in Section 2.3.2.1 Within the single cone-jet mode, size is not considerably affected by voltage where only a small decrease in size is detected when voltage is increased (Hong et al., 2008).

On the other hand, increasing the voltage results in morphology changes from spherical particles to elongated particles or beaded fibers to eventually only fibers if concentration is sufficiently high (Shenoy et al., 2005). This is owing to more charge acting on droplets with increased applied voltage, causing to stretching and elongation of droplets. It is therefore recommended to use moderate applied voltages that allow for the single cone-jet mode to take place while maintaining the spherical morphology of particles.

2.3.2.6 Effect of tip-to-collector distance

The lower limit of distance is determined by electric discharge. A small tip-to-collector distance can impair full solvent evaporation and consequently, wet microspheres impact the collector, leading to collapsing, coalescence and broad size distributions (Arya et al., 2009). Increasing the distance leads to better spherical morphologies since material (e.g. particle matrix) has enough time to diffuse within the droplet (Bock et al., 2011) and thus also reduced polydispersity. At constant applied voltage, a decrease in the tip-to-collector distance leads to rise in the strength of the electric field, thus resulting to a lower in particle size (Yao et al., 2008). Depending on the type of solvent used, an increase in tip-to-collector distance may also be detrimental for morphology.

2.3.3 Important of solvent

Solvents are needed to solubilize materials (e.g. polymers or/and lipid) prior to EHD spraying. The most broadly utilised solvent for EHD spraying particles loaded with food

ingredient components is dichloromethane, a chlorohydrocarbon with the lowest boiling temperature (40 °C) of the common solvents utilised in EHD spraying.

The boiling temperature of a solvent is the temperature at which the vapor pressure equals the ambient atmospheric pressure and it is representative of the solvent's volatility. Solvents with high boiling temperatures are vaporized less easily than solvents with low boiling temperatures and are thus less volatile. This means that materials (e.g. polymer) diffusion is increased in EHD sprayed droplets from solvents with high boiling temperatures. This affects the morphology and size of particles and it was previously shown that an increase in boiling point, corresponding to a lower in volatility, correlated with a decrease in particle size with smoother surfaces generated for solvents with boiling temperatures above 140 °C (such as chlorohydrocarbon, 146 °C) (Park & Lee, 2009). A large particle size and more textured surfaces can be observed with solvents with low boiling temperatures such as chloroform (61 °C) (Bock et al., 2011) and dichloromethane (40 °C) (Wu et al., 2009a). This is due to fast solvent evaporation, where less time is available for materials (e.g. polymer) chains to contract and re-arrange within the evaporating droplet exposed to electric field. Quicker evaporation can also cause in the formation of pores (Wu & Clark, 2008) and even hollow particles (Chang et al., 2010; Ciach, 2006). Importantly it was revealed that a decrease in vapor pressure weakens the forces of particle matrix entanglements (Meng et al., 2009). Therefore, the Coulombic repulsion is able to overcome the surface tension of evaporating droplets, leading to the ejection of highly charged and small off spring droplets.

2.4 Nanoencapsulation of food ingredient compounds

Nanoencapsulation is a flourishing area of research with major applications in the protection and delivery of active ingredients. It is a process of entrapping an active ingredient for instance food component (e.g., antioxidants, essential fatty acids, vitamins) within a wall

material (e.g., polymer, protein, lipids). Encapsulation helps not only in improving the stability, bioavailability and controlled release properties of the food component but also in masking unwanted odor and taste of the compound (de Vos et al., 2010).

Numerous methods for nanoencapsulation of food ingredient components (for instance, emulsification, coacervation, spray drying, nanoprecipitation, freeze drying, etc.) exist with their own advantages and disadvantages (Ezhilarasi et al., 2013). For example, nanoencapsulation by spray drying is possible only when modification in the apparatus design is made for retaining the nanoparticles. In case of emulsification method, nanoparticles are obtained in liquid state which needs appropriate drying method to achieve nanoencapsulates in powder form. In this context, EHD spraying utilises an extensive range of biodegradable, biocompatible, food grade, conducting polymer or/and lipid substances as encapsulated materials for entrapment and/or encapsulation of food ingredient components.

Common food ingredient component based encapsulating materials used in EHD spraying are whey protein concentrate (WPC), whey protein isolate, egg albumen, soy protein isolate, collagen, gelatin, zein and casein. Several investigations have shown the importance of the apparatus factors and solution properties on the morphology of protein based EHD spun fibers and EHD sprayed particles. For instance, WPC micro (1724 ± 524 nm), submicro (336.6 ± 218.8 nm) carriers were prepared for encapsulation of food ingredient food based ingredients that are prone to degradation (morphology of EHD sprayed WPC carrier). It was shown that change in pH of the solution leads to significant change in the carrier size as observably larger carriers were obtained at pH 6.4 (Lopez-Rubio & Lagaron, 2012).

Similarly, common polysaccharide based encapsulated materials utilised in EHD spraying are cellulose, alginates, chitosan and dextrans. For example, polysaccharides were EHD sprayed for the production of polyelectrolyte complex (polyanion: chitosan or calcium chloride

aqueous solution, polycation: sodium alginate solution) micro (80‑230 μm) suitable for food ingredient encapsulation (Fukui et al., 2010; Ghayempour & Mortazavi, 2013). On the other hand, EHD atomization for food component encapsulation is a relatively new concept and hence it is in its nascent stage. Investigations are shown to adjust the factors for EHD spraying by numerous polysaccharides biopolymers.

Recently, low molecular weight carbohydrate (for example, resistant starch, maltodextrin) based carriers were achieved by EHD spraying along with appropriate surfactants (Span 20, Tween 20, lecithin) (Perez-Masia et al., 2014). In two different investigations, zein was utilised as the polymer to encapsulate curcumin and docosahexaenoic acid in order to obtain and nanocarrier with average diameter in range of 175‑250 nm and carriers with average diameter 490 ± 200 μm respectively. The encapsulated docosahexaenoic acid revealed better chemical stability against degradation, improved stability to environmental conditions such as relative temperature, humidity and reduced off-flavour (Torres-Giner et al., 2010). Furthermore, the nanoencapsulated curcumin was found to possess improved shelf-life stability and better dispersion in aqueous food nanoparticles matrix (semi-skimmed milk), enabling its application as coloring agents in food products (Gomez-Estaca et al., 2012). The oxidative stability of beta carotene was also improved by EHD spray encapsulation utilizing WPC as encapsulating material (Lopez-Rubio & Lagaron, 2012).

Moreover, EHD spraying method has also been employed for encapsulation of probiotic Bifidobacterium strains in hydrocolloid-based smooth carriers with either pullulan or whey protein concentrate as encapsulating materials. The average diameter of pullulan encapsulated probiotic (457 ± 214 nm) was less than the WPC (529 ± 237 nm) carriers. Further, the whey protein concentrate carriers were created to improve the survival of the cells even at high relative humidity than the pullulan carriers. Also, the scientists emphasized

the absence of viability losses during EHD spray encapsulation process (Lopez-Rubio et al., 2012). The protection of food ingredient components by EHD spray encapsulation holds promising opportunities in the area of functional food development provided the focus is laid on optimisation and scaling-up of the process.

The benefits of EHD spraying method is high encapsulation efficiency, sustained release, light, greater thermal and shelf stability and improved protection of food ingredient compounds from chemical degradation. The biofood ingredient compounds encapsulated in EHD sprayed particles are shown to possess improved stability and functionality. Such encapsulates may be utilised as ingredients in functional foods. In this respect, EHD spraying seems to be a optimal for manufacturing nanoencapsulates appropriate for development of functional foods.

2.4.1 Techniques for nanoencapsulation of food ingredient compounds

Nanotechnology has been widely utilised in encapsulation and delivery system to develop agriculture pharmaceutics, and food industry in the recent years (Chen et al., 2006b; Farokhzad & Langer, 2009; Fathi & Mohebbi, 2010; Liu et al., 2008; Müller et al., 2007; Neethirajan & Jayas, 2011; Sanguansri & Augustin, 2006; Shimoni, 2009). It has emerged as one of the most promising scientific fields of research in recent decades. It concerns the understanding and manipulation of materials at dimensions of ~ 1-100 nm.

In the past few years, nanoparticle containing foods have been approved for use or entered experimental development (Fathi & Mohebbi, 2010; Neethirajan & Jayas, 2011; Rizvi et al., 2010; Sanguansri & Augustin, 2006) for example to deliver food ingredient components (Chen et al., 2006b; Shimoni, 2009). Recently, flavour encapsulation has become a popular technique in the food industry (Karathanos et al., 2007).

Most flavour compounds are highly volatile and chemically unstable as a result of oxidation, chemical interactions and volatilisation. So, encapsulation of flavour compounds is essential to stabilise them and offer their release when required (Choi et al., 2009). Also the properties of food ingredient compounds can be improved by encapsulating them, such as their prolonged residence time in the gastrointestinal tract, delivery, solubility, and the efficient absorption through cells (Chen et al., 2006c).

The successful utilisation of nanoparticles in various industries, particularly in biotechnology, is dependent largely on their uptake by the body tissue (e.g. via cell membrane), controlled and sustained release of food ingredient through polymer or/and lipid matrices and their stability.

Currently, several techniques are used for encapsulation (Dziezak, 1988) including liposome entrapment, coacervation, inclusion complexation, centrifugal extrusion, spray cooling, spray chilling or spray drying, extrusion coating, fluidized bed coating and rotational suspension separation (Gibbs et al., 1999; Zuidam & Heinrich, 2009).

2.4.2 Classification of nanocarrier systems

Polymeric and lipid nanoparticles represent the main classes of nanocarrier system capable of efficiently encapsulating a variety of food ingredient components to protect them from unfavourable environmental conditions by restricting the transfer of gases and maintaining the pH (Fang & Bhandari, 2010; Zimet & Livney, 2009). This enables increased storage periods, and improves bioavailability by releasing food ingredient components at a sustained rate (McClements et al., 2009; Mozafari et al., 2006)..

2.4.2.1 Lipid based nanocarrier system

Lipid based nanocarrier systems now under serious research can be divided into main classes, such as solid lipid nanoparticles, liposome, emulsions, microemulsions, nanoemulsions, multiple emulsions and filled hydrogel particles (Flanagan & Singh, 2006; Matalanis et al., 2011; McClements & Li, 2010; Velikov & Pelan, 2008; Weiss et al., 2008).

Lipid based nanocarrier systems have wide spectrum of applications as encapsulation and delivery carrier in pharmaceutical, food, and cosmetic areas, for example flavour, nutraceuticals, vitamins, and preservatives (Given, 2009; Sagalowicz & Leser, 2010; Sanguansri & Augustin, 2006; Velikov & Pelan, 2008). With respect to food delivery applications, lipid nanoparticles and liposome are effective carriers for both lipophilic and hydrophilic food ingredient component used in nutraceuticals, to increase oral bioavailability, efficiency and solubility (Fathi & Varshosaz, 2013; Lacatusu et al., 2013; Stratulat et al., 2014; Ting et al., 2014).

Liposomes, defined as the spherical shaped nanovesicles shaped by one or multiple concentric layer, have been extensively utilised owing to their good delivery efficiency, high compatibility and favorable kinetic release. In the recent years, several liposome containing food ingredients have been approved for use or entered trial development (da Silva Malheiros et al., 2010; Keller, 2001; LIU et al., 2013; Madrigal-Carballo et al., 2010). However, its major limitations are insufficient food ingredient component loading capacity, fast food ingredient component release, and instability in storage (Vyas et al., 2008).

Solid lipid nanocarrier, featured by a matrix made of solid lipid (Mehnert & Mader, 2001; Müller et al., 2000), there are general principles models for food ingredient component incorporation that are reported in the literature; Homogeneous matrix, food ingredient component enriched shell, and the Food ingredient component enriched core.

Homogeneous matrix model; food ingredient component dispersed uniformly in lipid matrix; this leads to prolong food ingredient component release (e.g. weeks) (Schwarz et al., 1994; zur Mühlen et al., 1998), acceptable biocompatibility, high encapsulation efficiency, high flexibility in controlled release manner, possibility of large scale production, slow degradation rate allows release for prolonged period and provide more protection against oxidation (Cavalli et al., 1993; Müller et al., 2000).

Food ingredient component enriched shell model; food ingredient component molecules are enriched in the shell of the nanoparticles, which has very fast release from nanoparticle (e.g. <5 min) (Heiati et al., 1998; Muller et al., 2002).

Food ingredient component enriched core model; food ingredient component precipitates first and the lipid monolayer formed surrounding the food ingredient component core, this results to a membrane controlled release rate governed by Fick's law of diffusion (Müller et al., 2002), most influenced by its physicochemical properties (e.g. partition coefficient) of the food ingredient component molecules (Cavalli et al., 1999; Souto et al., 2004). Up till now, lipid nanocarriers systems of food component such as flavour component have been intensively studied (Ezhilarasi et al., 2013; Fathi et al., 2012; Weiss et al., 2008).

2.4.2.1.1 The rational design of lipid based nanocarrier system

Recently nanoparticles have been gaining impetus scientifically and commercially in the pharmaceutical as well as the food industries (Awad et al., 2008; Gallarate et al., 2009; Varshosaz et al., 2010a; Varshosaz et al., 2009). Lipid based nanoparticles have been developed as an alternative to conventional carrier systems such as emulsions, liposome, etc. Owing to their unique properties including high encapsulation efficiency, small size, increased surface area, they have great potential in applications requiring controlled release, food ingredient stabilisation, etc. have high and enhanced food ingredient content, ability to

carry hydrophobic and lipophilic food ingredients, biodegradability and biocompatibility (Cavalli et al., 1993). They are also commercially viable and have gained regulatory approval (Müller et al., 2000; Smith & Hunneyball, 1986).

2.4.2.1.2 Lipid based nanocarrier system techniques

Numerous studies have been reported regarding the solid lipid nanoparticle, which are of lipid based shell nanoparticle manufactured by numerous techniques, which can be summarized in two main classes (Müller et al., 2000; Schwarz et al., 1994).

Hot homogenization method; this method results in lack of control over the physical and chemical properties of the solid lipid nanoparticles, loss of food ingredient to water phase and recrystallisation. Cold homogenization method; this technique results formation of food ingredient component enriched shell lead to high burst release (Müller et al., 2007). Such strategies meet the need to improve lipid nanoparticles with desirable physical and chemical and facilitate future scale up, which therefore deserves further development. It is thus ideal if any technique could be advanced to overcome the disadvantages of food component nanocarrier. One possibility is to engineer food component core with lipid shell nanoparticles as food component nanocarrier.

2.4.2.2 Polymer based nanocarrier system

Polymer nanoparticles have emerged as a highly promising area of scientific research and have been utilised in a wide spectrum of application areas in recent decades due to their unique properties, which include their ability to encapsulate and deliver food ingredient components (Chen et al., 2006b; Shimoni, 2009). The characteristics of polymer nanoparticles have to be adjusted according to the particular application.

2.4.2.2.1 The rational design of polymer based nanocarrier system

The polymeric material which can be designed to encapsulate food ingredient must be edible, biodegradable and able to form a barrier between the internal phase and its surroundings (creating a modified atmosphere restricting the transfer of gases (O_2, CO_2)) and also becoming a barrier for transfer of aromatic flavour compounds (Miller & Krochta, 1997).

2.4.2.2.2 Polymeric nanoparticles system techniques

The technique of nanoparticle production thus plays a vital role, as it is this that will largely determine the ability to predict and control the desired properties. Conventional processes for preparing polymer nanoparticles are frequently complex, commonly requiring multiple step processing, such as emulsification, drying, removal of surfactants (Ezhilarasi et al., 2013; Fathi & Mohebbi, 2010; Neethirajan & Jayas, 2011; Rizvi et al., 2010; Sanguansri & Augustin, 2006; Silva et al., 2012). This is not only time consuming but may reduce the degree of control over nanoparticle physicochemical properties and reduce product recovery; all of which increases the cost of production and uniformity of the final product. Further details on the different methods for polymer nanoparticle preparation can be found in the review by (Rao & Geckeler, 2011).

2.4.2.3 Polymer-lipid nanoparticle system

The use of a combination of polymers and lipids results in the formation of nanoparticles with a hydrophilic core and a hydrophobic shell. Both water soluble and insoluble food ingredient components can be encapsulated, including poorly soluble substances such as fatty acids, carotenoids, and phytosterols (Humberstone & Charman, 1997). The development of novel polymer-lipid nanoparticles for food ingredient component encapsulation with

predictable and controlled properties is essential to meet the requirements of food applications. Furthermore, it is crucial to select the appropriate encapsulation technique based on the nature of the core-shell particles, physicochemical properties of the materials, and required size.

2.4.2.3.1 Polymer-lipid nanoparticle system techniques

Conventional techniques for producing polymer-lipid nanoparticles are relatively complex, usually requiring a two or more step formulation process: firstly, development of nanoparticles of the core material (polymeric), and secondly, encapsulation of the core nanoparticles by the shell (lipid) (De Miguel et al., 2000; Thevenot et al., 2007). This often results in poor control over the final nanoparticle physicochemical structure. More details on polymer-lipid nanoparticle encapsulation can be found in the literature (Hadinoto et al., 2013; Mandal et al., 2013)

2.5 Tailoring of EHD sprayed particle characteristics

2.5.1 Morphology

The morphology of EHD sprayed particles is controlled by solvent evaporation and polymer diffusion (Almería et al., 2010). The EHD sprayed solution thus plays a major role in these mechanisms, where the nature of EHD sprayed solution (solubility, concentration) and solvent (boiling temperature, conductivity of solution, vapour pressure) together with the flow rate form the factors of morphology tailoring (Bock et al., 2011). Solution properties such as molecular weight and concentration can dictate the entanglement regime taking place, resulting to reproducible and solid EHD sprayed particles, when a certain degree of chain entanglement is obtained. Therefore in many studies, morphology is primarily related to solution concentration and molecular weight, where a reduction in concentration or an

increase in molecular weight encourages non-spherical morphologies such as wrinkled, hollow particles, shell-like, particles with tails or beaded fibers (Chakraborty et al., 2009; Enayati et al., 2010; Meng et al., 2009). As seen in Equation 3, flow rate also has a major influence on morphology through φ_{Ray}, the polymer volume fraction in a droplet at the Rayleigh limit.

2.5.2 Size

The size of EHD sprayed particles that contain food ingredient component significantly impacts their capabilities. For example, the release rate increases with a larger surface to volume ratio of the particles (Xie et al., 2006b) and is dependent on surface degradation and diffusion. Control of size is therefore crucial for designing release characteristics (Figure 7). The EHD spraying method can prepare particles with sizes ranging from micrometers to nanometers (Ijsebaert et al., 2001) and by selecting the precise parameters, low polydispersity can be achieved with relative standard deviations (RSD) within 2–27% of the average size (Xie et al., 2008c) and (Valo et al., 2009). This is advantageous in food ingredient component delivery since food ingredient component distribution within the particle matrix can be controlled more accurately with a single known particle size, allowing degradation rates and diffusion of encapsulated components to be well tailored to fit a required application (Gomez et al., 1998). The nanosize of EHD sprayed polymer/food ingredient component is thus less expected and most particles actually prepare micro-sizes.

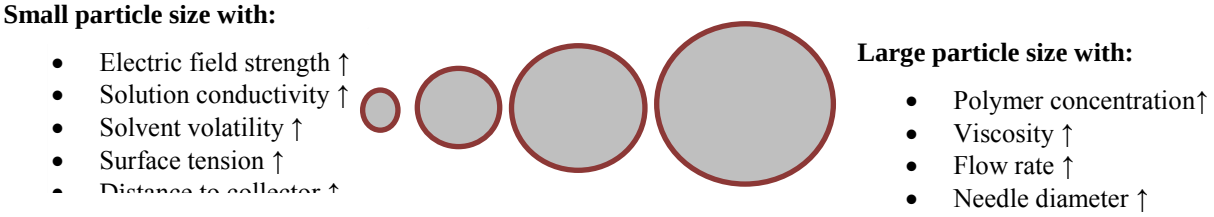

Figure 7: Illustrating the effect of parameters on particle diameter size (↑: increase).

2.5.3 Monodispersity

Monodispersity remains a very essential feature for particle sizes, particularly for release rate characteristics. It can be observed that many similar sizes can provide very different polydispersivities according to the processing parameters and also depend on the materials matrix, solvent and food ingredient choice. It is thus likely to achieve very low polydispersivity with EHD spraying method as low as 2.1% (Valo et al., 2009), by tailoring EHD spraying parameters, but this is a complex undertaking. It is achieved with increased polymer concentrations (higher viscosities) and reduced flow rates, reduced electrical conductivity of the EHD sprayed solutions and reduced applied voltages (Enayati et al., 2010; Enayati et al., 2011). This applies for the stable-cone jet mode recognized to be the only one able to prepare monodisperse particles and when parameters such as flow rate are used in the central cone jet region. Certainly, when flow rate is used close to the lower and upper limit of the cone jet region, the polydispersivity index of particles increases (Enayati et al., 2010).

The size of EHD sprayed particles is significantly effect by solution concentration and flow rate, where bigger particle sizes are most significantly achieved with an increase in solution concentration and flow rate and a reduction in conductivity (Bock et al., 2011). However, at increasing solution flow rates, the size distribution also becomes larger (Ijsebaert et al., 2001) and formation of secondary and satellite droplets can take place if the polymer network is not entangled enough. This leads to a bimodal size distribution which is quite common in EHD spraying and sometimes unavoidable (Bock et al., 2011; Ding et al., 2005; Hong et al., 2008; Jaworek, 2008).

Some strategies have been recommended to separate the two size populations by using a steel plate with a 3 cm circular hole as the grounded electrode, which assists to collect only the primary droplet population. Often a spatial separation occurs after the droplet break-up where

two regions of EHD spray can be seen during the stable cone-jet mode, since satellite/secondary droplets have a larger surface charge density but less mass than primary droplets. Therefore primary droplets can be found in the inner core of the spraying cone, while satellite/secondary droplets get ejected at the periphery of the cone (Hong et al., 2008).

By utilizing a plate with a circular hole as a screen on top of the collector, satellite/secondary droplets thus are left behind and only primary droplets are recovered ensuring monodispersity, although reduced yield may be of concern. Hartman et al. measured very small currents (31–57 nA) during EHD spraying and found that another way to reduce the frequency of satellite droplets is to lower the current by lowering the applied voltage or flow rate (Hartman et al., 2000). However, satellite/secondary droplets remain difficult to eliminate completely (Hong et al., 2008). These findings are described by the connection between particle size and EHD spraying parameters described by Hartman et al. in the stable single cone jet and shown in Equation 4 and Equation 5 (Hartman et al., 2000).

The droplet diameter size, *d*, can be modeled using different equations created by Delamora and Loscertales (Fernandez de la Mora & Loscertales, 1994) in 1994, Gañan-Calvo et al. (Ganan-Calvo et al., 1997) and Hartmann et al. (Hartman et al., 2000) (Equation 4 and Equation 5) for the single cone-jet. They are functions of the solution flow rate, *Q*, the solution density, ρ, the surface tension in ambient air, γ, the current, *I* and the liquid conductivity, *K* (α is a constant):

$$d = \alpha\left(\frac{\rho\varepsilon_0 Q^4}{I^2}\right)^{1/6} \qquad \text{Equation 4}$$

$$I \propto (\gamma K Q)^{1/2} \qquad \text{Equation 5}$$

Particle size is directly proportional to droplet size, where an increase in size is achieved with increasing solution flow rate and reducing surface tension, and is shown to correspond to an increase in solution concentration (Hao et al., 2006). But, as indicated previously, an increase in flow rate is also responsible for wider size distributions (Ijsebaert et al., 2001), thus a compromise requires to be made between dispersity and size. This is described in Section 2.3.2.1, where higher flow rates result to smaller φ_{Ray}. As indicated by Almeria et al., if increasing particle size is highly needed, while maintaining monodispersity, increased solution flow rates could be coupled with higher solution concentrations (Almería et al., 2010). As described in Section 2.3.2.2, the conductivity is actually a powerful parameter for governing particle size where the scaling laws from Gañan-Calvo show that a decrease in particle size can be achieved with an increase in electrical conductivity, according to Equation 6 (Ganan-Calvo et al., 1997):

$$d = \left(\frac{1}{K}\right)^{1/6} \qquad \text{Equation 6}$$

2.5.4 Loading and encapsulation

2.5.4.1 Definitions and methods

EHD spraying is an encapsulation process in which efficiency is measured by the traditional loading capacity (LC) and encapsulation efficiency (EE) parameters generally utilised in the area. EE represents the mass of food ingredient component successfully loaded in particles (m_{Loaded}) with respect to the original mass of food ingredient component available (m_{Total}) (Equation 7). Loading capacity is the mass of food ingredient component successfully loaded in particles (m_{Loaded}) as a fraction of the total mass of particles ($m_{Particles}$) (Equation 8):

$$EE = \frac{m_{Loaded}}{m_{Total}}$$ Equation 7

$$LC = \frac{m_{loaded}}{m_{particles}}$$ Equation 8

Extraction is generally utilised to determine these parameters. Briefly, particles are dissolved in solvent, usually identical to that used to initially solubilize the polymer, followed by the addition of an aqueous solution. The mixture is vortexed to extract the encapsulated food component to the aqueous phase, finally followed by centrifugation to separate the water and oil phases. The aqueous phase is then collected and examined. In some cases, solvent is left to evaporate before addition of the aqueous phase (Ding et al., 2005; Xie et al., 2006c; Xie et al., 2008c). From the literature, it seems that most studies only undertake one extraction, with the exception of Nie et al.'s study where a total of three extraction sets were performed for suramin recovery (Nie et al., 2010b). Doing only one extraction is quite restrictive considering that E (%) = 100D/(1 + D), where E is the amount extracted and D is the distribution coefficient. This might be an issue for full recovery of food ingredient component.

Last important consideration with the extraction process is that it does not represent the quantity of food ingredient component successfully encapsulated/loaded in particles but comprises also non-encapsulated food ingredient component which may be simply adsorbed on the surface, (which are responsible for the initial burst release often seen with such systems). This is an issue since very high EE are reported in the literature but there is rarely sufficient description of quantification of adsorbed versus encapsulated food ingredient component. Some LC/EE are therefore to be considered with caution if measured by the extraction method, as they are not representative of the real quantity of encapsulated/loaded

food ingredient component; this is a real shortfall in most studies. Interestingly, the determination of LC and EE is also presented via a "non-entrapped" suggested by Xu and Hanna (Xu & Hanna, 2006). Particles were centrifuged and the amount of free molecule was determined in clear supernatant by UV utilizing the supernatant of non-loaded particles as a basic correction. LC and EE were calculated according to Equation 9 and Equation 10:

$$\mathrm{LC} = \frac{\mathrm{A}-\mathrm{B}}{\mathrm{A}}\mathrm{X}100 \qquad \text{Equation 9}$$

$$\mathrm{EE} = \frac{\mathrm{A}-\mathrm{B}}{\mathrm{C}}\mathrm{X}100 \qquad \text{Equation 10}$$

where A is the original quantity of food ingredient component, B is the non-loaded quantity of food ingredient component and *C* is the total amount of particles. This method does not essentially take into account losses throughout particle production.

2.5.4.2 Influence of parameters on loading and encapsulation

In encapsulation processes, loading capacity and encapsulation efficiency are typically influenced by the processing factors, including particle formation. For instance encapsulation efficiency in double emulsion procedures is dependent on the balance between immiscibility and solvent evaporation rate between particle and water, rate of solution (e.g. polymer) precipitation and thus hardening rate of the sphere wall (Freiberg & Zhu, 2004). In EHD spraying, similar factors such as the nature of food ingredient component to encapsulated material (e.g. polymer) weight ratio, along with flow rates for instance, are parameters influencing loading capacity and encapsulation efficiency, and will be presented hereafter.

2.5.4.2.1 Loading capacities

High LCs are always required for better availability of the food ingredient component in targeted fields with minimal utilisation of carrier materials. Nevertheless, this can encourage possible changes of particle morphology that occur with increased loading, and thus possible change of release rate patterns. In a study from Hong et al., it was proven that an increase in the loading capacity led to a loss of sphericity of particles (Hong et al., 2008) which in turn affected the release rate patterns. The scaling laws of EHD spraying were nevertheless confirmed with almost no theoretical difference from non-loaded to loaded particles. Actual LCs in EHD spraying has also been revealed to be slightly reduced compared to theoretical loadings.

2.5.4.2.2 Encapsulation efficiencies

EHD spraying is known as a method which can offer high EE, and, also presents the great advantage that encapsulation of both types of hydrophobic and hydrophilic, are efficiently obtained compared to other approaches (Almería et al., 2011), mainly since there is no need of an emulsion step. In emulsion-based approaches, the existence of both aqueous and organic phases may actually result to better diffusion of the food ingredient component to one phase or the other according to their hydrophilicity/ hydrophobicity features and thus decreasing ultimate encapsulation efficiency. This is avoided with EHD spraying where emulsions are not needed. Encapsulation efficiency depends on the mixture of food ingredient component, wall materials matrix and solvent choice, where the nature of these components shows significant role.

2.6 EHD spraying and food ingredient component release characteristics

2.6.1 Choice of food ingredient component

Most food ingredient components such as food flavour are costly. For this reason the food ingredient delivery studies are first undertaken with model food flavours, to allow controlling of characteristics and parameters of EHD spraying particles in the first instance, before loading fragile and expensive food ingredients. Food ingredient component such as food flavour plays an important role in consumer satisfaction and influences further consumption of foods. Most available aroma compounds are produced via chemical synthesis or extraction. Food stuffs containing synthetic flavour are often avoided, because the consumers suspect that these compounds are toxic or harmful to their health (Teixeira et al., 2012).

Flavour stability in different foods has been of increasing interest because of its relationship with the quality and acceptability of foods, but it is difficult to control. Manufacturing and storage processes, packaging materials and ingredients in foods often cause modifications in overall flavour by reducing aroma compound intensity or producing off-flavour components (Lubbers et al., 1998). Flavours form very complex systems because there are many variables. Some are more stable in carbohydrates which are water soluble and some are more stable in lipid based coating.

Many factors linked to aroma affect the overall quality of the food, examples are physicochemical properties, concentration and interactions of volatile aroma molecules with food components (Landy et al., 1995). To limit aroma degradation or loss during processing and storage, it is beneficial to encapsulate volatile ingredients prior to use in foods or beverages. A summary of various food product such as fats and oils, aroma compounds and oleoresins, vitamins, minerals, colorants, and enzymes have been encapsulated (Jackson & Lee, 1991; Shahidi & Han, 1993), that have been loaded so far in particles.

The flavour compound being protected is locked up in a membrane that isolates it from the external medium.

The size of carrier formed can vary from a few millimeters to nanometers. The simplest of the carriers may consist of a core surrounded by a wall of uniform or non-uniform thickness. The core material may be composed of just one or several different types of ingredients and the carrier may be single or multilayered. The carriers are generally additives to a larger system and must be adapted to that system. Consequently, there are a number of performance requirements placed on microcarriers.

A limited number of encapsulating methods exist, but an enormous range of different materials can be used. These include proteins, carbohydrates, lipids, gums and cellulose. Each group of materials has certain advantages and disadvantages. For this reason, many coatings are actually composite formulations of any or all the above. The choice of wall materials depends upon a number of factors including: expected product objectives and requirements; nature of the core material; the process of encapsulation; economics and whether the coating material is approved by the Food and Drug Administration (US) or European Food Safety Authority (Europe).

For encapsulation of the flavour compounds, the carrier material must have no reactivity with the core material; be present in a form that is easy to handle, e.g. with low viscosity at high concentrations; allow a complete elimination of solvent in any processes requiring a phase of desolvatation; give the maximum protection of the food ingredient component against the external factors; ensure good emulsion-stabilisation properties and effective redispersion behaviour in order to release the flavour at the times and the place desired. A good knowledge of the physicochemical interactions occurring between aroma compounds and the main constituents of foods such as lipids, polysaccharides, and proteins, is required for food flavouring control. Major wall materials used for flavour encapsulation are reported in the literature.

2.6.2 Food ingredient component dispersion

Controlled dispersion of the food ingredient component within the particle is of upmost significance for reliable release rate. It was earlier stated that food ingredient component concentration in a particle to declines as we move outwards from the center with the increase of the particle diameter size (Hong et al., 2008). This is described by the diffusion mechanism of solutes, declaring that an increase in the droplet size provides a longer distance and time for diffusion of solutes, leading to a food ingredient component gradient within the particle. An EHD sprayed droplet contains food ingredient molecules which move and diffuse throughout solvent evaporation, providing the final particle. The level of intermolecular entanglement among food ingredient molecular dictates these parameters, affecting the diffusion rate of food ingredient molecules toward the center. When adding small molecules like food ingredient components to this system, they generally diffuse easily toward the droplet center due to the absence of intermolecular action. However the intermolecular entanglement of material matrix (e.g. polymer) food ingredient component is weakened, leading to a decrease in the diffusion coefficient of solutes expressed by the Stokes–Einstein Equation 11:

$$D = \frac{k_B T}{6\pi\eta R_H} \qquad \text{Equation 11}$$

where k_B is the Boltzmann's constant, η the viscosity of solvent, T the temperature, and R_H the hydrodynamic radius of solutes (Hong et al., 2008). Therefore by increasing the concentration of small solutes in a polymer droplet composed of big molecules, the diffusion coefficient decreases. Above a critical concentration value, the diffusion of solutes becomes slower than solvent evaporation and the small molecules are trapped on the surface of the droplet, leading to a molecule saturated layer of semi-solidified skin (Hong et al., 2008) and

(Ciach, 2006). Such a configuration is not ideal for the physical and release properties of particles, since with further evaporation of the droplet, the skin moves toward the droplet center, leading to particle collapse and a final wrinkled morphology, which does not lend itself to sustained and reproducible release properties. Ideal and homogeneous molecule dispersion, which is preferable for sustained release, is therefore obtained for low loadings, smaller particle size (which limits the food ingredient component gradient effect) and a good balance between the diffusion and evaporation mechanisms. If high loadings are needed, it is important to control diffusion and ensure that it does not become lower than evaporation. This can be balanced by utilizing a slow evaporating solvent. A few methods have been utilised to evaluate the incorporation of food ingredient components within the EHD sprayed particles, while they do not allow for physical visualisation of food ingredient components within the droplets (although TEM may be used to look at internal structure). Differential scanning calorimetry (DSC) relies on the fact that if a food ingredient component is well dispersed in the particle matrix, the melting transition of the food ingredient component will be suppressed either partially or completely (Ding et al., 2005). X-ray diffractometry (XRD) may also be utilised for examine the physical state of a food ingredient component within particle since features of the peaks mark the degree of crystallized ion of the food ingredient component with the particle matrix (Xie et al., 2008c).

2.6.3 Release kinetics of nanoparticles delivery systems

Particles for controlled food ingredient component delivery have been broadly investigated in the recent years and numerous reviews detail their preparation, the parameters influencing the release rates and the current complications faced during processes (Celebioglu & Uyar, 2012; Ezhilarasi et al., 2013; Fathi et al., 2012). Most of these reviews encompass nano - microparticles made from traditional fabrication approaches and limited information is

available on release rates from EHD sprayed particles. In general terms, release occurs through two distinct processes: passive diffusion and matrix (e.g. polymer) degradation. Ideally a controlled release rate would indication a zero-order release pattern, meaning a constant release rate over time. However the release rate from particles is commonly divided in two different mechanisms: firstly: The initial burst release of food components contained on and in the surface of the particle owing to the leaching occurring at the wall of the particle as it becomes hydrated (Freiberg & Zhu, 2004). Secondly: The slower and more constant release of food components from the core of the particle as it degrades.

Release patterns can be influenced by chemical and physical parameters: the nature of the matrix particles, the nature of the loaded food component, its distribution, the morphology of microspheres, their size distribution and porosity (Sokolsky-Papkov et al., 2007) and (Freiberg & Zhu, 2004). In EHD spraying, similar factors are able to tailor release rates and they are discussed in the next section.

2.6.3.1 Size

The size of particles which encapsulate food ingredient components is dominant in tailoring release rate patterns. A greater surface area to volume ratio (smaller particles) results in quicker release rate, since particles are more easily penetrated by fluids, favoring easier diffusion of molecules and faster degradation of the particle matrix. However, it is essential to highlight that it is not size itself that controls the release rates but it has more to do with the particles matrix (e.g. polymer or/and lipid), food ingredient component and solvent choice and processing factors that are utilised in each case, as explained in Section 2.3. Although an increase in matrix material (e.g. polymer or/and lipid) concentration is generally shown to increase size and decrease release rates and burst release at high concentrations, the contrary is seen for loadings. An increase in loading is commonly responsible for increased sizes too,

but creates quicker release rates and burst, especially on the submicron scale (Xu & Hanna, 2007). In the case of emulsions, the organic/aqueous phase factor has small influence on release rate patterns although size is significantly affected, as a consequence from reduced electrical conductivity with increased organic phase, and thus increased size, as described in Section 2.3.

The burst release stage is mostly diffusion-driven while the second stage providing a slower release is erosion-driven. It was shown by Almeria et al. that the burst release stage was greatly affected by particle size and particle agglomeration, whereas the slower release part was much less dependent on particle size (Almería et al., 2011). Agglomeration however was shown to affects release rates for hydrophilic food ingredient component, since sizes of particle clusters result in orders of magnitude bigger than single particles.

2.6.3.2 Morphology

Along with size distribution, morphology is another main feature for governing food ingredient component release behavior, morphology is directed by the wall materials, food ingredient component and solvent selection and processing parameters (Ding et al., 2005). More pores were found in wrinkled particles allowing for molecule adsorption instead of encapsulation. Water diffusion is more accessible in porous particles and result to the quick diffusion of adsorbed food ingredient component, responsible for the high burst release.

In denser particles, the rate of water diffusion is decreased, allowing for desirable zero-order release rate patterns. Similarly to wall materials (e.g. polymer) concentration, the weight average molar mass, generally known as molecular weight is another important factor for tailoring particles and their release rate patterns, since both factors direct the viscosity of solutions. The morphology of high molecular weight particles was spherical while the low molecular weight particles displayed an irregular morphology. The solvent is another factor

to governor particle morphology, owing to vary evaporation rates that result to more or less porous structures, respectively.

2.6.3.3 Nature of matrix nanoparticles

It is accepted that degradation of particles primarily occurs in amorphous regions, followed by a slower degradation of the crystalline regions of particles (Freiberg & Zhu, 2004). Freiberg et al. stated that low crystallinity allows enhanced food ingredient component dispersion and increased food ingredient component and material particle interactions while the degree of crystallinity is also influenced by the concentration, the food ingredient component loading and removal rate of solvent (Freiberg & Zhu, 2004). Thus, the utilise of particle matrix with highly crystalline structures enables the production of particles with uniform and reproducible physical properties (Bock et al., 2011), but might be insufficient for optimal food ingredient component dispersion and release rate properties.

2.6.3.4 Nature of food ingredient components

Interactions among loaded food ingredient component and particle matrix direct the location of food ingredient component within particle matrix and affect the behavior of release rate (Valo et al., 2009). The food ingredient components and their site within the particles affected the release rate patterns: loading of hydrophilic food ingredient component in the shell and hydrophobic food ingredient component in the core provided a sequential release, while the opposite led to the food ingredient components being released in parallel (Nie et al., 2010a).

The physical and chemical properties of the food ingredient component with the nanoparticle have a great effect on release rate pattern. For similar size distributions and loadings,

dramatic differences can be seen when variable the hydrophobicity and hydrophilicity of the food ingredient component encapsulated.

2.6.4 Stabilities of nanoparticles delivery systems

EHD spraying remains a process that employs solvents and thus the possibility of food ingredient component stability needs to be evaluated and compared to traditional encapsulation approaches to verify its superiority. So far, limited studies have addressed this issue, nonetheless they present promising results. The methods commonly employed are Fourier transform infrared (FTIR), ultraviolet (UV) spectroscopy (Pareta & Edirisinghe, 2006; Xie et al., 2008a; Xie et al., 2008b). Although promising advancement has been made, more studies are necessary to evaluate a greater variety of food ingredient component (food flavour agents) in contact with organic solvent, and various polymer or/and lipid, since the purity and source of food ingredient, and the nature of polymer or/and lipid can also influence the stability of loaded food ingredient component.

2.6.5 Release modelling of nanoparticles delivery systems

2.6.5.1 Introduction

To provide a particular release profile from a system, it is necessary to know the exact mass transport mechanisms involved in the food ingredient component release, and to predict quantitatively the resulting release kinetics. Many mathematical models have been used to design a number of simple and complex delivery systems and to predict the overall release behavior. They allow the measurement of some important physical parameters and resorting to model fitting on experimental release data. It is very important to know how to use these equations to understand the different factors that affect the release velocity and how the dissolution behaviors can vary and influence the efficiency. Therefore, this section describes

the main mathematical models of release, namely Higuchi, zero-order, Hixson-Crowell, first-order, and Ritger-Peppas models, respectively (Higuchi, 1963; Ritger & Peppas, 1987; Sezer et al., 2011). The concept, definitions and physicochemical properties involved in each model are discussed and the equations reported.

2.6.5.2 Zero-order model

Food ingredient component dissolution from dosage forms that do not disaggregate and release the food ingredient component slowly can be represented by the equation:

$$Q_t = K_0 t \qquad \text{Equation 12}$$

Where Q_t is the amount of ethylvanillin released in time t, and K_0 is the zero order release constant with units of concentration/ time. The plot made: Cumulative % food component release vs. time

2.6.5.3 First order model

This model has also been used to describe absorption and/or elimination of some food ingredient components although it is difficult to conceptualize this mechanism on a theoretical basis. The release of the food ingredient component which followed first order kinetics can be expressed by the equation:

$$\log Q_0 - \log Q_t = K_1 t \qquad \text{Equation 13}$$

Where Q_0 is the initial amount of the ethylvanillin in the nanoparticles, Q_t is the amount of ethylvanillin released in time t and K_1 is the release constant for first-order rate.

The plot made: log cumulative of % food component remaining vs. time

2.6.5.4 Higuchi model

This model is based on the hypotheses that (i) initial food ingredient component concentration in the matrix is much higher than food ingredient component solubility; (ii) food ingredient component diffusion takes place only in one dimension (edge effect must be negligible); (iii) food ingredient component particles are much smaller than system thickness; (iv) matrix swelling and dissolution are negligible; (v) food ingredient component diffusivity is constant; and (vi) perfect sink conditions are always attained in the release environment. Accordingly, model expression is given by the equation:

$$Q_t = K_H t^{(\frac{1}{2})}$$ Equation 14

Where Q_t is the amount of ethylvanillin released over time t, and K_H is the Higuchi dissolution constant. The plot made: cumulative % food component release vs. square root of time

2.6.5.5 Hixson-Crowell model

Hixson and Crowell (1931) recognized that the particles regular area is proportional to the cube root of its volume. They derived the equation:

$$Q_0^{\frac{1}{3}} - Q_t^{\frac{1}{3}} = K_{HC}\, t$$ Equation 15

Where Q_0 is the initial amount of the ethylvanillin in the nanoparticles, Q_t is the amount of ethylvanillin released in time t and K_{HC} is the release constant for Hixson-Crowell release. The plot made: cube root of food component % remaining in matrix vs. time

2.6.5.6 Ritger-Peppas model

Power law is a more comprehensive semi-empirical equation to describe food ingredient component release from polymeric systems. This model was developed by (Ilyasoglu & El, 2014; Ritger & Peppas, 1987) as a semi-empirical model, establishing the exponential relationship between the release and the time:

$$\frac{Q_t}{Q_\infty} = kt^n \qquad \text{Equation 16}$$

Where Q_t the amount of ethylvanillin released at time t, and Q_∞ is the amount of ethylvanillin released at infinite time (is the amount of ethylvanillin at the equilibrium state (sometimes very close to the amount of ethylvanillin contained in the dosage form at the beginning of the release process), thus $\frac{Q_t}{Q_\infty}$ is the fractional ethylvanillin release at time t, k is the release rate constant incorporating geometric and structural features of the nanoparticles, and n is the exponent of release (related to the food ingredient component release mechanism) in function of time t.

The power law model is useful for the study of release from polymeric systems when the release mechanism is not known or when more than one type of phenomenon of release is involved (Peppas, 1985; Peppas & Narasimhan, 2014). Actually, it can be seen as a generalization of the observation of the superposition of two apparently independent mechanisms of food ingredient component transport, relaxation, and diffusion. Depending on the value of n that better adjusts to the release profile of food ingredient component in a matrix system, it is possible to establish a classification, according to the type of observed behavior; Fickian model (Case I) and Non-Fickian models (Case II, Anomalous Case and Super Case II). In the Fickian model (Case I), n = 0.5 and the food ingredient component release are governed by diffusion. The solvent transport rate or diffusion is much greater than

the process of polymeric chain relaxation. Equilibrium of absorption in the surface exposed of the polymeric system takes place rapidly, leading to conditions of time-dependent links.

Table 1: Interpretation of release models of active agent from polymeric matrices with different geometries (Kosmidis et al., 2003 and Peppas, 1985)

Release mechanism model	**Geometry**	**Release exponent (n)**	**Time in function of n**
Fickian diffusion	Planar (thin films)	0.50	$t^{0.50}$
	Cylinders	0.45	$t^{0.45}$
	Spheres	0.43	$t^{0.43}$
Anomalous transport	Planar (thin films)	0.50 < n < 1.0	$t^{0.50<n<1.0}$
	Cylinders	0.45 < n < 0.89	$t^{0.45<n<0.89}$
	Spheres	0.43 < n < 0.85	$t^{0.43<n<0.85}$
Case I transport	Planar (thin films)	1.0	$t(^{a})$
	Cylinders	0.89	$t^{0.89}$
	Spheres	0.85	$t^{0.85}$
Super Case II transport	Planar (thin films)	n > 1	$t^{n>1}$
	Cylinders	n > 0.89	$t^{n>0.89}$
	Spheres	n > 0.85	$t^{n>0.85}$

a: Zero-order release.

The kinetics of this phenomenon is characterized by diffusivity. When n = 1, the model is non-Fickian (Case II), the release rate corresponds to zero-order release kinetics and the mechanism driving the food ingredient component release is the swelling or relaxation of polymeric chains.

This is another extreme type of behavior. Moreover, when $0.5 < n < 1$, the model is non-Fickian or anomalous transport, and the mechanism of food ingredient component release is governed by diffusion and swelling. The diffusion and swelling rates are comparable. The rearrangement of polymeric chains occurring slowly and the diffusion process simultaneously cause the time-dependent anomalous effects. Finally, the Super Case II model is characterized when $n > 1$, constituting an extreme form of transport. Table 1 summarizes this classification that constitutes very important information, because the different values of n are not always taken into account, leading to misinterpretations of experimental results.

To determine the exponent n, it is recommended to use the portion of release curve until the point where $\frac{Q_t}{Q_\infty} < 0.60$. In all cases, it is assumed that the release occurs in just one direction and that the relationship between the width and thickness of the matrix is a maximum of 1:10 (Peppas, 1985).

2.7 Summary

The technique of EHD spraying has emerged as a promising technique to prepare nanoparticles with encapsulated and/ or entrapped food ingredient component which may be released as the nanoparticle. The morphology and size of the particles prepared are of dominant importance to enable reproducibility and appropriate efficacy of the system. This chapter has described the several parameters and interplays of the processing parameters which affect the production of EHD sprayed particles and have highlighted the shortfalls

associated with many current techniques. Importantly it has also emphasized the essential to thoroughly evaluate and the release profiles, availabilities of the entrapped and and/or encapsulated food ingredient component. Only when all of these concerns are well tackled can a delivery system for the use in targeted food ingredient delivery.

Chapter 3 Materials and Experimental Methods

3.1 Introduction

This introduces and describes the materials and experimental methods used to obtain the results in this thesis. For each of the materials and method details of the supplier and product are given and the methods are explained. The first section comprises an overview of the materials used and explains some of the properties and common application of the materials. Further, the section explains criteria for the food ingredient components, polymer and lipid used. The second section introduces and explains the methodology used for all preparative and analytical work. A brief theoretical background is also provided for most of the analytical methods used. The following section describes the preparation of nanoparticles. The last section describes in-vitro release experiment e.g. determination of food ingredient component encapsulation efficiency and loading capacity and release rate.

3.2 Materials

The main materials used in this project are the model food ingredient components vanillin (VA), ethylvanillin (EV), ethylmaltol (EMA), and maltol (MA). The encapsulating materials were stearic acid (SA) and ethylcellulose (EC) in powder form. 95% (vol) ethanol or doubled distilled water (DDW) was used as a solvent. All materials were purchased from Sigma-Aldrich (Poole, Dorset, UK).

3.2.1 Lipid - Stearic acid

The fatty acid nature of the saturated 14, 16 and 18 - carbon chain (e.g. stearic acid) (Table 2), butterfat, and palmitic acid) at normal human body temperature is commonly used in selecting the lipid matrix to prepare lipid nanoparticles (Bocca et al., 1998; Cavalli et al.,

1997; Gasco et al., 1992; Mehnert & Mader, 2001; Zhang et al., 2000). These form the bulk of fatty acid in animal body tissue (Bruss, 1997).

Table 2: Stearic acid chemical structure and component properties.

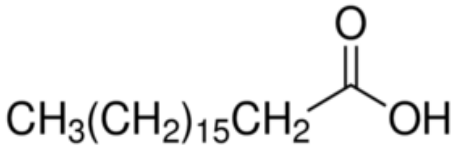	
Properties	
Chemical formula	$C_{18}H_{36}O_2$
Molar mass	284.48 g·mol^{-1}
Density	0.9408 g/cm^3 (20 °C) 0.847 g/cm^3 (70 °C)
Melting point	69.3 °C (156.7 °F; 342.4 K)
Boiling point	361 °C (682 °F; 634 K) decomposes 232 °C (450 °F; 505 K) at 15 mmHg
Solubility in water	0.003 g/L (20 °C) 0.34 g/L (25 °C) 1 g/L (37 °C)
Solubility in ethanol	0.9 g/100 mL (10 °C) 2 g/100 mL (20 °C) 4.5 g/100 mL (30 °C) 13.8 g/100 mL (40 °C)

Nanocarriers prepared using SA are approved by regulatory authorities and hence their application for the delivery of food ingredient is acceptable. Furthermore, SA is known to have a neutral effect on the plasma lipid profile as it is rapidly converted to oleic acid within the body (Bonanome et al., 1992) and it does not increase plasma cholesterol concentration like other saturated fatty acids (Hegsted et al., 1965).

SA has been chosen as the carrier material owing to its excellent entrapment efficiency, biocompatibility and low toxicity (Phadke et al., 1994). Due to its hydrophobic nature, SA reduces flavour dissolution and flavour release when included in the formulation, and slows the release kinetics at higher SA levels (Dave et al., 2004), thus to develop an attractive opportunity to develop food ingredient component delivery method.

3.2.2 Polymer - Ethylcellulose

Ethylcellulose (EC), a derivative from cellulose etherification, is soluble in a wide variety of solvents, such as esters, aromatic hydrocarbons, alcohols, ketones, and chlorinated solvent. The solubility paramter range varies with the degree of substituation of the hydroxyl group in the polymeric cellulosic backbone with the ethosyl groups. Solution of EC in aromatic hydrocarbons are highly viscous; whereas solvent like ethanol yelid solutions having low viscosity (Rekhi and Jambhekar, 1995).

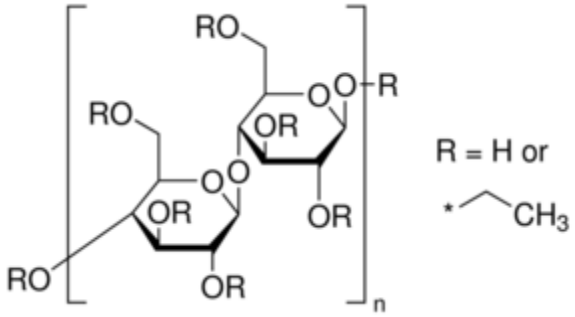

Figure 8: Chemical structure of ethyl cellulose. R = H or C_2H_5 depending on degree of substitution. EC sample in this work have 48% ethoxyl substation.

Ethyl cellulose is one of the most commonly used polymers in coating because of the various advantages it offers to formulations, such as film forming, minimum toxicity, excellent physical and chemical stability (Rao & Murthy, 2002). EC was chosen as the primary polymer to illustrate this method due to its long history in fiber manufacturing (Cuculo, Aminuddin, & Frey, 2000), abundant availability, biocompatibility and its increasing application in the food engineering industry (Ahmad, Gunduz, et al., 2012). EC is commonly used as an emulsifier, thickening agent and dietary fiber in food products primarily due to its cost effectiveness. In addition, these properties also make EC useful in a wide range of other biotechnology fields such as biomedical applications and filtration (Kim, Kim, Kang, Marquez, & Joo, 2006). Other varieties of cellulose are also gaining interest in the food sector. The material is expected to play a major role as a food additive, in food packaging, and in the preparation of composite materials (Chang, Chen, Lin, & Chen, 2012).

3.2.3 Solvent - Ethanol

Ethanol (C_2H_5OH) is a common organic solvent that is widely used in chemistry, biochemistry, and molecular biology. In our research general purpose research grade ethanol (99%) was purchased from Sigma Aldrich (Poole, UK) and had the following physical properties; density: 789 kg m^{-3}, molecular weight: 46 g mol^{-1}, viscosity: 1.3 mPa s, boiling point: 78 °C.

The electrical conductivity of the solvent has a direct influence on the size of the particle produced. The solvent, with a higher dielectric constant results in smaller sized particle (Xie

et al., 2006a). Therefore, ethanol having a large dielectric constant 24.3 at (~25^{o}C) is likely to produce small particles.

3.2.4 Food ingredient component

Most flavour compounds are chemically unstable and highly volatile as a result of chemical interactions, oxidation and volatilisation. Hence, encapsulation of flavour compounds is essential to stabilise them and initiate their release when required (Al-Omran et al., 2002; Choi et al., 2009; Madene et al., 2006). To test these hypotheses, ethylvanillin, Vanillin, ethylmaltol, and Maltol (Table 3), widely used in food industry, were selected as a model hydrophilic component for encapsulation in the polymer, lipid, and polymer-lipid hybrid nanoparticles.

3.2.4.1 Vanillin

Vanillin is a white crystalline material melting at about 81 ^{o}C. The purity is generally above 99.0% w/w on dried basis. In vanillin obtained from guaiacol, ethyl vanillin can be an impurity comprising up to 250 ppm. Calcium stearate is occasionally added (0.5%) to improve flow-ability. Vanillin has a characteristic pleasant smell and taste of vanilla which is the reason for its widespread use. Vanillin has a vapour pressure of 0.33 Pa and saturated air has a concentration of 0.00029 % at 25 ^{o}C, corresponding to 18.0 mg/m3. Vanillin is soluble in water and solubility increases with increasing temperature.

At 25 ^{o}C the solubility is 10 g/l. Log Pow value ranges from 1.21 to 1.35 (calculated and measured) indicating that vanillin is unlikely to bioaccumulate. The pH of a 5 % solution of vanillin in water is 4.3. The phenol group of vanillin has a pKa value of 7.38. With increasing pH the molecule will loose a proton, become negatively charged and more soluble in water.

Table 3: Food flavour component chemical structure and component properties.

Ethylvanillin	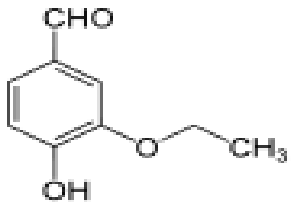	**Vanillin**	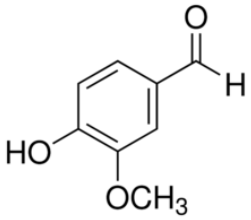
Ethylmaltol	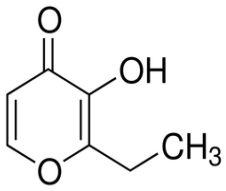	Maltol	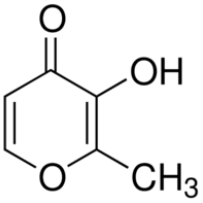

Properties				
	Vanillin	**Ethyl vanillin**	**Maltol**	**Ethylmaltol**
Molecular formula	$C_8H_8O_3$	$C_9H_{10}O_3$	$C_6H_6O_3$	$C_7H_8O_3$
Molar mass	152.15 g mol^{-1}	166.17 g mol^{-1}	126.11 g mol^{-1}	140.14 g mol^{-1}
Density	1056 kg m^{-3}	1186 kg m^{-3}	1348 kg m^{-3}	1261 kg m^{-3}
Melting point	81 to 83 °C; 178 to 181 °F; 354 to 356 K	76 °C (169 °F; 349 K)	161 to 162 °C (322 to 324 °F; 434 to 435 K)	85–95 °C (185 to 203 °F; 358 to 368 K)
Boiling point	285 °C (545 °F; 558 K)	295.1 °C (563.2 °F; 568.2 K)	284.70 °C (544.46°F; 556K)	161 °C (322 °F; 434 K)
Solubility in water	10 gm ml^{-3}	20 gm ml^{-3}	10 gm ml^{-3}	20 gm ml^{-3}
Ethanol	50mg ml^{-1}	50mg ml^{-1}	40mg ml^{-1}	50mg ml^{-1}

3.2.4.2 Ethylvanillin

Ethyl vanillin is a chemically synthesized flavoring agent related to vanillin or artificial vanilla. Natural vanilla extract is very complex, consisting of hundreds of compounds, while ethyl vanillin consists of just one compound. Nevertheless, it gives off an aroma very similar to that of vanilla. Ethylvanillin is used as a model hydrophilic food ingredient component, wide used on in food and cosmetic, pharmaceutical industries (Manojlovic et al., 2008).

Ethyl vanillin has a much stronger flavour than natural vanilla, however, so it is less expensive to use in large-scale food production. It is also easier to preserve than vanilla extract. Ethyl vanillin is used in chocolate, maple syrup, ice cream, and beverages, and is actually utilised in many fragrances as well. Ethyl vanillin is a very important raw material for a myriad of fragrance compounds and other additives. It is found in cosmetics, deodorant, and perfume. It is also used in the electroplating industry (which involves coating the surface of a conducting material with a metal), and as a brightener to whiten paper and fabric. Ethyl vanillin is safe to use in small quantities as it is used for imparting flavour to foods. Long term studies with mice have shown that ethyl vanillin does not cause cancer. Furthermore, ethylvanillin is the synthetic analog of vanillin, and natural vanillin has been shown to have some anti-oxidant effects in laboratory experiments.

3.2.4.3 Maltol

Maltol is a naturally occurring organic compound that is used primarily as a flavour enhancer. It is found in the bark of larch tree, in pine needles, and in roasted malt (from which it gets its name). It is a white crystalline powder that is soluble in hot water, chloroform, and other polar solvents. Because it has the odor of cotton candy and caramel, maltol is used to impart a sweet aroma to fragrances. Maltol's sweetness adds to the odor of

freshly baked bread, and is used as a flavour enhancer in breads and cakes. It is registered as a flavour component in the EU.

3.2.4.4 Ethylmaltol

Ethylmaltol is an organic compound that is a common flavourant in some confectioneries. It is related to the more common flavorant maltol by replacement of the methyl group by an ethyl group. It is a white solid with a sweet smell that can be described as caramelized sugar and cooked fruit. The conjugate base derived from ethylmaltol, again like maltol, has a high affinity for iron, forming a red coordination complex. In such compounds, the heterocycle is a bidentate ligand.

3.3 Preparation of the solution

Encapsulated materials (e.g. pure SA, pure EC, and SA and EC) were dissolved in ethanol using a magnetic stirrer in different concentrations (1–5 mg/ml). To each of these spraying solutions was added (1-5 mg/ml) of food ingredient component (e.g. EV, VA, EM, and MA) and stirred again until a clear solution was obtained. All the spraying solutions with and without food ingredient component were characterised by measuring properties such as surface tension, viscosity and density at the ambient temperature 25±2 °C.

3.4 Characterisation of solvents and solutions

The solutions were characterised for their density, surface tension, viscosity, electrical conductivity at a temperature of 25±2°C, ambient pressure (101.3 kPa) and a relative humidity of 45-60%. Surface tension was determined using (plate method) a Kruss tensiometer (Model-K9, Kruss GmbH, Germany), viscosity was measured using a U-tube viscometer (75 ml Cannon-Fenske Routine Viscometer, Cannon Instruments, USA) and

electrical conductivity using a Jenway 3540 conductivity meter (Bibby Scientific Limited, Staffordshire, UK).. Both the viscometer and tensiometer were standardized and calibrated before measurement using ethanol and distilled water. The densities of the solutions were measured using the well-established standard 25 ml density bottle method (VWR, Lutterworth, UK).

3.4.1 Density

The density of the solutions used in the experiments was measured using a 25 ml standard density bottle (VWR International, Lutterworth, UK). An electronic balance (AND HF-1200G A&D Instruments Ltd., Japan) was used to measure the mass of the empty density bottle and the mass of the bottle filled with solution. The density value of each solution was measured five times and the mean value and standard deviation were calculated. The density ρ (kg m^{-3}) was obtained each time.

3.4.2 Surface tension

Using a Kruss Tensiometer K9, the surface tension of the solutions (standard Wilhelm's plate method) was measured. Each solution was added to a 20 ml tall glass container (beaker) and it was placed at the tensiometer platform. Then, the rectangular shape plate was hung from the tensiometer hook and the tensiometer was calibrated before use (set to zero). The edge of the plate was moved at the surface of the solution in such a way that a meniscus could be formed between the liquid and the plate due to the surface tension force of the liquid. The plate was then steadily lifted and the surface tension value was taken when the plate was just about to detach from the liquid surface. The process was repeated five times for each solution in order to minimize errors and the average value and standard deviation of the surface tension was calculated. The plate was thoroughly cleaned after every measurement.

3.4.3 Viscosity

The viscosity of the solution was determined using a U-Tube glass viscometer (BS/U type, VWR International Ltd, Lutterworth, UK). In order to calculate the viscosity with a U-Tube viscometer, ethanol or acetone was infused into it in order to clean it. Then, the time taken for a standard volume of distilled water to pass through the U-tube capillary was noted for five passes and the mean time value was calculated. The experiment was repeated with other solutions five times by following the same procedure as water. The viscosity mean value was obtained for each solution

3.4.4 Electrical conductivity

The electrical conductivity of the solutions was determined using a Jenway 3540 conductivity meter (Bibby Scientific Limited, Staffordshire, UK). All the instruments were calibrated before use according to the manufacturer's instructions. The conductivity electrodes were always cleaned with acetone or ethanol to remove any excess solutions or liquids that remained in the probes. The probe was also rinsed with distilled water, after cleaning with ethanol, and dried before measurements. The electrodes were kept immersed in the solutions for 10 min and the electrical conductivity values shown on the meter were recorded. The mean values of three consecutive readings for conductivity were taken.

3.4.5 Solubility studies

Solubility of nanocarriers materials (e.g. polymer or /and lipid) and food ingredient component in ethanol were measured by adding the solutes little by little into a container with 10 ml of ethanol while continuously stirring until the solution reached the cloud point was reached or the solutions began precipitating out. The solutions were occasionally heated slightly using a hot plate to aid the dissolution process.

3.5 Preparation of nanoparticles

Nanoparticles were prepared using a single-needle EHD spraying setup as shown in Figure 1. The spraying system consisted of a high voltage electrical power source (Glassman Europe Ltd., Tadley, UK), with a mechanical syringe pump (PHD 4400, Harvard Apparatus, Edenbridge, UK) with high precision and adjustable flow rate, a stainless steel needle set into an epoxy resin and connected to the high voltage supply. The inner and outer diameters of needle were 450 µm and 870 µm, respectively.

The polymeric solutions containing the food ingredient components, were loaded into a 10 ml plastic syringe (BD Plastic, Sunderland, UK). This syringe was mounted on the Harvard syringe pump and was connected to the stainless steel needle at one end via silicone tubing. The syringe pump controlled the flow rate of spraying solution into the needle. A video camera with an in-built magnifying lens (Leica S6D JVC-color) was used to observe the needle tip at all times during collection of nanoparticles in order to understand the spraying behaviour on the application of applied voltage.

The system operating parameters e.g. flow rate, collection distance and voltage, were used to control nanoparticle formation. The nanoparticles were only collected at the applied voltages which furnished a stable cone-jet. The nanoparticles generated from the jet were collected onto a microscopic slide containing distilled water. The particles were then left to dry in a desiccator under vacuum.

All five samples were sprayed at varying flow rate (10 - 25 µl/min), with the collection distance kept between 100-150 mm from the needle end and with the applied voltages between 0-20 kV. All the experiments were repeated three times.

3.6 Particle characterisation

3.6.1 Size diameter and surface morphology

3.6.1.1 Scanning electron microscope

The nanoparticles diameter and surface morphology were studied using the JEOL JSM-6301F field emission scanning electron microscope (SEM). JEOL JSM-6301F is equipped with an emitter that can achieve a resolution of ~1.5 nm. The samples were collected in glass slides or glass containers and then left to dry under ambient conditions for 72 hours. Then, they were vacuum-coated with gold at 40 mA for 120s using a sputtering machine (Edwards sputter coater S1 50B), prior to observation. SEM images were obtained at 3 and 5 kV acceleration voltage. The average nanoparticle size was determined, using ImageJ software (National Institutes of Health NIH, Maryland, USA) from ~300 particles for each set of processing conditions.

3.6.2 Nanoparticles inner structure

3.6.2.1 Transmission electron microscopy

Transmission electron microscopy (TEM) is transmitting a beam of electrons through an ultra-thin specimen, interacting with the nanoparticles as it passes through. TEMs are capable of imaging at a higher resolution than optical microscope, due to the small de Broglie wavelength of electrons. TEMs at high magnification can also distinguish between two or more materials due to the material composition and the different absorption of electrons and in each material (the information mentioned, were obtained from the TEM instruction manual).

In the experiments, Transmission electron microscopy (TEM) images of the nanoparticles were also obtained (JEOL-1010 TEM, Tokyo, Japan) at an accelerating voltage of 80

kV. One millilitre of the nanoparticle solution was spread onto a copper grid for observation. The nanoparticle samples were then stained with a 2% solution of uranyl acetate for 30 seconds and allowed to dry. Samples of EHD sprayed nanoparticles were also placed in a tube, containing 10 ml of DDW at ambient room temperature for 90 days, and then observed again using TEM.

3.6.3 Physical form of nanoparticle

3.6.3.1 Fourier transform infrared (FTIR) spectroscopy analysis

The chemical structure of obtained nanoparticle was characterised by Fourier Transform Infrared Spectrometer (FT-IR). FT-IR spectra were measured using Perkin-Elmer, 2000 FT-IR spectrometer, UK. 2mg powdered samples of nanoparticles with and without food ingredient components, were individually mixed with Potassium bromide (KBr) and pelletised using a hydraulic press. Potassium bromide being transparent to IR furnished spectra for each of the component studied. The spectra were recorded in the range of 400–4000 cm^{-1}. The FT-IR spectra were obtained by averaging 256 scans at a resolution of 1 cm^{-1}. Samples of EHD sprayed nanoparticles were stored dry for 90 days at the ambient temperature (25±2 ^{O}C), and then observed again using FTIR.

3.6.3.2 Differential scanning calorimetry

Differential scanning calorimetry (DSC) is a thermoanalytical technique in which the difference in the amount of heat required to increase the temperature of a sample and reference is measured as a function of temperature. Both the sample and reference are maintained at nearly the same temperature throughout the experiment. Generally, the temperature program for a DSC analysis is designed such that the sample holder temperature increases linearly as a function of time. The reference sample should have a well-defined heat

capacity over the range of temperatures to be scanned. DSC was performed on samples of nanoparticles with and without food ingredient components to determine whether there were any interactions with the core-shell components.

In order to determine the phase transition temperatures of the nanoparticles with and without food ingredient components, (10–20 mg) dried samples of nanoparticles with and without food ingredient components were placed in open aluminum pans. A reference pan was filled with 100 µl of distilled water to increase the sensitivity of the measurements (Li et al., 2002; Zheng et al., 2004).

The pans were then thermally scanned over a temperature range of 20-300 ^{O}C at 10 ^{O}C/min heating rate using a Netzsch STA 449C Jupiter Calorimeter (NETZSCH, Germany), under helium purge, then allowed to cool down to 20 ^{O}C to observe exothermic and recrystallisation phenomena. Melting endotherm, and temperature (^{O}C) data were generated using Universal analysis *Proteus* software (NETZSCH, Germany).

3.6.3.3 X-ray diffraction

X-ray diffraction (XRD analysis or XRPD analysis) is a unique method in determination of crystallinity of a compound. XRD analysis is based on constructive interference of monochromatic X-rays and a crystalline sample: The X-rays are generated by a cathode ray tube, filtered to produce monochromatic radiation, collimated to concentrate, and directed toward the sample. The interaction of the incident rays with the sample produces constructive interference (and a diffracted ray) when conditions satisfy Bragg's Law ($n\lambda=2d \sin \theta$). This law relates the wavelength of electromagnetic radiation to the diffraction angle and the lattice spacing in a crystalline sample.

The characteristic x-ray diffraction pattern generated in a typical XRD analysis provides a unique "fingerprint" of the crystals present in the sample. When properly interpreted, by comparison with standard reference patterns and measurements, this fingerprint allows identification of the crystalline form.

The powder X-ray diffraction pattern of nanoparticle sample was determined using Thermo-ARL Xtra; Thermo Scientific diffractometer using Cu Kα1 radiation (λ = 1.542Å). The generator voltage was set at 40 kV and the current at 30 mA. The nanoparticle sample was scanned over the 2θ angular range 3°–40° with a step size of 0.02° and a scanning speed of 4° min^{-1}.

3.6.4 Component physical stability

Physical stability was studied by placing samples prepared using EHD spray in a dessicator at ambient temperature for 90 days and then examining them using FTIR to observed changes in their physical.

3.7 Component detection

3.7.1 UV spectroscopy

The UV spectroscopy was used in our experiments to obtain the food ingredient component release profiles of the food components. In order to measure the food components (e.g. ethylvanillin) concentration in the samples, ultra-violet wavelength light in the region of 200 – 400 nm is transmitted by the UV spectrophotometer through it. The light absorbance observed at a specific wavelength due to the ethylvanillin composition is directly related to the concentration of ethylvanillin in the sample. When the ethylvanillin concentration is sufficiently low in the solution, a linear relationship between the absorbance and

concentration of ethylvanillin in the solution exists and is given by the Beer-Lambert law (Parnis & Oldham, 2013) (Equation 17).

$$A = \varepsilon \times \ell \times c \qquad \text{Equation 17}$$

where A is the absorbance (no units, $A = \log_{10} \frac{P_o}{P}$) P: the intensity of transmitted light, P_o: the incident intensity, ε the attenuation coefficient (L mol^{-1} m^{-1}), ℓ the distance the light travels through the material (m) and c the concentration of food ingredient component (mol l^{-1}). To calculate the food ingredient component release and the experimental entrapment efficiency of food component (e.g. ethylvanillin) in the dressing nanoparticles samples, a calibration curve was prepared and used for finding the linear relationship between the absorbance and the food component (e.g. ethylvanillin) concentration. In our experiments the UV spectroscopy measurements were carried out using a Perkin Elmer Lambda 35 UV-vis spectrophotometer (Cambridge, UK) in the wavelength region 200 - 400 nm for a period of 15 hours. Calibration curves were prepared for the concentration range 0.001 - 0.5 mg/ml (1 - 50 ppm) of food component (e.g. ethylvanillin) dissolved in distilled water. Although food component (e.g. ethylvanillin) absorbs light also at a wavelength of 278 nm was chosen as the reference wavelength for the experiments because it has a higher extinction coefficient and thus a much stronger and clearer absorbance signal could be achieved from the UV spectrophotometer. Furthermore, the UV spectra of distilled water were compensated for in the data analysis. All the measurements were repeated three times.

3.7.2 Loading capacity, encapsulation efficiency and burst

The encapsulation efficiency was determined according to the method verified previously by Eltayeb *et al*. (Eltayeb et al., 2013b). Nanoparticles were produced with varying concentrations of nanocarrier materials (between 1-5%) and food ingredient component

(between 1-2.5 %wt) at a flow rate of 10 – 25 µl min^{-1} and applied voltage of 10 -19kV. Following collection in DDW, the resulting nanoparticle suspension was centrifuged (B4i Centrifuge, Jouan, ST. Herblain, France) at 4000 rpm for 10 min at 25±2 °C. The total amount of food ingredient component in the liquid was investigated by dispersing the nanoparticles in 10 ml of DDW and examining using UV spectrophotometry (Perkin Elmer, Lambda 35, UV/ Vis spectrophotometer, Waltham, USA) before and after filtering through 200nm syringe filters.

The amount of food ingredient component encapsulated in the nanoparticles was calculated by subtracting the amount of food ingredient component in the DDW from the total amount of the food ingredient component in the nanoparticle solution. Encapsulation efficiency (EE) and loading capacity (LC) were determined according to equations (Equation 7 and Equation 10) and (Equation 8 and Equation 9) respectively.

3.8 *In vitro* release experiment

The aim of this study was to assess the in vitro release kinetics of nanoparticles were prepared using EHD techniques. The release of the encapsulated food ingredient components from the nanoparticles inserted into 3 different media was determined via UV spectroscopy.

3.8.1 Release rate

In this study, samples (1 ml) of food ingredient component loaded nanoparticles were collected in tubes, containing 10 ml of DDW. The amount of food ingredient component released was obtained by UV–spectrometry, as described above. Release studies were conducted over 15 hours and repeated five times for each set of nanoparticles and the results combined to obtain the cumulative food ingredient component release rate, which was plotted as a function of time.

3.8.2 Release rate models

The objective of this study is to review the spectrum of mathematical models that have been developed to describe food ingredient component release from nanoparticles. The major advantages of these models are: (i) the elucidation of the underlying mass transport mechanisms; and (ii) the possibility to predict the effect of the nanoparticles design parameters (e.g., shape, size and composition of nanoparticles) on the resulting food ingredient component release rate, thus facilitating the development of new food engineering products. The choice of the appropriate mathematical model when developing new food products or elucidating food ingredient component release mechanisms strongly depends on the desired or required predictive ability and accuracy of the model. To determine the appropriate mathematical model, the food ingredient component release rate profile data was fitted using Higuchi, zero-order, Hixson-Crowell, first-order, and Ritger-Peppas models, respectively (Higuchi, 1963; Ritger & Peppas, 1987; Sezer et al., 2011) and release equations are given in section 2.6.5.

Chapter 4 Preparation, Characterisation and Release Kinetics of Ethylcellulose Nanoparticles Encapsulating Food Flavour

4.1 Introduction

Food grade polymeric nanoparticles have the potential to play a key role in the future of food component delivery which is an essential characteristic of functional foods. For this potential to be realized, it is important to study both the loading and release characteristics of the encapsulated material from the particle matrix as a function of particle size, material properties and processing conditions. In this chapter, ethylcellulose nanoparticles encapsulating ethylvanillin as a model food component were prepared by EHD processing.

In this chapter, aim was to use EHD processing to prepare polymeric nanoparticles, ≤100 nm in diameter, encapsulating a food component and to study their release characteristics. Ethylcellulose (EC) was used as a model hydrophobic polymer since it has been approved and accepted by both the United States Food and Drug Administration (FDA) and the European Union (EU) for food, cosmetic and pharmaceutical applications.

Investigated the different polymer concentrations for which a stable cone-jet could be obtained during EHD processing; and by tuning the operating parameters (flow rate and applied voltage), EV encapsulating nanoparticle populations with varying mean size (≤100 nm) and size distributions were obtained. EV release was expected to occur through two different processes: "burst" release of EV encapsulated near the surface of the EC nanoparticle due to hydration (Freiberg & Zhu, 2004); and slower release from the polymer matrix as it degrades. The release profiles can be influenced by the properties of the polymer (e.g. molecular weight), its concentration, the nature of the loaded food component, its concentration and distribution and the nanoparticle size distribution (Freiberg & Zhu, 2004).

These in turn may be controlled by the EHD operating parameters. Smaller particles typically give rise to higher release rates, due to the higher surface area to volume ratio and hence more rapid penetration by water.

4.2 Preparation of polymer nanoparticle

Appropriate quantities of EC were dissolved in ethanol using a magnetic stirrer to obtain solutions with concentrations of 2.5, 5.0, 7.5, and 10 (w%). EV was added to each of these polymeric solutions to obtain concentrations of 1, 2.5 or 5 (w%); followed by further stirring until a clear solution was obtained.

Table 4: List of solution compositions from which nanoparticles were prepared

Formulation	**Polymer concentration (wt%)**	**Food component loading (wt%)**	**Flow rate (µl min^{-1})**
P1	10.0	1.0	25
P2	10.0	1.0	20
P3	10.0	1.0	15
P4	10.0	2.5	15
P5	7.5	5.0	15
P6	7.5	1.0	15
P7	10	5.0	15
P8	5.0	1.0	15
P9	7.5	2.5	15
P10	2.5	1.0	15

Optimisation of the operating parameters and formulation with regard to their influence on nanoparticle physical properties and food component release rate was carried out prior to this

work (Eltayeb et al., 2013a; 2013b) and the operating parameters for this study (e.g. polymer concentration, food component and flow rate) selected accordingly as detailed in the (Table 4).

The applied voltage and distance between the needle tip and collector were adjusted in order to obtain a stable cone jet. A series of EV loaded nanoparticle samples were successfully prepared with various EC concentrations under different EHD processing conditions. The EHD jetting mode is a function of the applied electrical potential difference (Jaworek, 2008).

In this study a stable cone-jet was established over a range of liquid flow rates from 15 to 25 µl min^{-1} and applied voltages from 13.6 to 14.5 kV. This was found to be necessary for forming uniform nanoparticles. With increasing polymer concentration, the voltage required to generate nanoparticles increased and eventually the jet became unstable. (Enayati et al., 2010).

4.2.1 Influence of polymer concentration

Polymer concentration plays an important role in the entanglement regime which dictates particle or fiber formation and is an essential parameter to control in order to optimize the process. It is known that the polymer concentration will affect the surface tension, viscosity, and electrical conductivity of the liquid phase, all of which will in turn affect the EHD process (Xu & Hanna, 2008).

An increased conductivity of a solution implies that more charge is carried by the electrospraying jet. In general, a low electrical conductivity is preferred to obtain quasi-monodisperse particles, since a higher conductivity may favor elongated particles or even fibers if the polymer concentration is high enough. Correlating with viscosity, stable electrospraying is known to be achieved only when viscosity is high or conductivity is low.

For instance the initial studies were carried out to optimise the EC concentration, and it was found that the surface tension and viscosity of the solution increased with polymer concentration (Figure 9a) which increases the mean nanoparticle size (Doshi & Reneker, 1995). This was explained by the low diffusion rate of EC chains where a shell of solid EC would form on the surface of the droplets. For lower polymer concentrations in the 2.5 – 5% range, the shell would be thinner but a similar overall size would be obtained, while for concentrations 7.5 - 10% a high polymer concentration was established on the surface of the droplet with less solvent evaporation, resulting in a larger final particle size. All these results underline the strong effect and inter-dependence of flow rate coupled with concentration on particle size. In addition, the electrical conductivity of the solutions decreased noticeably with increasing EC concentration (Figure 9b), which again increases nanoparticle size.

4.3 Polymer nanoparticle characterisation

The diameter of the polymer nanoparticles ranged between 10 and 90 nm depending on the operating conditions. The corresponding size distributions were relatively narrow with a polydispersity index (expressed as the relative standard deviation to the average size of one formulation) ranging between 17 and 34% (see Table 5). Figure 10b (1–3) further demonstrates how nanoparticle size was a function of the both the EC concentration and operating conditions.

4.3.1 Influence of flow rate influence

After the selection of polymer solutions, flow rate is arguably the second most important parameter in electrospraying and together with the solution parameters (concentration and conductivity) can control polymer entanglements and Coulomb fission.

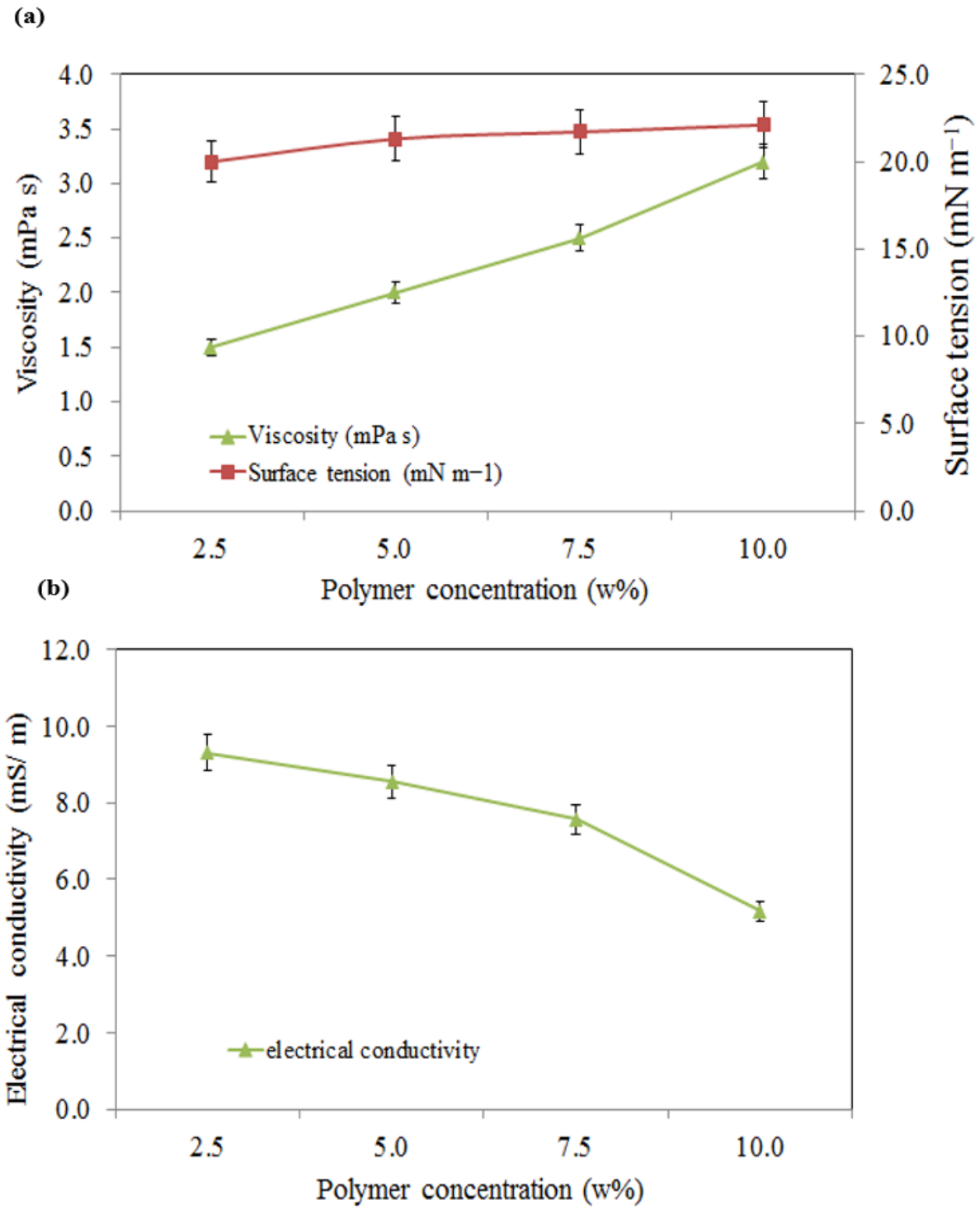

Figure 9: (a) Effect of EC concentration on surface tension, and viscosity of solution. (b) Relationship between concentration and electrical conductivity of EC solution. Error bars indicate standard deviation from the mean.

Flow rate thus has consequences for both the morphology and size of particles and must be judiciously chosen since both these characteristics will influence the food ingredient component dispersion within the polymer matrix, ultimately affecting food ingredient component release.

The size of electrosprayed polymer particles is greatly influenced by flow rate and polymer concentration, where increased particle sizes are most significantly obtained with an increase in flow rate and polymer concentration and a decrease in conductivity ((Figure 10).

Particle size is directly proportional to droplet size, where an increase in size is obtained with increasing flow rate and decreasing surface tension, and is shown to correspond to an increase in polymer content (Figure 10 (a1)). However, as stated earlier, an increase in flow rate is also responsible for broader size distributions (Figure 10 (b1)), thus a compromise needs to be made between particle size and polydispersity. For instance with an increase in flow rate from 10 to 25 µl min^{-1} the nanoparticle mean size increased by 19% (Figure 10 (a1)) and the polydispersity index also increased (Figure 10 (b1)). This result is consistent with previous studies (Eltayeb et al., 2013a; Jaworek & Sobczyk, 2008).

4.3.2 Influence of polymer concentration

Nanoparticle size also increased with polymer concentration (Figure 10 (a2)) and this is most likely as a direct result of the increase in viscosity (Figure 10(b2)) (Jaworek & Sobczyk, 2008; Rohner et al., 2004).

4.3.3 Influence of ethylvanillin concentration

Increasing the EV concentration reduced the nanoparticle mean size (Figure 10 (a3)). This may be explained by the reduction in electrical conductivity of the liquid (Figure 10 (b3).

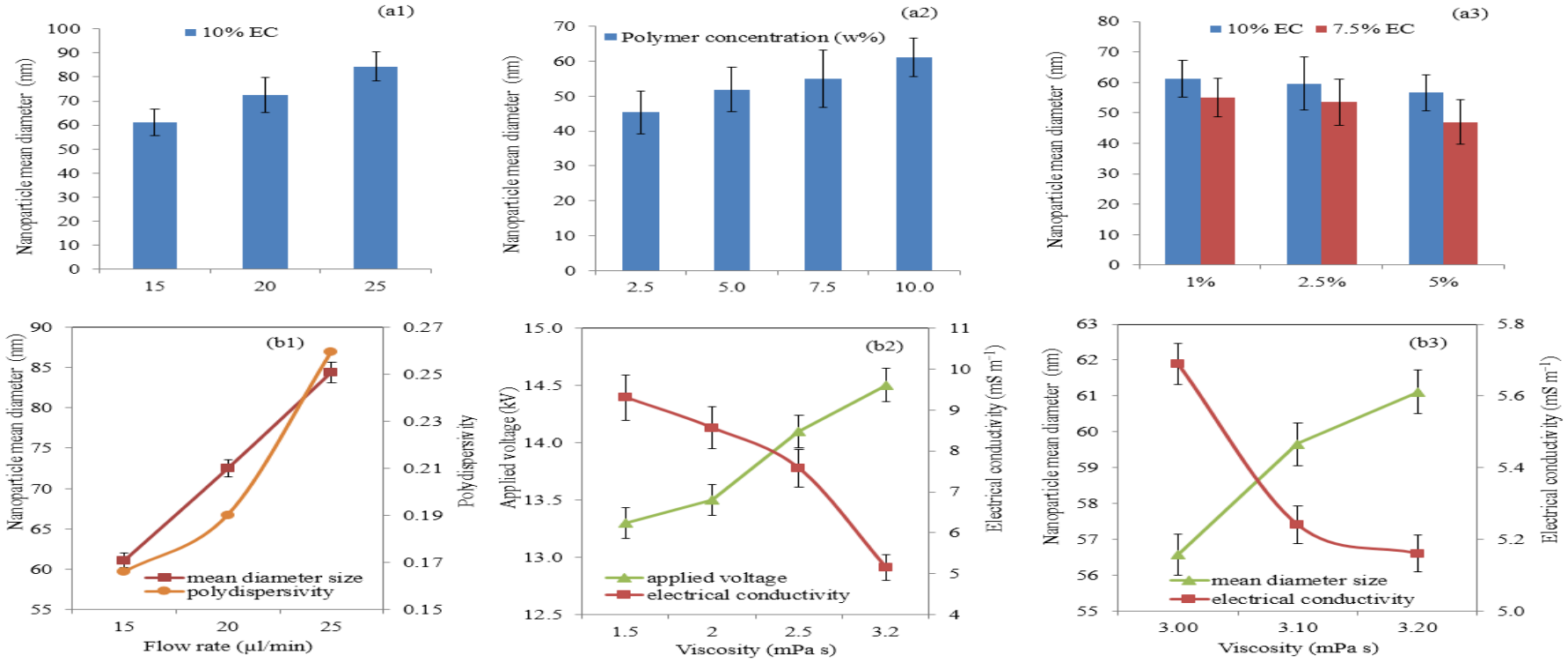

Figure 10: Mean diameter of nanoparticles prepared at different: (a1) flow rates, (*a2*) polymer loading and (*a3*) food component concentrations. (b1) Mean diameter and polydispersity of nanoparticles prepared at different flow rates. (b2) Effect of solution electrical conductivity and viscosity on applied voltage, of formulations P3, P6, P8, and P10. (b3) Effect of solution electrical conductivity and viscosity on nanoparticle mean diameter, for particles from solutions P3, P4, and P7 (see Table 4). Error bars indicate standard deviation from the mean. $n \approx 300$ nanoparticles. Error bars indicate standard deviation from the mean.

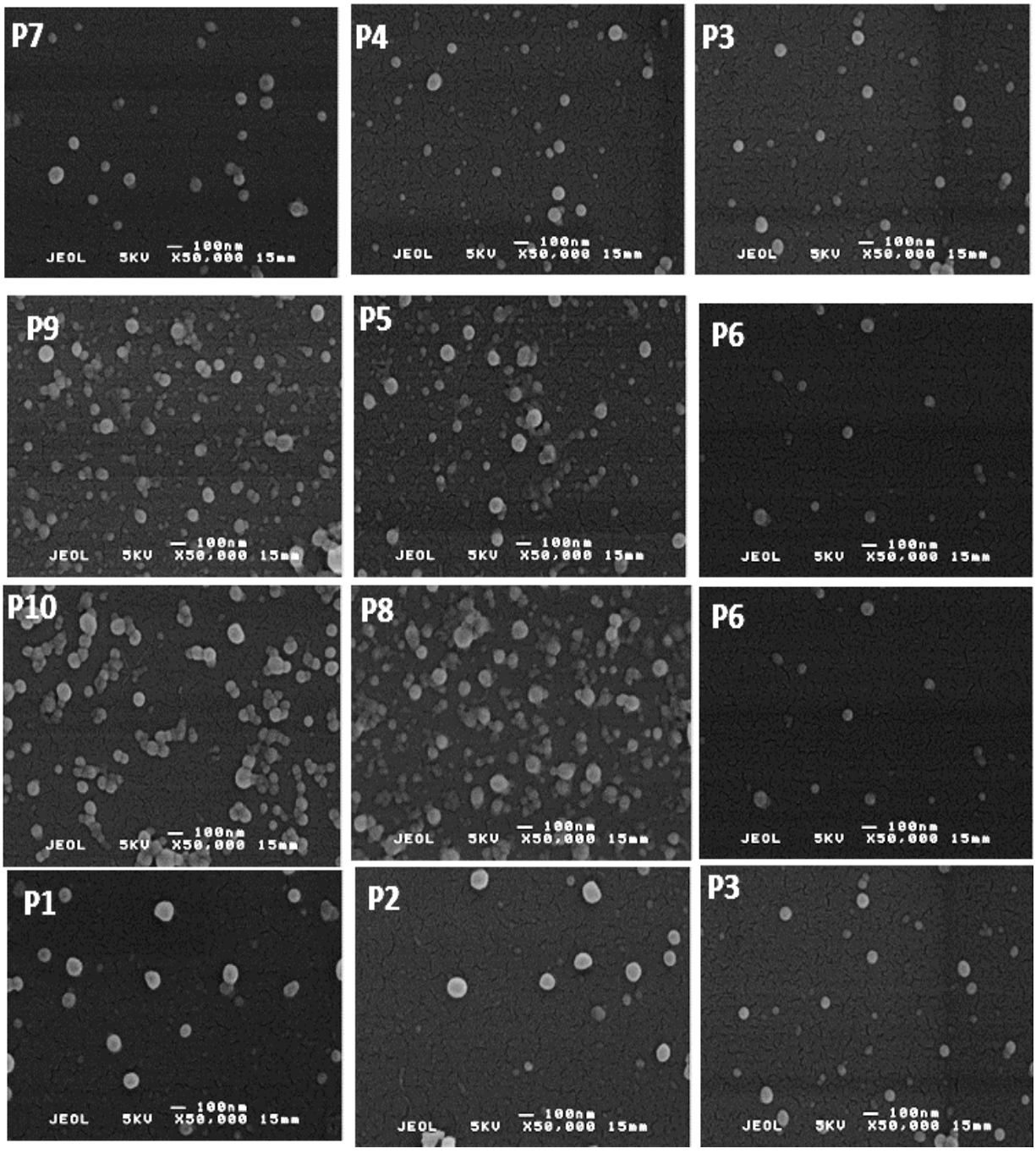

Figure 11: Scanning electron microscopy images of nanoparticles obtained from each solution in Table 4.

The effect was less pronounced however than that for the corresponding EC concentration (Figure 10(b2 and b3)) in agreement with previous work by the authors (Eltayeb et al., 2013a; 2013b).

4.3.4 The surface morphology of the polymer nanoparticles

Nanoparticle size and morphology were investigated using SEM. Dried nanoparticles with and without the food component were vacuum sputter coated with gold for 2 min, at 40 mA, and mounted on Al stubs with double sided carbon tape, prior to SEM examination, which was carried out at 5 kV. ImageJ software was used to measure the standard deviation and mean of the nanoparticle diameter. Approximately 250 to 300 nanoparticles were measured for each set of processing conditions. Figure 11 shows SEM images of the polymeric nanoparticles. As may be seen, the nanoparticles were predominantly spherical in shape and this was the case for nearly all processing conditions investigated. Solutions P3 & P6 generated the most stable cone jet at a flow rate of 15µl min^{-1} with an applied voltage of 14.5 kV and a collection distance of ~150 mm. This corresponded to the most uniform nanoparticles with mean diameters of 61 ±3 and 55 ±5 nm, respectively.

4.3.5 Structure of the polymer nanoparticles

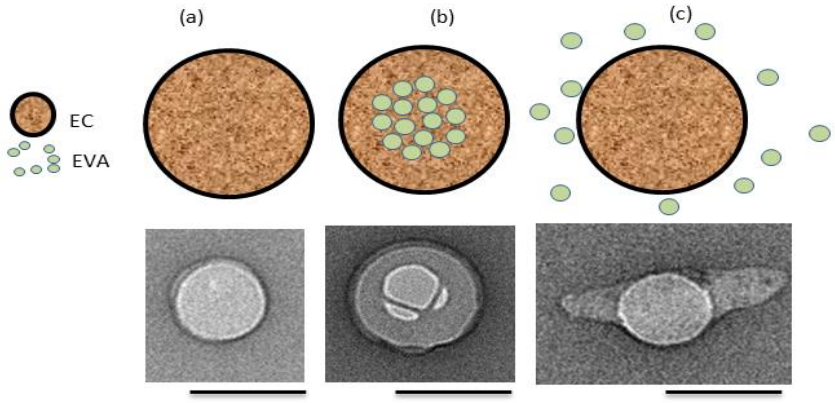

Figure 12: Schematic representation and related transmission electron microscopy of (a) EC nanoparticles, (b) EC nanoparticles encapsulating EV, and (c) EC nanoparticles after release (15 h). The images were taken for particles from solution P3 (see Table 4). Average size is 61 ±3, scale bar = 100 nm.

The internal structure of the nanoparticles was investigated using TEM (Figure 12a-c) including before and after EV release. Figure 12a shows the solid matrix structure of the EC particles. Figure 12b shows EV encapsulated and distributed evenly within the EC nanoparticles. Figure 12c shows the particles following EV release.

4.3.6 Chemical structure

Figure 13(a, b, and c) reveals the FT-IR spectrographs of the EV, EC, and EV-EC respectively. FTIR was used to check any chemical interactions between EV and EC. The spectrum of EV (Figure 13a) shows peaks at 3366, 2918, 1580, and 1701 cm^{-1} which belong to phenolic (-O-H) stretching, asymmetric stretching of alkenes (-CH-) of the OCH_2 group, aromatic C=C stretching vibration (Vieira et al., 2006) and the carbonyl (C=O) stretching vibration (González-Baró et al., 2008), respectively. In addition to this, peaks at around 1111 cm^{-1} are attributed to C-O stretching and 524 cm^{-1} corresponds to vibration and bending (Zheng et al., 2009). The IR spectra peaks of EC (Figure 13b) indicates a peak at 3482 cm^{-1} which is assigned to the –OH groups on the closed ring structure of the EC (Desai et al., 2006). These can be attributed to the intra and inter molecular hydrogen bonding due to the –OH groups (Ravindra et al., 1999). The IR spectra peaks of EV-EC (Figure 13c), located at (3482 to 2976) cm^{-1} and (2976, 2871) cm^{-1} are attributed to O-H and C-H stretching, respectively, of the EC structure (Li & Yang, 2008).

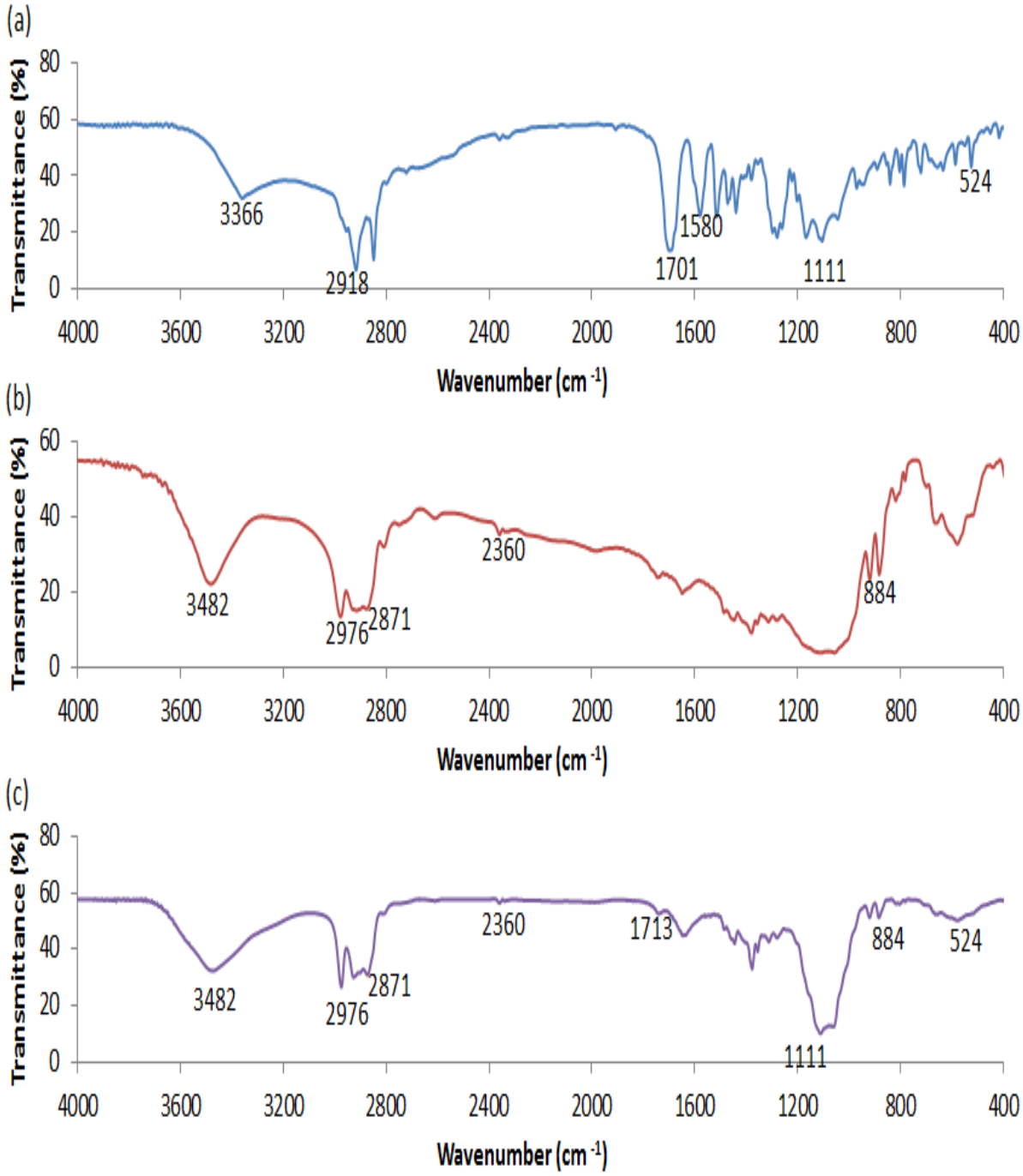

Figure 13: FT-IR spectra of: (a) pure EV; (b) pure EC, and (c) EV-EC nanoparticles, 10 wt% EC nanoparticles containing 1 wt% EV, prepared at flow rate 15 µl min^{-1} and applied voltage 14.5 kV.

Nanoparticle FTIR spectra obtained from the Figure 13 a, b, and c indicated peaks which were a summation of the characteristic peaks obtained with the pure EV and pure EC. The

peak at ~1713 cm^{-1} belongs to the carbonyl (C=O) stretching vibration, the peaks at ~1380 cm^{-1} are attributed to C-O stretching and 884 cm^{-1} corresponds to vibration and bending (Li & Yang, 2008). However, the C=O band shifted from 1701 to 1713 nm, which indicates hydrogen bonding formed between O-H and C-H in EV within EC (Li & Yang, 2008). Therefore, no degradation or chemical interaction occurred between EV and EC.

4.4 Loading capacity, encapsulation efficiency and burst

The encapsulation efficiency was determined according to the method verified previously by Eltayeb *et al*. (2013b). Nanoparticles were produced with varying concentrations of EC (from 2.5 to 10%) and EV (from 1 to 5, wt%) at a flow rate of 15 µl min^{-1} and applied voltage of 13.6 to 14.5 kV.

An increase in loading generally leads to a decrease in EE, as seen in electrosprayed EC (10%) loaded with ethylvanillin, where a 1, 2.5, and 5% loading, respectively led to 84, 83, and 78% encapsulation efficiency, respectively. This was attributed to the partition coefficient, referring to the equilibrium solubility of the ethylvanillin in the EC against the equilibrium solubility of the ethylvanillin in the solvent and responsible for diffusion of the ethylvanillin into the EC phase. Similar polymer solutions P6, P9, and P5 and electrospraying conditions, an increase of EV loading from 1% to 5% decreased EE from 80% to 71% in EC particles. This was also shown for EC particles encapsulating EV where EE increased with decreasing EV:EC ratio. This latter may be explained by an increase in viscosity when decreasing the EV:EC ratio, leading to better encapsulation. Furthermore, a strong correlation was found between EV:EC weight ratio with respect to encapsulation efficiencies. Size affects encapsulation efficiencies as well, where smaller particle sizes lower the EE. For polymer solutions P3, P2, and P1, an increase of flow rate from 15 – 25 µl min^{-1} slightly decreased EE from 84% to 81% in EC particles.

Table 5: Characteristic of EC loaded EV: loading capacity, encapsulation efficiency, burst, nanoparticle mean size, and polydispersity. Data present mean ± SD, n = 3

Solution	Loading capacity (%)	Encapsulation efficiency (%)	Burst (%)	Nanoparticle mean size (nm)	Polydispersity (%)
P1	83.0	81.0	6.0	84 ±5	21
P2	82.0	82.0	4.0	73 ±6	17
P3	81.0	84.0	3.0	61 ±3	16
P4	80.0	83.0	6.0	60 ±5	17
P5	65.0	71.0	27.0	57 ±5	21
P6	79.0	80.0	11.0	55 ±5	23
P7	75.0	78.0	16.0	54 ±4	32
P8	74.0	74.0	17.0	52 ±9	24
P9	71.0	73.0	18.0	47 ±7	31
P10	67.0	71.0	22.0	45 ±4	34

Loading capacity (LC) and encapsulation efficiency (EE) were determined according to equations (Equation 10) and (Equation 9) respectively.

Solution P3 (surface tension 21.3 ±0.05 mN m^{-1}, viscosity ~3.2 ±0.70 mPa s and electrical conductivity 5.16 ±0.16 mS m^{-1}) gave rise to the highest encapsulation efficiency (83%) as indicated in Table 5. This concentration was therefore selected for encapsulating EV (1, 2.5 and 5, wt%).

4.5 Release profiles

The food component release rate results are shown in section. As expected, EV release from the EC took place at a rate that varied over 15 h, involving two steps; an initial burst release

followed by a diffusion driven release. Particles prepared from solution P10 with an EV concentration of 1% took approximately 2 h to release ~40% of EV compared with 36%, 23% and 14% for P8, P6 and P3, respectively (Figure 14). The food component release rate decreased as the amount of EC concentration was increased, and nanoparticles from solution P3 with 10% EC concentration exhibited the most linear release.

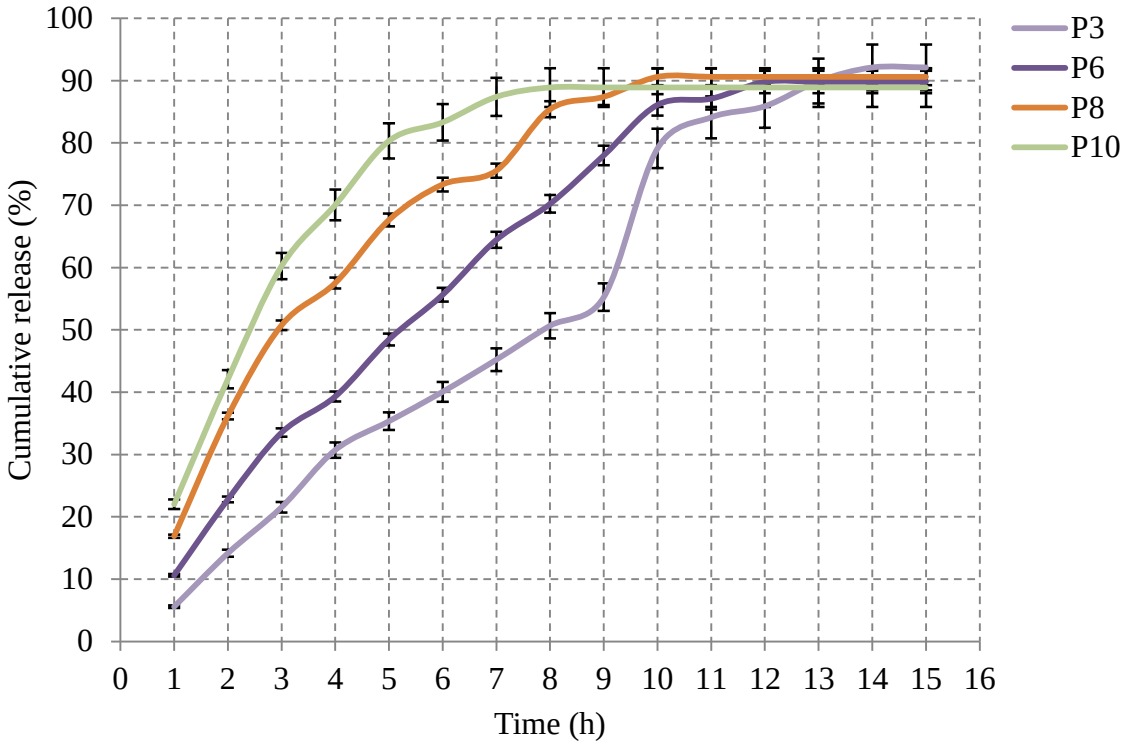

Figure 14: EV release profile for nanoparticles prepared from solutions P3, P6, P8, and P10 (see Table 4).

The release rate from nanoparticles prepared from solutions P10 and P8 was higher compared with those from P6 and P3, and this is likely to have been due to the lower amount of EC present in the nanoparticle matrix and the increase in the surface-area to volume ratio of the nanoparticles with decreasing size.

Figure 15 shows the effect of EV concentration on the release profile. The loading and encapsulation efficiency of EV at different concentrations (1, 2.5 and 5 wt%) in the

nanoparticles from solutions P3, P4, and P7 were found to be 81, 80, and 75 and 84, 83 and 78%, respectively, e.g. the loading and encapsulation efficiency of the nanoparticles decreased as the amount of EV increased. EV (1 wt%, by weight) was encapsulated within nanoparticles (P3) with 84% encapsulation efficiency.

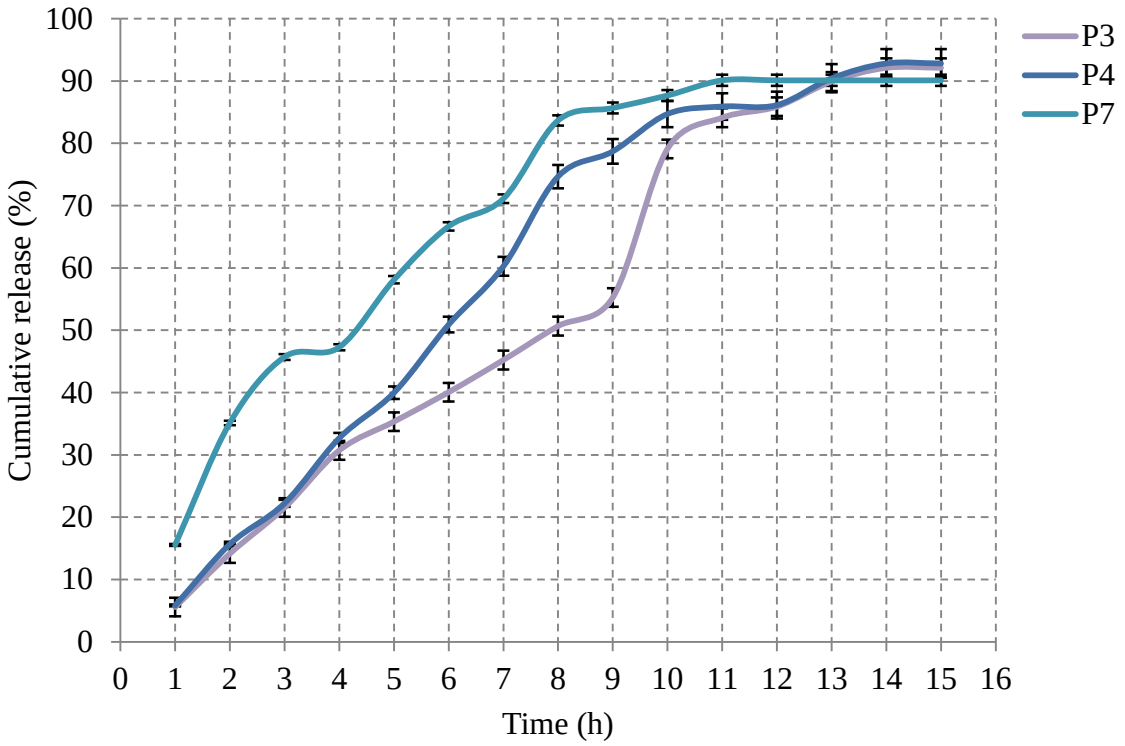

Figure 15: EV release profile for nanoparticles prepared from solutions P3, P4, and P7 (see Table 4),

Figure 16 shows the effect of EV concentration on the release profile. The loading and encapsulation efficiency of EV at different concentrations (1, 2.5 and 5 wt%) in the nanoparticles from solutions P6, P9, and P5 were found to be 79, 71, and 65 and 80, 73 and 71%, respectively, e.g. the loading and encapsulation efficiency of the nanoparticles decreased as the amount of EV increased. This was shown for EC particles encapsulating EV where EE increased with decreasing EV:EC ratio. This latter may be explained by an increase in viscosity when decreasing the EV:EC ratio, leading to better encapsulation

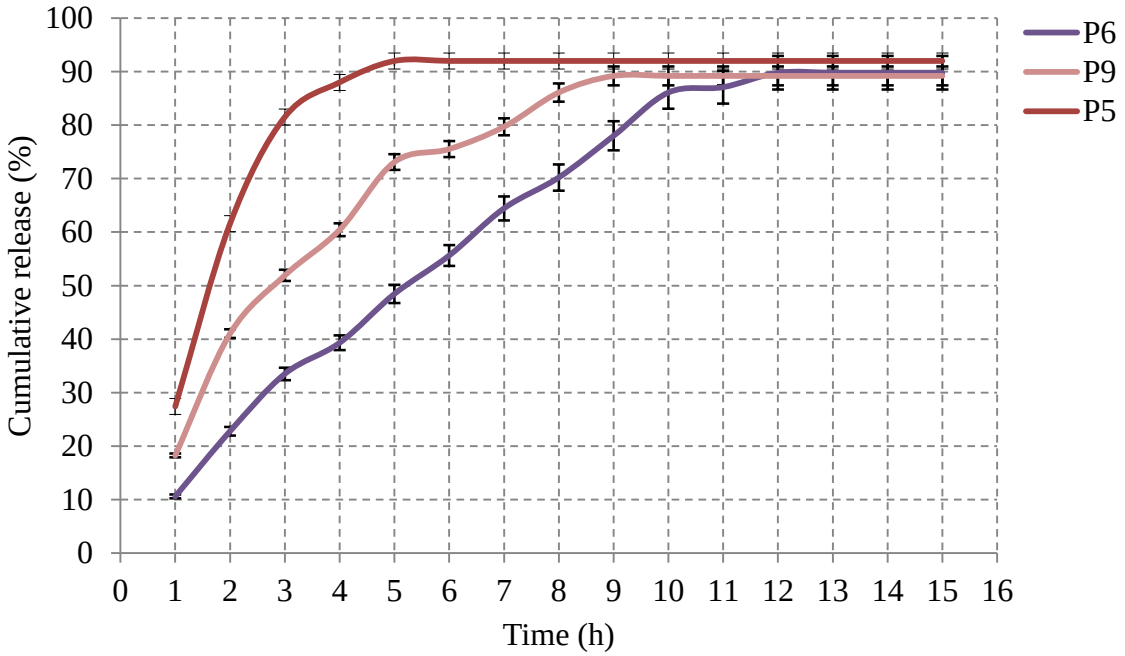

Figure 16: EV release profile for nanoparticles prepared from solutions P5, P6, and P9 (see Table 4),

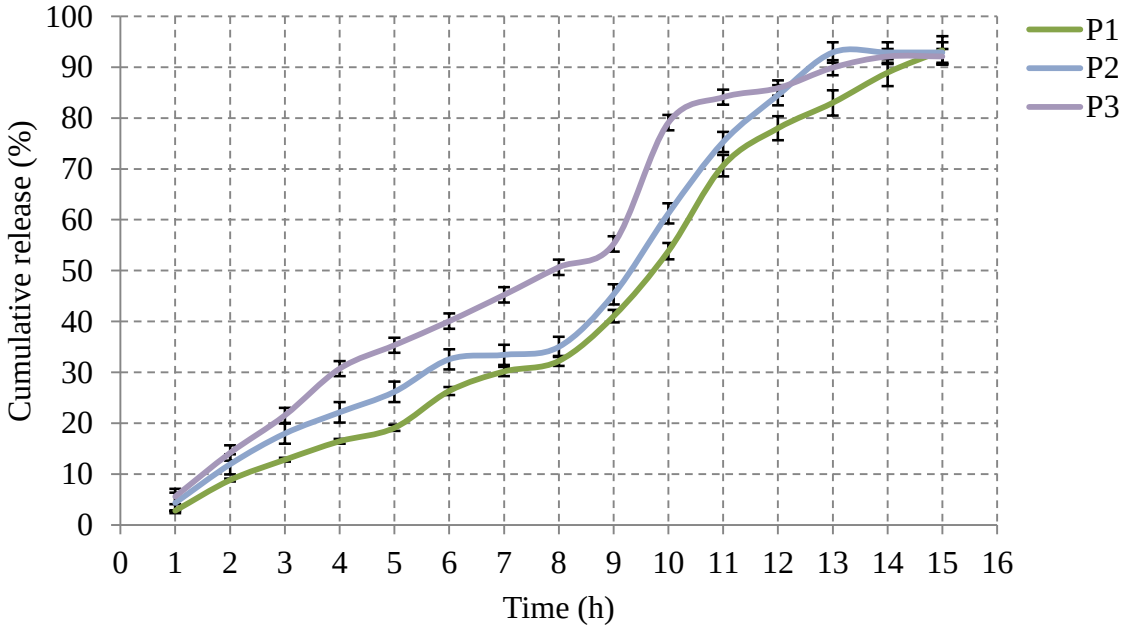

Figure 17: EV release profile for nanoparticles prepared from solutions P1, P2, and P3 (see Table 4).

The effect of flow rate on food component release rate (Figure 17) shows that as flow rate increased the release rate decreased. Nanoparticles from solutions P1 and P2 both released their payload more slowly than those from P3.

The effect of food component loading on food component release is consistent with previous studies (Eltayeb et al., 2013a; 2013b) and can be explained by the fact that the decreased food component loading increases the relative amount of ethylcellulose acting as a diffusional barrier.

Figure 17 indicates the correlation between nanoparticle size and food component release rate. Nanoparticles from solutions P1 and P2 were larger and therefore had a lower surface area to volume ratio and released EV more slowly than nanoparticles from solution P3. They could also have had a different structure due to slower ethanol evaporation during particle formation (Yao et al., 2008). The food component loading had a similar but smaller influence on nanoparticle mean size by changing the EC concentration of the polymer solution, with a large amount of food component loading causing an increase in mean particle size.

The flow rate was also found to affect nanoparticle size, as expected. These two parameters were directly proportional to each other. The maximum level of release achieved over the 15 h indicated that some EV remained encapsulated within the EC nanoparticles. This is unsurprising as EC is practically insoluble in water.

4.6 Release models

In this section, the food component release rate profile data was fitted using Higuchi, zero order, Hixson-Crowell, first order, and Ritger-Peppas models, respectively (Higuchi, 1963; Ritger & Peppas, 1987; Sezer et al., 2011) and release equations are given in section 2.6.5.

Table 6 Model parameters for food component release from nanoparticles. R^2, k and n represent correlation coefficient, release rate and release exponent, respectively.

	Zero-order		**First-order**		**Higuchi**		**Hixson-Crowell**		**Ritger-Peppas**		
Formulation	R^2	K_0	R^2	K_1	R^2	K_H	R^2	K_{HC}	R^2	k	n
P1	0.961	7.80	0.71	0.112	0.893	46.85	0.97	0.213	0.983	1.34	0.99
P2	0.955	7.58	0.76	0.142	0.898	44.88	0.96	0.197	0.975	1.11	0.82
P3	0.969	1.57	0.88	0.012	0.957	38.40	0.92	0.181	0.985	1.03	0.90
P4	0.930	8.05	0.94	0.137	0.970	31.74	0.85	0.176	0.970	1.09	1.11
P5	0.399	15.40	0.57	0.085	0.546	21.12	0.36	0.054	0.642	0.15	0.23
P6	0.887	19.25	0.96	0.110	0.973	16.20	0.84	0.143	0.975	0.83	0.81
P7	0.850	29.88	0.94	0.109	0.936	2.08	0.77	0.114	0.940	0.60	0.60
P8	0.792	36.11	0.93	0.111	0.904	5.43	0.70	0.104	0.911	0.55	0.57
P9	0.736	40.53	0.88	0.094	0.862	11.83	0.65	0.094	0.882	0.46	0.52
P10	0.597	48.27	0.78	0.082	0.763	21.80	0.55	0.080	0.830	0.42	0.48

The fits are obtained by applying Microsoft Excel's trendline analysis to linearised forms of the equations, and the goodness-of-fit statistics are those reported by that procedure. Although this means that the values of R^2 are not strictly comparable, they have been used as a guide to selecting the best model. Although both the Higuchi and Ritger-Peppas models are strictly applicable only to the early stages of release, here they are applied to the whole release profile.

For all the nanoparticle formulations shown in Table 6, based on their correlation coefficients (R^2), the poorest fit was to the first order model ($R^2 = 0.906$) and the best fitting model was found to be the Ritger-Peppas model ($R^2 = 0.985$). The values of n for most of the nanoparticles prepared were found to be >0.48 and <0.89, indicating that release occurred through a non-Fickian diffusion mechanism.

4.7 Summary

This chapter has demonstrated that simple single needle EHD processing can be used to prepare nanoparticles from a food grade polymer encapsulating a food component with high encapsulation and loading efficiency. Adjusting the EHD processing parameters allowed the nanoparticle size to be controlled in a reproducible manner whilst maintaining a relatively narrow size distribution. This is important because the release of the food ingredient was found to be very sensitive to nanoparticle size. It was shown that the release of the ethylvanillin from the nanoparticles was sustained over 15 h; and that the release period could be controlled, again by varying the processing parameters.

Chapter 5 Preparation, Characterisation and Release Kinetics of Stearic Acid Nanoparticles Encapsulating Food Flavour

5.1 Introduction

Nanotechnology has been widely utilised for encapsulation and controlled release of food ingredients in the pharmaceutical, cosmetic, and food industries in recent years. For these applications the nanoparticles must be stable, non-toxic, have high encapsulation efficiency and loading capacity and enable the release kinetics of the flavour component to be tailored to meet specific requirements.

In this chapter, EHD processing was used to form stearic acid nanoparticles encapsulating ethylvanillin. Both materials are widely used in the food industry (Manojlovic et al., 2008) and representative of typical hydrophobic coating and hydrophilic flavour components respectively. Since stearic acid is a natural lipid extracted from animal fat; expect the lipid nanoparticles should be safe and biocompatible for food applications.

This chapter utilises an EHD technique to prepare core-shell lipid nanoparticles with a tunable size and high food ingredient loading capacity, encapsulation efficiency and controlled release.

Using stearic acid and ethylvanillin as model shell and food ingredients respectively, we identify the processing conditions and ratios of lipid:ethylvanillin required to form nanoparticles. The internal structure of the lipid nanoparticles was studied by transmission electron microscopy which confirmed that the ethylvanillin was encapsulated within a stearic acid shell. Fourier transform infrared spectroscopy analysis indicated that the ethylvanillin had not been affected by the processing.

5.2 Preparation of lipid nanoparticles

Stearic acid and ethylvanillin were dissolved in ethanol with concentrations ranging from 1 to 5 w% and 1 to 4 w%, respectively. The solutions were mixed using a magnetic stirrer at room temperature until optically transparent. The solutions were fed through silicone tubing from a 10 mL plastic syringe driven by a high precision syringe pump into a stainless steel needle with internal diameter 450 μm, at a flow rate of 15 μl min^{-1}. The applied electrical potential difference between the needle and a ground electrode was varied between 13 – 15 kV, using a high voltage power supply. Once a stable cone jet had been obtained, nanoparticles were collected either on a glass microscope slide, or in a vial containing DD water for the release studies, both of which were kept at distance of ~100 mm from the needle tip. The jet created at the tip of the needle during nanoparticle production was observed using a video camera. Optimization of the operating parameters and formulation with regard to their influence on nanoparticle physical properties and ethylvanillin release rate was carried out prior to this work (Eltayeb et al., 2013a; Eltayeb et al., 2013b) and the operating parameters for this study (i.e. lipid concentration, solution flow rate, distance between needle tip and collector) were selected in order to produce a stable cone jet and controlled nanoparticle formation (Eltayeb et al., 2013a; Eltayeb et al., 2013b).

5.3 Lipid nanoparticle characterisation

5.3.1 Size, morphology and internal structure

As showed in Figure 18, nanoparticles were successfully prepared using a single step EHD technique at a flow rate of 15 μl min^{-1} with an applied voltage of 14.5 kV and a collection

distance of ~100 mm. Uniform nanoparticles with a mean diameter of 65±6 nm (Figure 18a, b) were obtained. Lipid assembles around the ethylvanillin core to form shell (Figure 18c).

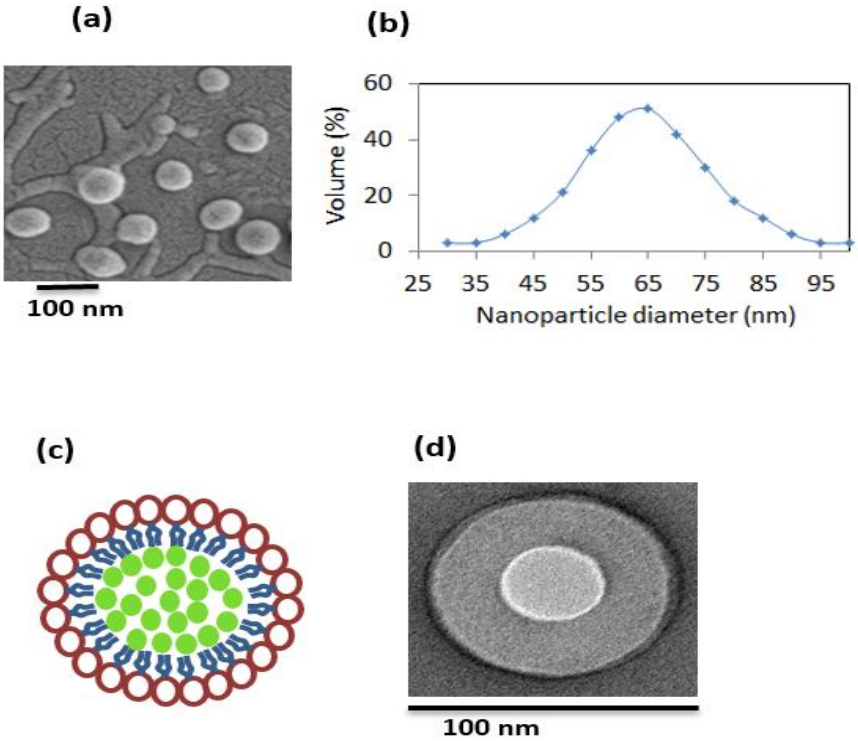

Figure 18: Schematic illustration; (a) SEM image of 4 wt% stearic acid lipid nanoparticle encapsulating 1.6 wt% EV structure at an applied voltage of 14.5 kV and flow rates 15 $\mu l.min^{-1}$. (b) Size distributions of nanoparticles containing EV. (c and d) schematic and corresponding TEM image of nanoparticle. Average size is 65±6 nm. Scale bar100 nm.

To characterise the structure of the lipid nanoparticles, they were examined by TEM with negative staining of the lipid by 2% solution of uranyl acetate to improve its electron density. This indicated an EV rich core surrounded by and SA rich outer layer (Figure 18d). The thickness of the stearic acid rich layer (~20 nm). The concentration of SA will change the solution viscosity, surface tension and conductivity; this will in turn alter the behaviour of the jet and hence the characteristics of the nanoparticles produced (Wu et al., 2015).

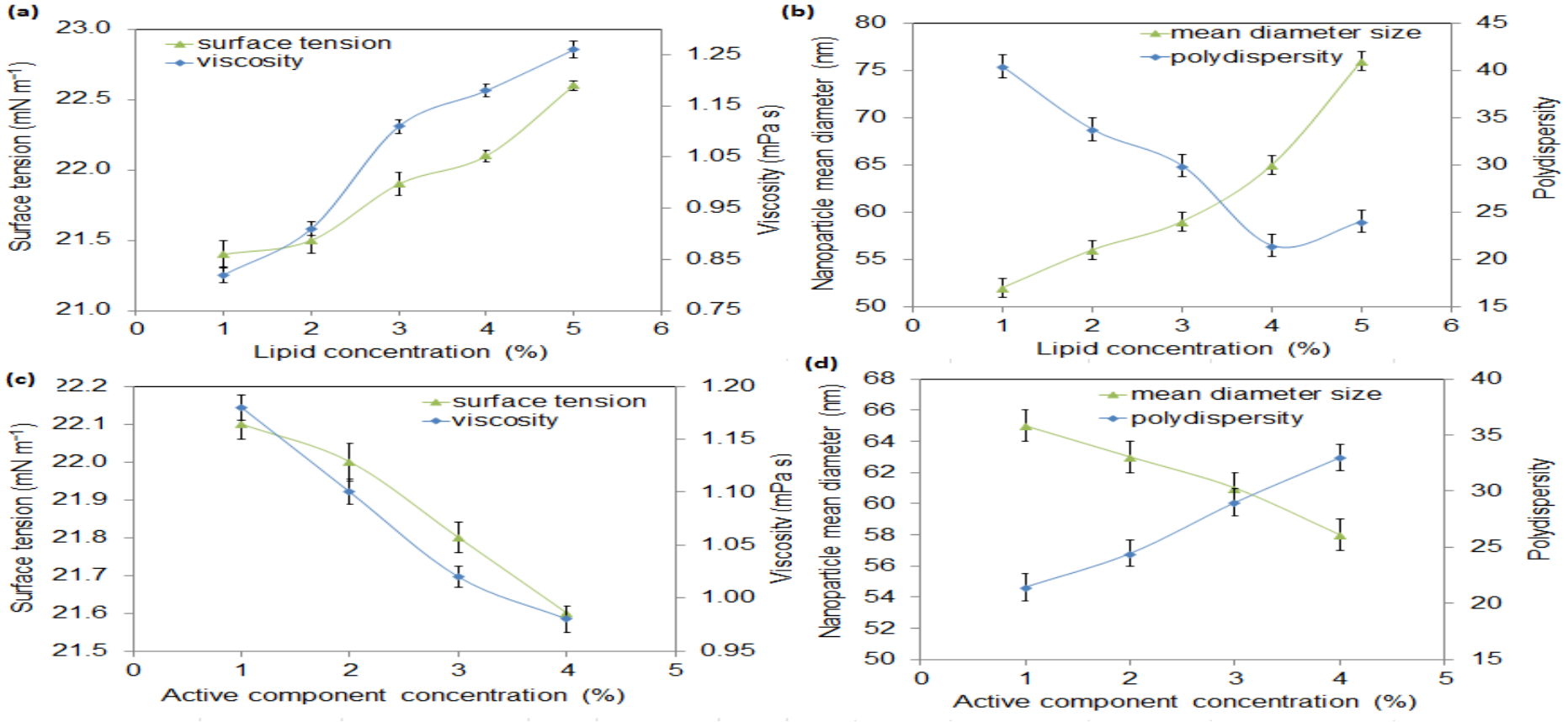

Figure 19: (a) effect of lipid concentration surface tension and viscosity of solution, (b) Mean diameter and polydispersity of nanoparticles prepared at different stearic acid lipid concentrations. Effect of EV weight concentration on 4 wt% of lipid solution on: (c) surface tension, and viscosity, (d) Mean diameter and polydispersity. $n \approx 300$ nanoparticles.

5.3.2 Influence of lipid concentration on nanoparticles

As shown in Figure 19 (a, b), varying the lipid weight ratio from 1 to 5 wt% to encapsulate 1 wt% ethylvanillin solutions, viscosity (0.82 to 1.26 mPa s) and surface tension (21.4 to 22.6 mNm^{-1}) results in nanoparticles with diameters from 52−76 nm, for ethylvanillin delivery application (Eltayeb et al., 2013a; Eltayeb et al., 2013b).

Keeping the SA weight constant at 4 wt%, we varied the ethylvanillin weight concentration ratio from 1 to 4 wt%, inherent viscosity demonstrated that nanoparticle size can fine-tune in a highly reproducible manner while slightly affecting surface tension. For example, when the viscosity of the SA-EV solution was decreased from 1.18 to 0.98, the nanoparticle size decreased from 65±6 nm (polydispersity = 21%, N = 300) to 58±4 nm (polydispersity = 33%, N= 300) (Figure 19b), while the nanoparticle solution surface tension only slightly fluctuated in the range of 22.1 to 21.8 mNm^{-1} Figure 19 (c, d) (Doshi & Reneker, 1995; Jaworek & Sobczyk, 2008; Rohner et al., 2004; Xu & Hanna, 2008). The observed influence of ethylvanillin inherent viscosity on nanoparticle solution was consistent with what has been previously reported for SA/EC hybrid nanoparticles (Eltayeb et al., 2013b).

5.3.3 X-ray diffraction

The X-ray diffraction (XRD) patterns obtained are shown in Figure 20. Figure 20a shows the pure ethylvanillin crystal structure. The (XRD) pattern for the ethylvanillin loaded lipid nanoparticles (Figure 20c) was identical to the peaks assigned to a standard lipid crystal structure (Figure 20b). As the (XRD) pattern of the ethylvanillin loaded lipid nanoparticles did not show any peak corresponding to the ethylvanillin, pure ethylvanillin is present in the centre and pure SA at the surface of the particle, which further confirmed particle structure.

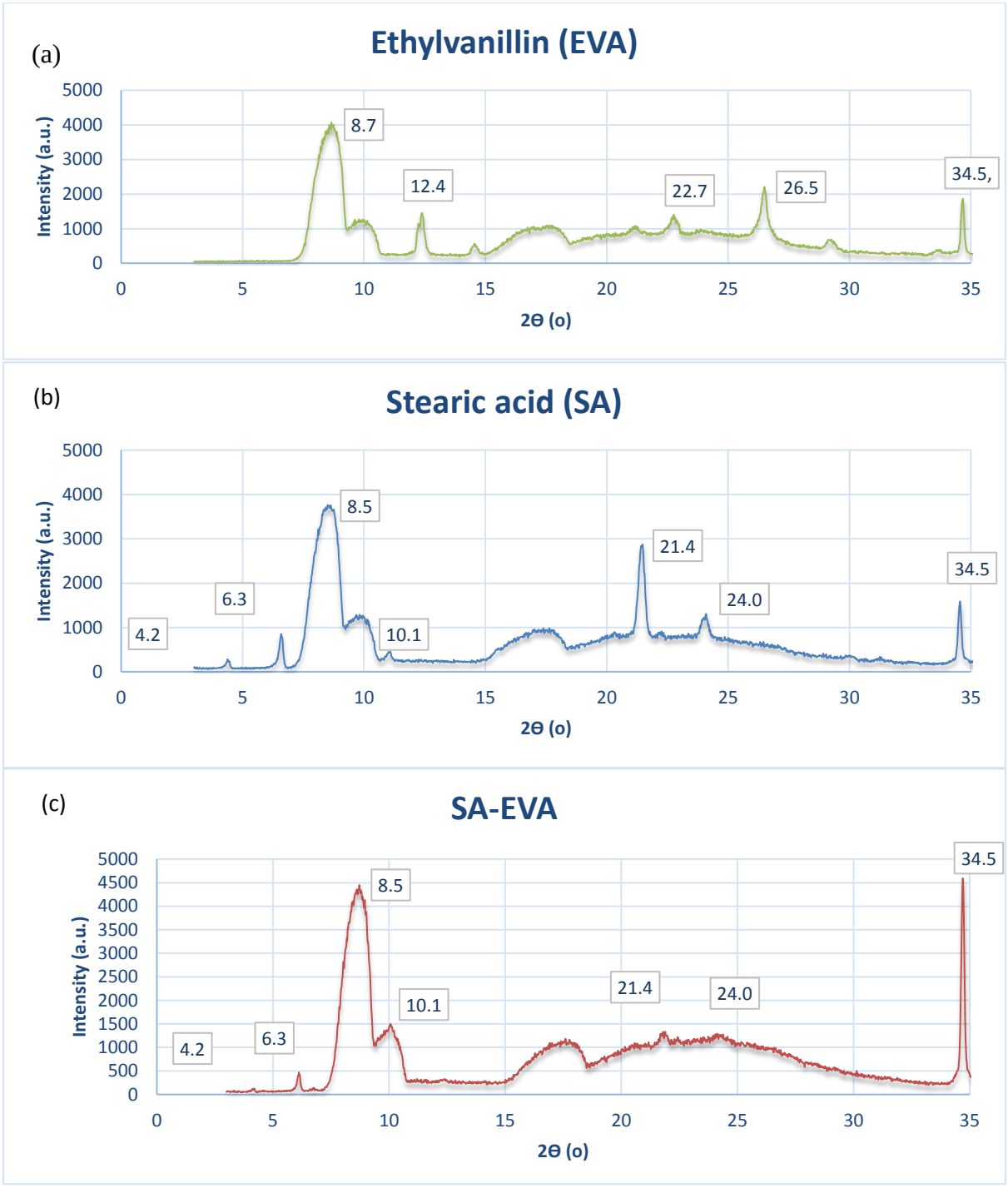

Figure 20: Comparison of the XRD curves of; (a) pure EV; (b) pure SA, and (c) EV with SA nanoparticles, 4 wt% SA nanoparticles containing 1.6 wt% EV, prepared at a flow rate 15 µl min^{-1} and applied voltage 14.5 kV. All curves were recorded with the same temperature calibration.

5.3.4 Chemical structure

The FTIR spectrum of EV (Figure 21a) shows peaks at 3366, 2918, 2850, and 1701 cm^{-1} which belong to phenolic (-O-H) stretching, asymmetric stretching of alkenes (-CH-) of the OCH_2 group, aromatic C=C stretching vibration (Vieira et al., 2006) and the C=O carbonyl stretching vibration (González-Baró et al., 2008), respectively.

In addition to this, peaks at ~1111 cm^{-1} were seen, belonging to C-O stretching and at 524 cm^{-1} corresponding to vibration and bending (Zheng et al., 2009). The spectrum of SA (Figure 21b) shows two strong absorption peaks at 2953 cm^{-1} and 2852 cm^{-1} that are attributed to the asymmetric and symmetric stretching vibrations of its -CH_2 group.

The strong absorption peak at 1711 cm^{-1} corresponds to the stretching vibration of the carbonyl C=O group. The absorption peaks around 1471 cm^{-1} represent the bending vibration of -CH_3 groups. The absorption peaks from 1310 cm^{-1} to 1105 cm^{-1} represent the rocking vibration of the -CH_2 group. The nanoparticle spectra shown in Figure 21c exhibited peaks that were a combination of the characteristic peaks obtained with pure EV and pure SA. However, the C=O band shifted from 1701 to 1711 nm, which indicates hydrogen bonding formed between O-H and C-H in EV with SA nanoparticles. This indicates that there was no degradation or chemical interaction occurred between EV and SA.

5.4 Encapsulation efficiency, loading capacity and release profile

Next, I examined the EV loading capacity, encapsulation efficiency, and release profile from the SA lipid nanoparticles prepared from solutions with different SA concentrations from 1 to 5 wt%. We hypothesized that the SA at the shell of the ethylvanillin core may serve distinct functions; improving ethylvanillin loading capacity and encapsulation efficiency, and decreasing the water diffusion rate into the ethylvanillin core.

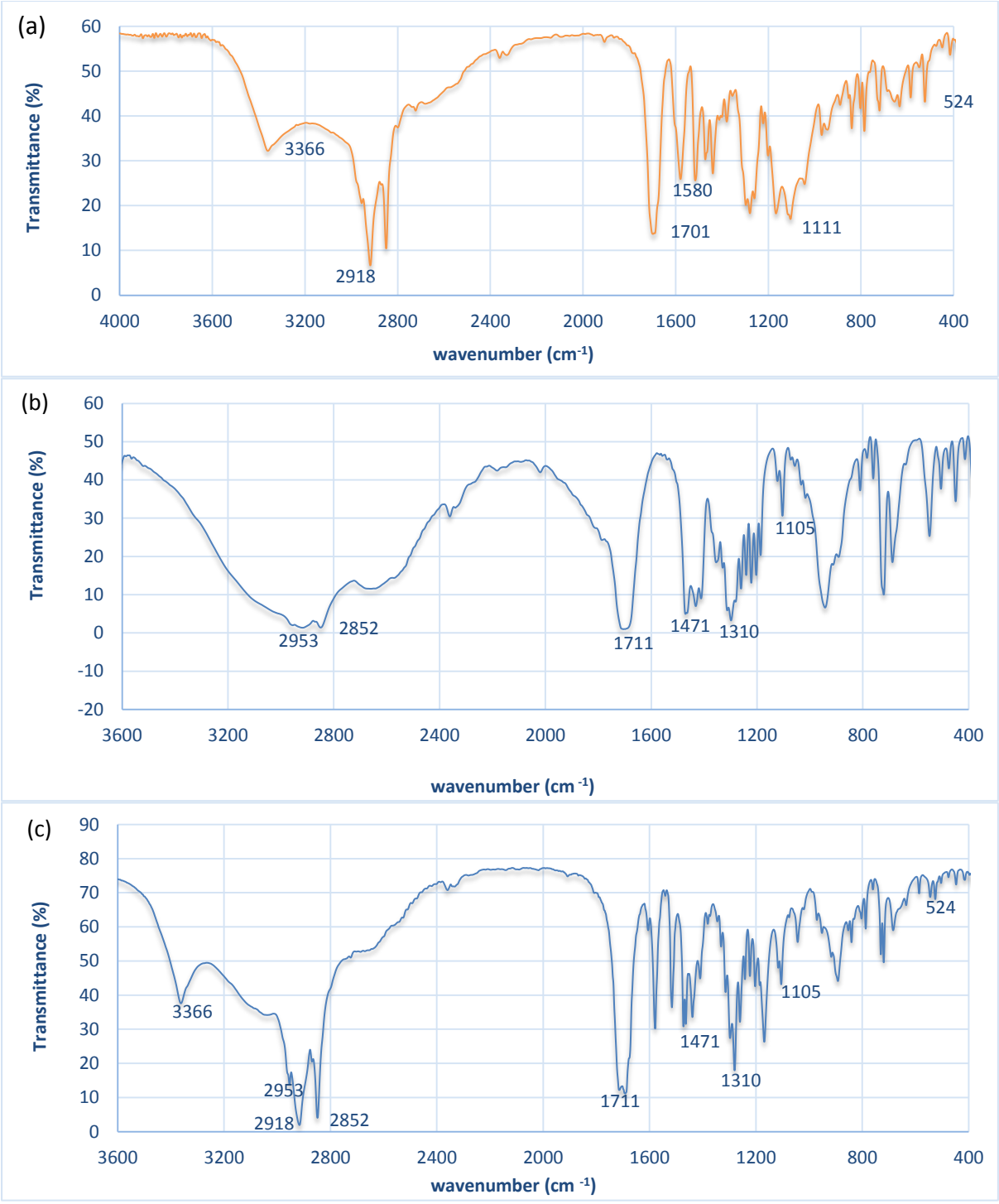

Figure 21: FT-IR spectra of: (a) pure EV; (b) pure SA, and (c) EV with SA nanoparticles, 4 wt% SA nanoparticles containing 1.6 wt% EV, prepared at flow rate 15 µl min^{-1} and applied voltage 14.5 kV

This would in turn reduce the hydrolysis rate of the ethylvanillin resulting in slower release from the nanoparticles. To examine these hypotheses, ethylvanillin (EV), a commonly used food flavour, was chosen as a model hydrophilic flavour component to be encapsulated in the SA lipid nanoparticles. As shown in Figure 22a and Table 7, for nanoparticles prepared from the EV: SA 1:4 solution, 71 ± 3% of EV was encapsulated into the nanoparticles. In contrast, EV encapsulation efficiencies for the nanoparticles prepared from 1, 2, 3 and 5% solutions were 48 ± 3, 55 ± 4, 62 ± 6 and 61 ± 9%, respectively. The relatively low encapsulation efficiency of the 5 wt% lipid nanoparticles may have been due to the increase in diameter and/or less hydrophobic core than the 4 wt% lipid nanoparticles.

In addition, the encapsulated EV was released from the lipid nanoparticles at a control rate over 240 min (Figure 22b). When all lipid nanoparticles were each loaded with EV at approximately 1 w %, it took the 4 w% lipid nanoparticles around 60 min to release ~5% of EV versus 12, 20, 48, and 44 for 1, 2, 3 and 5 w% lipid nanoparticles, respectively. These results suggest that the SA at the interface of the core acts as a shell that helps to protect the ethylvanillin inside the nanoparticles. We further observed that the EV loading capacities of these nanoparticles were relatively high. For instance, when the EV input was 1, 2, 3 and 4 w%, the measured loading capacity reached 0.6, 1.2, 1.8 and 1.6%, respectively (Figure 22c).

However, EV encapsulation capacity decreased when the initial flavour component input was increased to ~4 w%. We also observed that EV was released from the nanoparticles at a control manner until its loading capacity was higher than ~1.8% (Figure 22d).

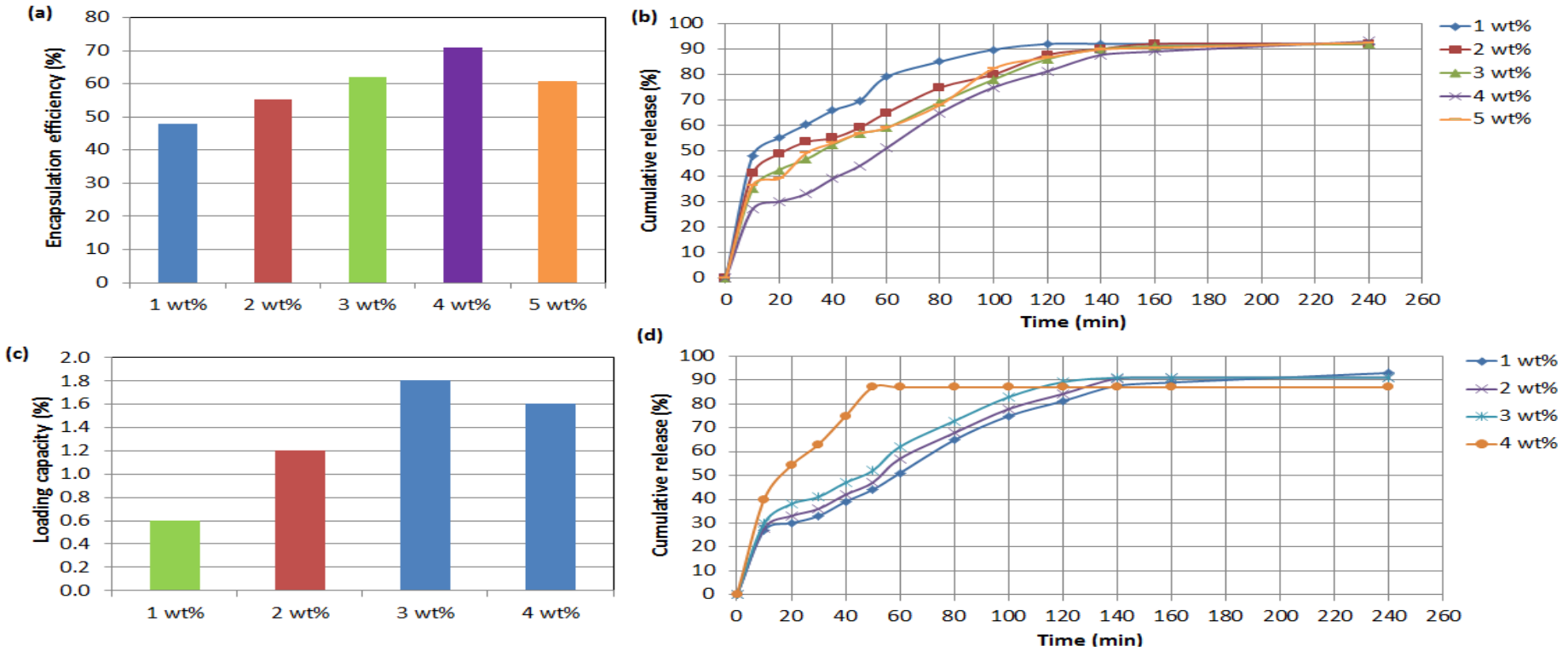

Figure 22: (a) EV encapsulation efficiency of lipid nanoparticles prepared from solutions 1, 2, 3, 4, and 5 w% of the SA, (b) EV release profile for lipid nanoparticles prepared from solutions 1, 2, 3, 4, and 5 w% of the SA, (c) EV loading capacity of lipid nanoparticles at various initial flavour component inputs ranging from 1 to 4 w% of the EV, and (d) EV release profle for nanoparticles prepared from 1 to 4 w% of the EV solutions.

They are effective electrosprayed lipid nanoparticles for ethylvanillin encapsulation, and have been shown to increase encapsulation efficiency, single process, with less cost as compared to literature (Ezhilarasi et al., 2013; Fathi et al., 2012; Kriegel et al., 2009).

Table 7: Characteristic of SA loaded EV: loading capacity, encapsulation efficiency, burst, nanoparticle mean size, and polydispersity. Data present mean ± SD, n = 3

Formulation	Lipid concentration (wt %)	Food component loading (wt%)	Loading capacity (%)	Encapsulation efficiency (%)	Burst (%)	Nanoparticle mean size (nm)	Polydispersity (%)
L1	10	1	46	48	46	52 ±4	40
L2	20	1	51	55	41	56 ±9	34
L3	30	1	57	62	35	59 ±5	30
L4	40	1	64	71	27	65 ±3	21
L5	50	1	56	61	36	76 ±4	24
L6	40	2	60	69	28	63 ±2	24
L7	40	3	60	67	30	61 ±7	29
L8	40	4	40	54	40	58 ±6	33

5.5 Release models

Release studies were conducted over 240 mins and repeated three times for each set of lipid nanoparticles and the results combined to obtain the cumulative ethylvanillin release rate, which was plotted as a function of time.

Next, we examined which release model of the (1.6:4 w%; EV:SA) lipid nanoparticles gave the best fit to the experimental results. The released profile was incorporated into the several release models the Higuchi, zero-order, Hixson Crowell, first order, and Korsmeyer Peppas and among them the best fit model was determined based on regression coefficient (R^2) value. We further observed that the best fitting model was the zero-order model release with R^2 0.976 and n = 0.45 (Table 8). The zero order release indicated that release of the ethylvanillin from the SA lipid depends upon the time of the ethylvanillin in it and also described the Fickian diffusion mechanism of the ethylvanillin from the nanoparticles.

Table 8: Model parameters for food component release from nanoparticles. R^2, k and n represent correlation coefficient, release rate and release exponent, respectively.

	Zero-order		First-order		Higuchi		Hixson-Crowell		Ritger-Peppas		
Formulation	**R^2**	**K**	**R^2**	**k**	**R^2**	**k**	**R^2**	**k**	**R^2**	**K**	**N**
L4	0.976	15.40	0.8425	0.1451	0.943	2.25	0.9735	0.1562	0.947	1.09	0.45
L6	0.968	18.69	0.8984	0.1412	0.923	6.19	0.964	0.1495	0.950	1.03	0.48
L7	0.954	24.48	0.9161	0.1457	0.903	12.80	0.9451	0.1373	0.953	0.92	0.42
L8	0.655	53.72	0.7031	0.0811	0.596	47.62	0.6318	0.074	0.769	0.52	0.24

The ethylvanillin release from lipid nanoparticle followed the zero order kinetics. The release rate seemed to be mainly dependent on the ethylvanillin lipid interactions and partitioning, therefore, it may be concluded that the physicochemical properties of the flavour component core from the lipid nanoparticles are of primary importance.

5.6 Summary

In summary, we have demonstrated that lipid nanoparticles encapsulating a model flavour component (ethylvanillin) can be produced by EHD spraying. We found that the diameter and size distribution of the nanoparticles could be controlled by varying the lipid:ethylvanillin concentration ratio in the sprayed solution. The nanoparticles were found to have a core-shell structure, with the thickness of the outer lipid layer being dependent upon the concentration of lipid in the processed solution.

The encapsulation efficiency and loading capacity were similarly found to be dependent on the lipid: ethylvanillin concentration ratio; although there was found to be a limit above which both started to decrease. It was shown that the release of the ethylvanillin described by a zero-order release model and was a function of the nanoparticle size, and lipid: ethylvanillin concentration ratio. This technique for preparation of lipid nanoparticles in one step may be useful for production of lipid based nanoparticles with different characteristics for food applications.

Chapter 6 Preparation and Characterisation of Polymer-Lipid Nanoparticles Encapsulating Food Flavour

6.1 Introduction

A key challenge in the production of multicomponent nanoparticles for food applications is obtaining reproducible monodisperse nanoparticles with the minimum number of preparation steps. In this chapter, show that polymer-lipid core-shell nanoparticles composed of stearic acid and ethylcellulose and containing model food components can be produced in a one step process using EHD techniques.

The conditions under which a stable cone-jet was formed were identified and by varying the EHD processing parameters, nanoparticles with a tunable size less than ≤100 nm were produced. The reason prepared polymer-lipid core-shell nanoparticles to encapsulate food components was to limit flavour degradation or loss during processing and storage because of increase of degradation time of polymer-lipid core-shell nanoparticle.

Polymer-lipid core-shell nanoparticle is able to provide more protection against chemical reactions such as oxidation. It is beneficial to encapsulate volatile ingredients prior to use in foods or beverages. These nanoparticles are composed of a hydrophilic polymeric core for encapsulation, and a lipid shell. The overall structure of the nanoparticles produced was examined by multiple methods, including transmission electron microscopy and differential scanning calorimetry to confirm that they were of core-shell form.

6.2 Preparation of polymer-lipid core-shell nanoparticles

6.2.1 EHD processing

Nanoparticles were prepared using a single-needle EHD spraying setup. The spraying system consisted in a high voltage electrical power source, with a mechanical syringe pump with high precision and adjustable flow rate, a stainless steel needle connected to the high voltage supply. The solutions containing the food ingredient, were loaded into a 10 ml plastic syringe.

This syringe was mounted on the Harvard syringe pump and was connected to the stainless steel needle at one end via silicone tubing. The syringe pump controlled the flow rate of spraying solution into the needle.

A video camera with an in-built magnifying lens was used to observe the needle tip at all times during collection of nanoparticles in order to understand the spraying behaviour on the application of applied voltage. The system operating parameters e.g. flow rate, collection distance and voltage, were used to control nanoparticles formation. The nanoparticles were only collected at the applied voltages which furnished a stable cone-jet. The nanoparticles generated from the jet were collected onto a microscopic slide containing distilled water. The particles were then left to dry in a desiccator under vacuum.

All five samples were sprayed at varying flow rate (10 - 25 µl/min), with the collection distance kept between 100-150 mm from the needle end and with the applied voltages between 0-20 kV. All the experiments were repeated three times.

The polymer-lipid nanoparticles solutions were sprayed at varying voltages and flow rates to obtain the stable cone-jet, which is essential for obtaining uniform sized droplets during the

spraying. The droplets generated by cone-jet can be near-monodisperse and are very fine. Determination of the appropriate applied voltage required to generate a stable jet is important to achieve the control needed throughout the spraying process to generate the particle.

6.2.2 Influence of flow rate

Initially, the voltage (1 – 20 kV) was increased in small increments until a stable-cone jet was formed (13-15 kV). A stable cone jet could only be achieved when the flow rate was 10 or 15 µl/min. The spindle mode was observed between 10 - 12 kV, and the multi-jet mode between 16-20 kV for all the flow rate 10 - 25 µl/min. Samples were collected on glass slides coated with distilled water to give a cushioning effect and prevent flattening of spherical nanoparticles.

Increasing the viscosity of solutions (by increasing EC concentration) results in a shift of the cone-jet mode to higher voltages. This is because of the lower conductivity of more viscous solutions: a stronger electric field should be applied to overcome the surface tension and liquid viscosity to form the cone jet. It is very important to keep in mind that only in the stable cone-jet mode is the production of monodisperse particles possible. Only then can the size and morphology of particles be controlled by carefully changing other parameters.

6.2.3 Influence of applied voltage

EHD processing parameters such as applied voltage, needle diameter, and flow rate in addition the concentrations and chemical composition of the EHD spraying solution influence the spraying process and the properties of the final products. Of these, the applied voltage is a key factor. As the applied voltage increases, EHD jetting modes change significantly (Jaworek, 2008).

In this study when the voltage was increased from 8 kV to 14kV, a cone-jet was formed at 10 µl/min , which is essential for generating uniformly sized and stable particles with sizes below 100nm (Enayati et al., 2010). Further increasing the voltage (16kV) gave rise to multiple jets and above 19kVunpredictable, unstable multi-jets formed (Nie et al., 2010a).

6.2.4 Influence of physical properties of the solutions

The major physical properties of the solutions which affect nanoparticle generation and formation in EHD method, are viscosity and surface tension, both of which are influenced by polymer concentration (Pham et al., 2006). These are shown in Table 9. Initial experiments were carried out to adjust the EHD process parameters using various concentration of polymer-lipid in different ratios, dissolved in ethanol.

Table 9: Characteristics of solutions containing SA and EC (mean ± S.D., n = 5).

Solution	Lipid:Polymer (wt/wt%) ratio	Density (g/m^{-3})	Surface tension (mN m^{-1})	Viscosity (mPa s)
PL1	5:0	793±0.00	22.3±0.06	1.2±0.11
PL2	4:1	795±0.00	23.0±0.20	2.1±0.1
PL3	3:2	796±0.00	23.0±0.22	2.8±0.04
PL4	2:3	802±0.00	23.4±0.26	3.2±0.06
PL5	1:4	806±0.00	23.5±0.29	3.5±0.02

High concentration stearic acid solutions (5 wt%) resulted in blockage of the needle. Adding EC to the solution, it was observed that the surface tension of the spraying solution increased as the amount of EC increases. Therefore, the concentration of EC in the spraying solution seems to play a role in the EHD process. Decreasing the surface tension of the solution in general, decreases the average particle size (Doshi & Reneker, 1995).

The particle shape is also affected by the solvent volatility, apart from the spraying liquid flow rate. An increase in the amount of EC, results in an increase in the viscosity, and thus, is expected to increase the particle size (Jayasinghe & Edirisinghe, 2002).

SA/EC, 4:1, w/w ratio was found to be the most effective in terms of producing smallest nanoparticles and high encapsulation efficiency, as it did not cause any blockage of the stainless steel needle and furnished particles in the nano-range. This concentration was chosen for encapsulating food component, with a minimum amount of ethylcellulose in suspension (1 wt%), thus having the lowest surface tension (23 mN m^{-1}) and lowest viscosity (~2 mPa s).

Table 10: Characteristics of SA/EC and EV solutions (mean ± S.D., n = 5).

Solution	**Food component (wt%)**	**Lipid:Polymer (wt/wt%) ratio**	**Density (g/m^{-3})**	**Surface tension (mN m^{-1})**	**Viscosity (mPa s)**
PL2	-	4:1	795±0.00	23.0±0.20	2.1±0.1
PL21	1.2	4:1	782±0.00	24.5±0.31	2.20±0.06
PL22	1.6	4:1	786±0.00	23.0±0.15	2.13±0.08
PL23	2.5	4:1	792±0.00	22.7±0.32	2.07±0.05

The combination of low surface tension and low viscosity can give the smallest polymer-lipid nanoparticles in diameter in EHD spraying (Trotta et al., 2010). Polymer-lipid nanoparticles were produced using a flow rate of 10 and 15 µl/min, a collection distance was approximately 100 - 150 mm, and an applied voltage of 13 – 15 kV. Table 10 Lists the physical properties of various concentrations of food component in polymer-lipid system (4:1) dissolved in ethanol. It

was observed that the viscosity and surface tension of the spraying solution decreased as the amount of food component increased.

6.2.5 Influence of solvent

To prepare polymer-lipid nanoparticles, the primary requisite is a food grade solvent with a low boiling point, high volatility and high lipid solubility. Ethanol being capable of dissolving lipids, e.g. SA as well as EC, and being acceptable in food formulation, was selected as a solvent for preparing polymer-lipid nanoparticles. Due to its high volatility it is easily evaporated form the surface of nanoparticles as they form. Hence, the collection distance has to be optimised so as to allow evaporation of all ethanol from the surface, giving, polymer-lipid nanoparticles encapsulated food component.

6.3 Nanoparticles characterisation

6.3.1 Influence of flow rate

The surface morphology of the obtained polymer-lipid nanoparticles was studied using scanning electronic microscopy (SEM). The SEM images were used to calculate the standard deviation, mean diameter and polydispersivity index for each of the nanoparticle samples studied. Approximately 300 nanoparticles were measured, using the image analysis software ImageJ. Being the product of the stable cone-jet, the SEM images confirmed that food component encapsulated polymer-lipid nanoparticles diameter obtained were ranged between 10 - 100 nm diameter (polydispersity index 23%). Flow rate has tremendous effect on the nanoparticle size as only 10 and 15 µl/min flow rate furnished stable cone-jet.

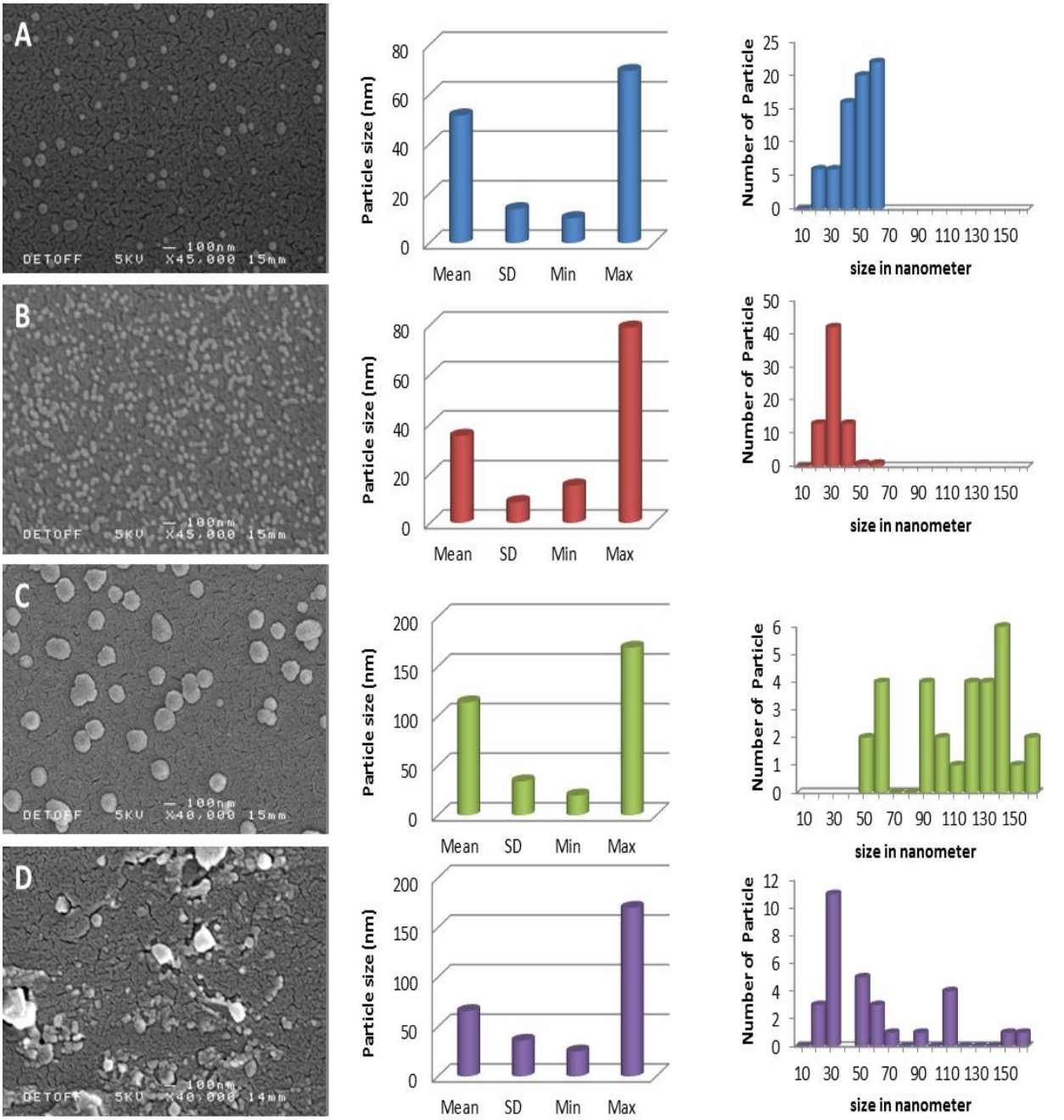

Figure 23: Particle size distribution of polymer-lipid nanoparticles from sample 4:1:1.7; SA/EC and EV (wt/wt%) (Table 10) at an applied voltage of 13-15 kV at different flow rates (µl/min) (a) 10, (b) 15, (c) 20, and (d) 25.

Other processing parameters were concentration of SA, EC and food component, applied voltage (13 - 15 kV), collection distance from the needle tip e.g. 100-150mm. SEM images (Figure 23a and b) confirmed the spherical shape of polymer-lipid nanoparticles and indicated a homogenous distribution. However, size ranges (Figure 23c and d) between 20 to 170 nm in diameter were obtained indicating the size of polymer-lipid nanoparticles is highly dependent on flow rate and applied voltage (Tang & Gomez, 1996).

6.3.2 Influence of applied voltage

Images of the nanoparticles formed under ambient conditions are shown in Figure 24A.

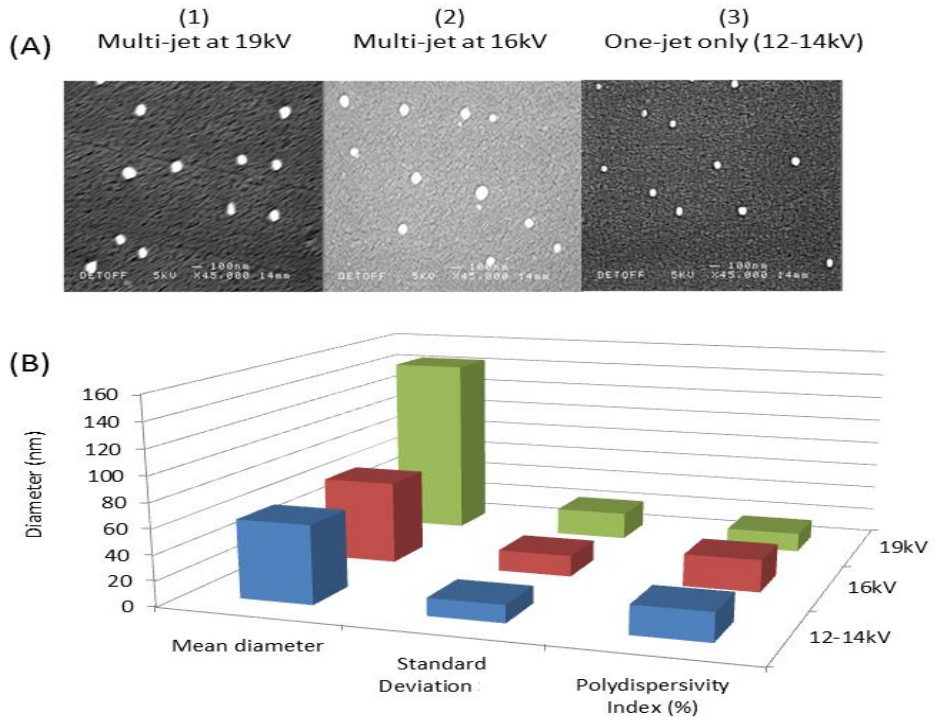

Figure 24: SEM images of nanoparticles prepared under ambient conditions (A) at 12-14kV, 16kV, and 19kV; (B) corresponding size distributions of nanoparticles prepared. Flow rate used was 10 µl/min.

Under an applied voltage of 12-14kV, the nanoparticles had an average diameter of 62±14 nm (Figure 24B). Particles prepared with voltages of 16 and 19kV were less uniform in size and shape, and had an average diameter of 66±17 nm (Figure 24B and C). The lower applied voltage of 12kV provided a more stable cone-jet and correspondingly resulted in more uniform nanoparticles.

6.3.3 Chemical structure

Figure 25 (a-c) shows the IR spectra for food component, polymer-lipid nanoparticles, and food component encapsulated polymer-lipid nanoparticles respectively. FTIR spectroscopy was done to determine the chemical interactions among inert ingredient e.g. SA, EC and food component e.g. EV.

The IR spectra peaks of food component encapsulated polymer-lipid nanoparticles (Figure 25 c), located at peaks 3493, 2941 cm^{-1} and 2853cm^{-1} which usually overlaps with the absorption band of C–H vibration result by stretching vibration of O–H group. Figure 25 b and c shows a peaks at 3478 and 3493 cm^{-1} which is due to the -OH groups present on the structure of the ethylcellulose repeating units (Desai et al., 2006) . Also, it represents the intra- and intermolecular hydrogen bonding due to the -OH groups (Ravindra et al., 1999).

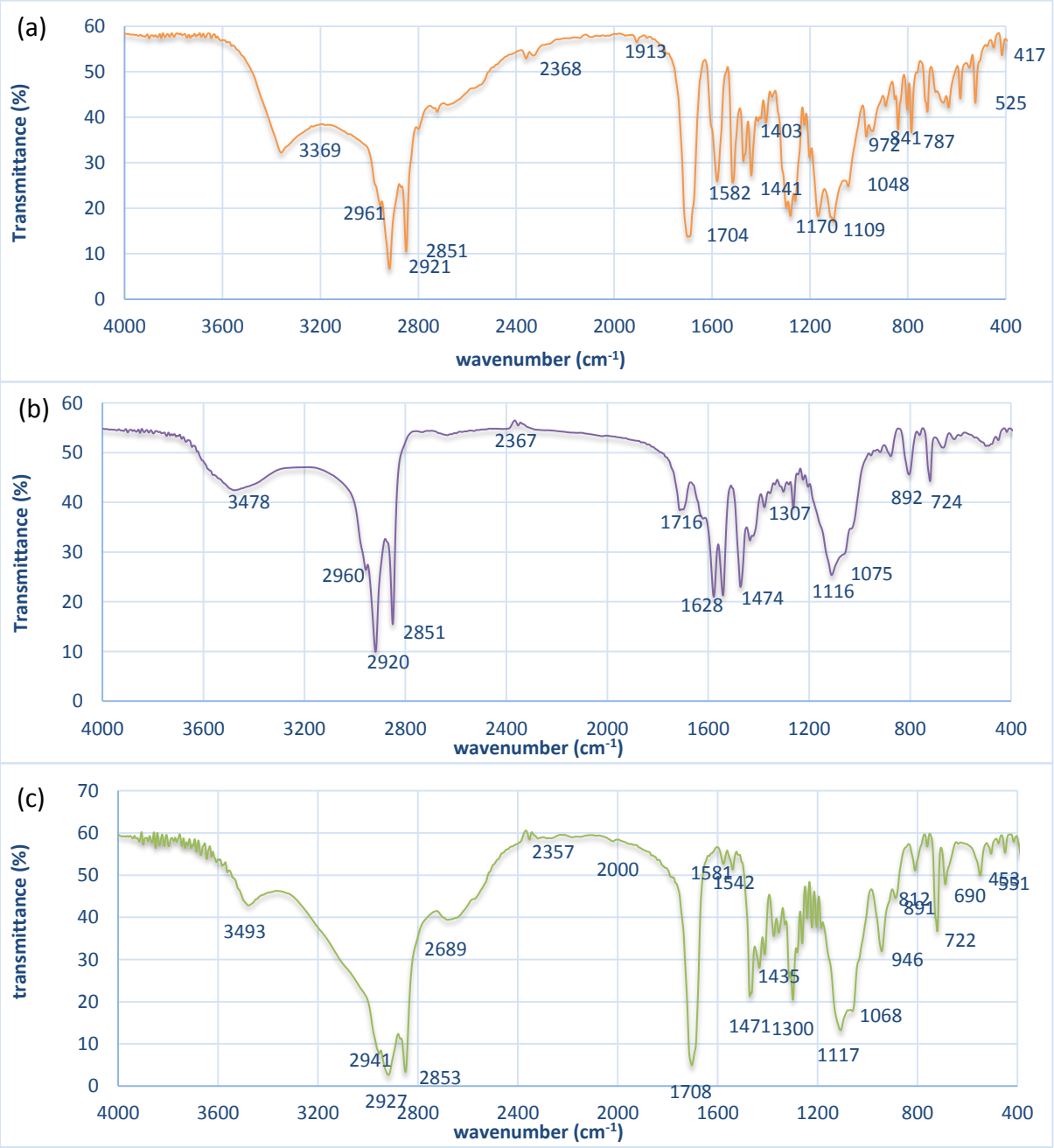

Figure 25: FT-IR spectra of: (a) pure food component (ethylvanillin); (b) polymer-lipid nanoparticles, and (c) EV encapsulated polymer-lipid nanoparticles.

While the peak at around 1708 cm^{-1} belongs to the stretching vibration of carbonyl group (C=O) and the peak at 1471 cm^{-1} is the $–CH_2$ bending peak, 1300 cm^{-1} represents C–H and C–C bending group and 722 cm^{-1} and 960 cm^{-1} corresponds to rocking vibration and bending, which are all characteristic for chain of stearic acid (Wang et al., 2011). The peak at around 1117 cm^{-1} is attributed to C–O stretching. Form the FT-IR spectra of food component, polymer-lipid nanoparticles, and food component encapsulated polymer-lipid nanoparticles, it is clearly seen that the FT-IR spectrum of the all the peaks of food component, polymer-lipid nanoparticles, and food component encapsulated polymer-lipid nanoparticles has no significant new peaks indicates there are no chemical reaction between food component and SA/EC. The only small difference is the peak positions in the food component, polymer-lipid nanoparticles, and food component encapsulated polymer-lipid nanoparticles. These changes are attributed to the interactions between oxygen atom of carbonyl group (C=O) (Wang et al., 2011) and of SA and hydrogen atom of hydroxyl group (O–H) of EV.

6.4 Entrapment efficiency and loading capacity

A UV spectrophotometer was used to measure the absorbance of the solution with a known concentration. A calibration curve was prepared for known concentrations of food component e.g. EV at a wavelength of 320 nm. The encapsulation efficiency of the polymer-lipid nanoparticle was found by quantifying the entrapped food component in polymer-lipid nanoparticle. Measurement of food component (e.g. ethyl vanillin) entrapment efficiency and loading capacity were performed by EHD spraying 1 ml of spraying solution and dispersing the polymer-lipid nanoparticle in 10 ml of double distilled water (collection liquid) kept at 25±2 °C.

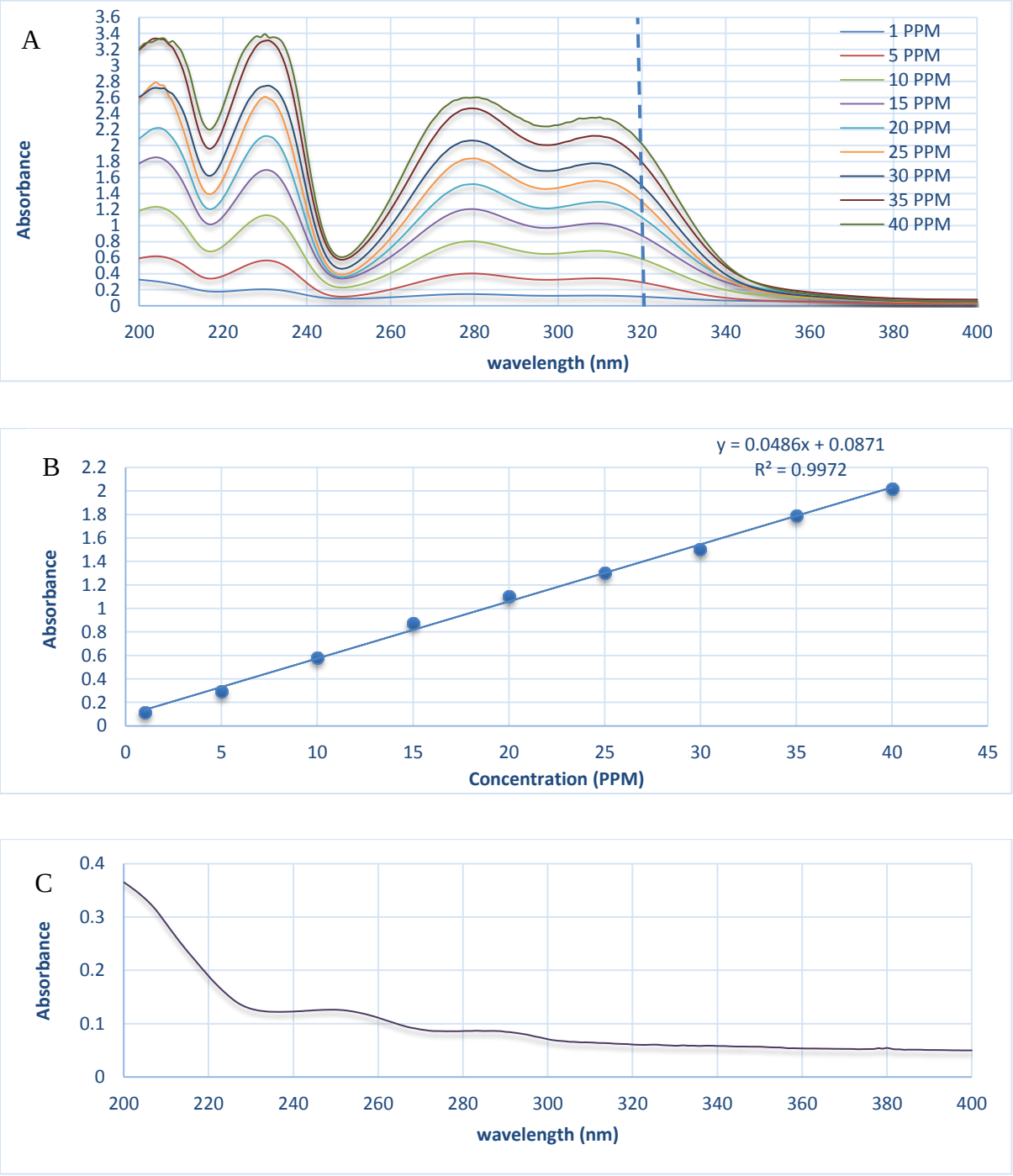

Figure 26: UV spectra (200 – 320) of (a) EV in different concentration (1 - 40 ppm), (b) calibration curve, and (c) EV encapsulated polymer-lipid nanoparticles.

These polymer-lipid nanoparticle dispersed in double distilled water were subjected to stirring for about 10 min.

Knowing the initial amount of food component used in preparing the food component encapsulated polymer-lipid nanoparticles, the percentage of food component encapsulated in the polymer-lipid nanoparticle (encapsulation efficiency) was obtained by (Equation 7and Equation 10) and (Equation 8 and Equation 9) respectively.

UV spectroscopic analysis of polymer-lipid nanoparticles indicated the presence of food component with in polymer-lipid nanoparticles (Figure 26). The total amount of food component leached ones into the supernatant (water) after centrifugation was calculated by the absorbance at 274 nm (Figure 26c). Food component was encapsulated within polymer-lipid nanoparticles with a 88.5% entrapment efficiency and a 89% loading capacity, indicating higher entrapment efficiency as well as a high loading capacity.

6.5 Formation of core-shell structure

TEM images of the nanoparticles were also obtained at an accelerating voltage of 80 kV. One millilitre of the nanoparticle solution was spread onto a copper grid for observation. The nanoparticle samples were then stained with a 2% solution of uranyl acetate for 30 seconds and allowed to dry. TEM images of the nanoparticles prepared from a cone-jet with and without food component are shown in Figure 27. Here, all the nanoparticles exhibited similar levels of contrast, indicating layered structure.

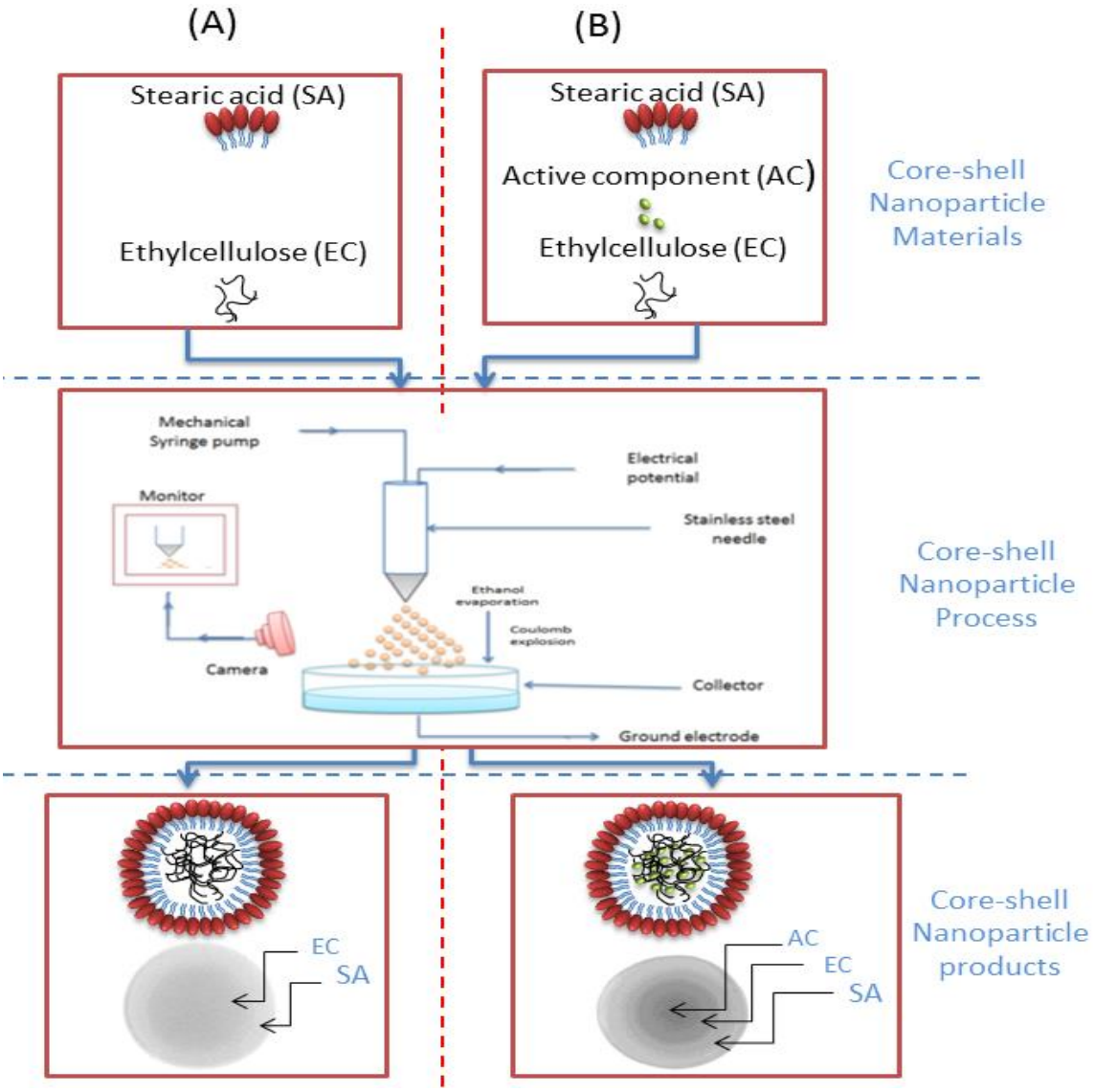

Figure 27: EHD sprayed core-shell polymer-shell nanoparticle assembly and process; (A) nanoparticle without, and (B) with encapsulated EV.

Figure 27(A, B) shows the assembly and process of EHD preparation of core-shell nanoparticles (A) with no food component, (B) encapsulating an food component, the solution jet is accelerated towards the collector, and then ethanol evaporates gradually, resulting in the formation of nanoparticles, with a layered structure.

Figure 27(A, B) shows the nanoparticles as white/black domains shell-core structure because the samples were pretreated by a negative staining technique. Negative staining is one such contrast enhancement method. Negative staining for light microscopy is an indirect staining where the background instead of the specimen is stained the unstained specimen appears as bright object against a dark background hence the name Negative Staining. Similarly staining for transmission electron microscopy the specimen is unstained whereas the background appears dark, as the heavy metals used for negative staining do not penetrate the specimen but stain the background dark. Water-soluble 2% uranyl acetate stain the area not occupied by the nanoparticles. Consequently, electron beam goes through the areas where the nanoparticles are only as they cannot pass through the areas where the heavy metal is. Figure 27(A) shows two layers (shell-core) structures which are attributed to SA and EC respectively. However, Figure 27(B) shows an extra inner layer, attributed to the food component, encapsulated within the core (EC).

6.6 Structure stability of nanoparticle and suitability for delivery application

In this section, show that polymer-lipid core-shell nanoparticles composed of stearic acid and ethylcellulose and containing model food components (Vanillin (VA), ethylmaltol (EMA), and Maltol (MA)) can be produced in a one step process using EHD techniques. The conditions under which a stable cone-jet was formed were identified and by varying the EHD processing parameters, nanoparticles with a tunable size less than ≤100 nm were produced. The overall structure of the nanoparticles produced was tested by multiple measures to ensure that they were core-shell polymer-lipid nanoparticles containing food component rather than a homogenous matrix. Also, demonstrates the suitability of these polymer-lipid nanoparticles for food

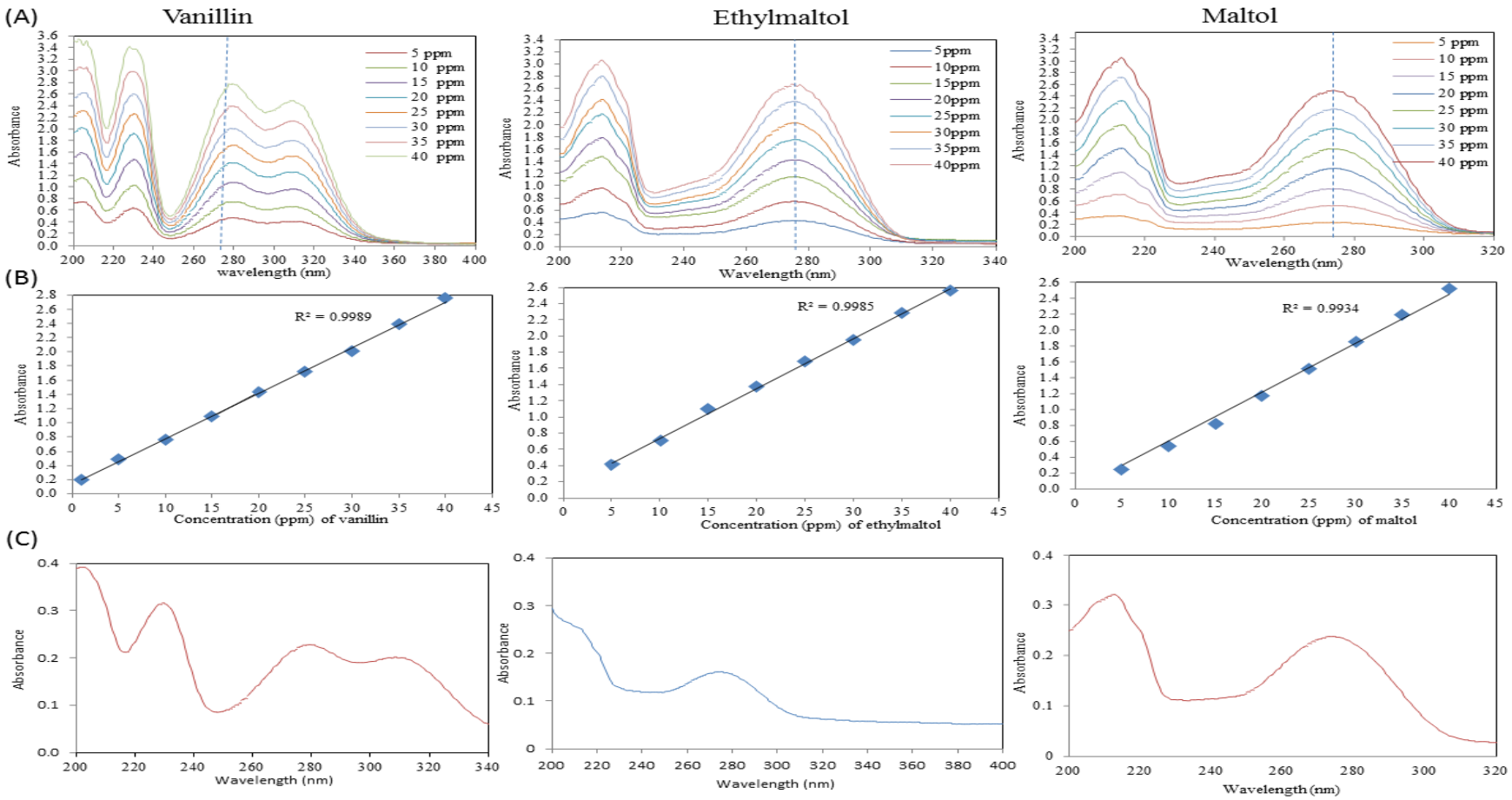

Figure 28 Absorption spectra of VA, EMA, and MA; (a) at different concentrations (1 - 40 ppm), (b) calibration curves, and (c) food component release from nanoparticles.

component encapsulation and delivery applications. Demonstrates the suitability of the one step single needle EHD has the ability to produce a core-shell polymer-lipid nanoparticle structure.

6.6.1 Suitability of polymer-lipid nanoparticles for delivery applications

The nanoparticle solution was centrifuged at 4000 rpm for 10 min at 25±2 °C. The amount of food component released was measured using UV spectrophotometry.

A calibration curve of various food component concentrations (5–40 ppm) versus absorbance was plotted. The amount of food component released was subtracted from the total amount of food component in the nanoparticles to calculate the amount encapsulated according to Equation 9 respectively.

The overall structure of the nanoparticles produced was tested by multiple measures to ensure that they were core-shell polymer-lipid nanoparticles containing food component rather than a homogenous matrix. During the collection of the nanoparticles, some food component was also released into the DDW. The amount released of VA, EMA, and MA in the supernatant from the nanoparticle solutions was found to be 13%, 13.2%, and 10.3% respectively, meaning that 86.8%, 87%, and 89.7% of the food component VA, EMA, and MA (Figure 28) respectively was encapsulated in the nanoparticles. This demonstrates the suitability of these polymer-lipid nanoparticles for food component encapsulation and delivery applications.

6.6.2 Interactions between the nanoparticles and water molecules

Core-shell nanoparticles were stored in DDW for 90 days at the ambient temperature (25±2 ^{O}C), then a drop (~1 ml) of the nanoparticle solution was again observed using TEM. As illustrated in Figure 29, during the nanoparticle storage in DDW interactions between the nanoparticles and water molecules occur, due to hydrogen bonding. This results in

penetration of the water into the nanoparticles augmented by hydrophobic repulsion from the solvent and favorable intermolecular interactions on the structure of the nanoparticles. Finally, the food component molecules are released into the DDW leaving hollow SA-EC nanoparticles (Figure 29B). On the basis of the observations described above, it is clearly evident that the one step single needle EHD has the ability to produce a core-shell polymer-lipid nanoparticle structure.

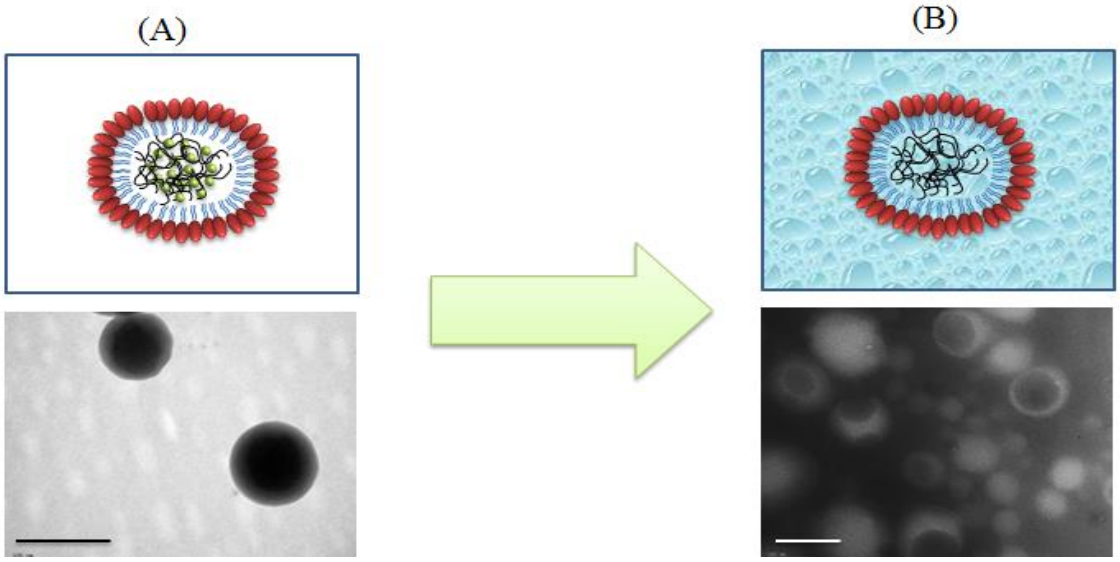

Figure 29: Schematic and corresponding TEM image of nanoparticles: (A) immediately after collection and before food component release, (B) after food component release. Scale bar 100nm.

6.6.3 Suitability of nanoparticles for shelf life stability of nanoparticles

Samples of EHD sprayed nanoparticles were stored dry for 90 days at the ambient temperature (25±2 ^{O}C), and then observed again using FTIR. Figure 30(A-C) shows the IR spectra (day 0, and 90) for core-shell polymer-lipid nanoparticles with and without food component e.g. VA, EMA, and MA respectively.

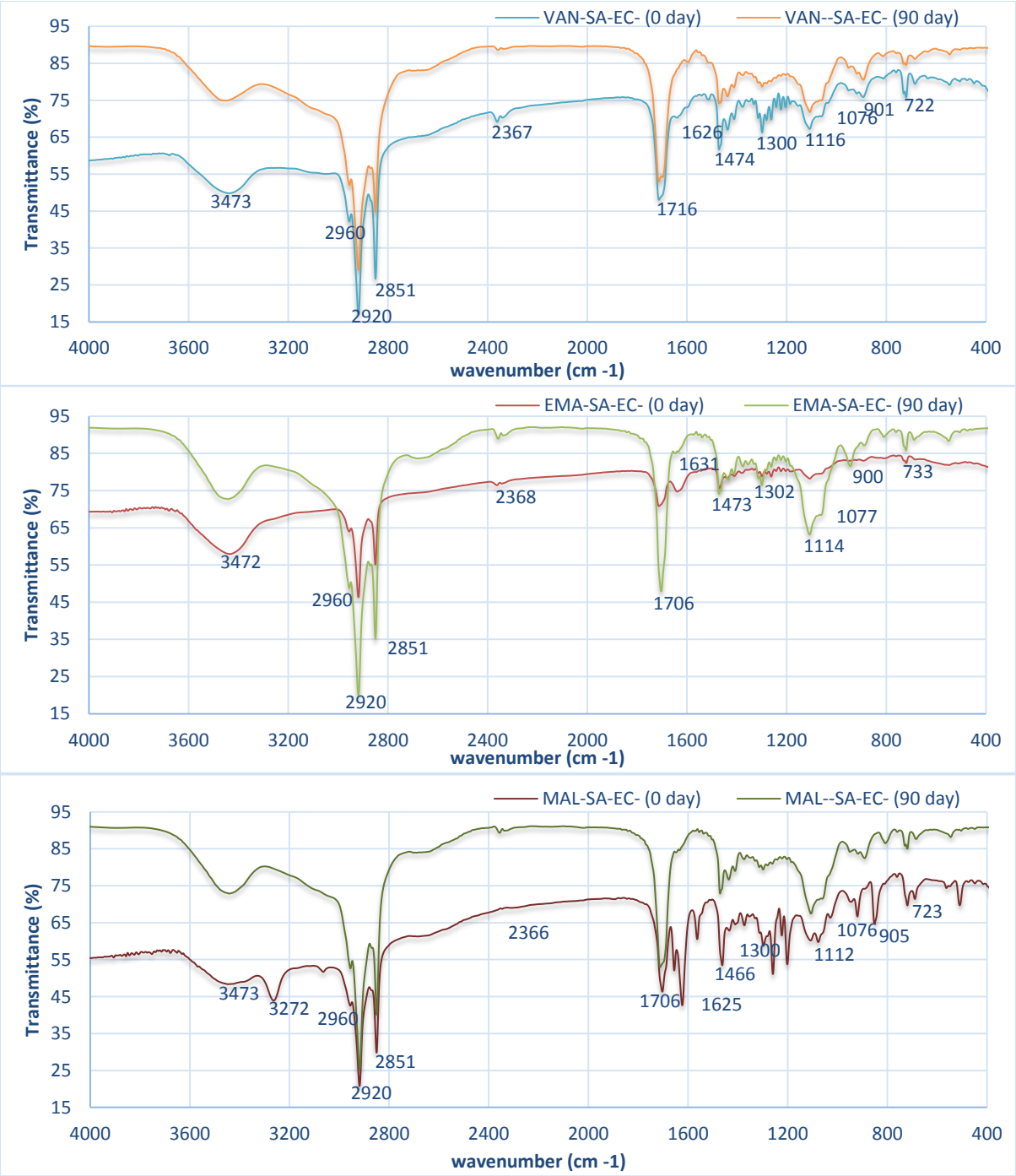

Figure 30 Comparison of the FTIR spectra of: (A) nanoparticles containing SA/EC only (for day 0 only), and nanoparticles (SA/EC) encapsulating food components (for day 0, and 90) (B) VA, (C) EMA, and (D) MA.

The IR spectra peaks of the latter (Figure 25B) were located at 3478 cm^{-1} and 2851cm^{-1} which overlaps with the absorption of C–H vibration result by stretching vibration of O–H group.

Figure 30(A-C) shows a peak between 3473 - 3472 cm^{-1} represents the intra- and inter-molecular hydrogen bonding due to the -OH groups (Ravindra et al., 1999) present on the structure of the ethylcellulose (Desai et al., 2006). The peak at ~1716 cm^{-1} belongs to the stretching vibration of the carbonyl group (C=O) and the peak at 1474 cm^{-1} is the $–CH_2$ bending peak, 1300, 1307 cm^{-1} represents C–H and C–C bending group and 722 cm^{-1} and 892 cm^{-1} corresponds to rocking vibration and bending, which are all characteristic for chain of stearic acid (Wang et al., 2011).

The peak at around 1112, 1116 cm^{-1} is attributed to C–O stretching. From the spectra of EC SA, and food component it is clearly seen that the FT-IR spectrum of the all the peaks of SA, EC, and food component has no significant new peaks. There are small shift in the peak positions, due to the interactions between the oxygen atoms of the (C=O) (Wang et al., 2011) of SA and the hydrogen atoms of the O–H and C-H of the food components e.g. EMA, MA (Li & Yang, 2008).

6.6.4 Physical form of nanoparticles

The physical for of food component and food component loaded nanoparticles was analysed using DSC and measured between 10 and 300 ^oC at a heating rate of 10 $^oC\ min^{-1}$. Figure 31 shows DSC thermograms for (A) empty nanoparticles (SA/EC) only, and nanoparticles (SA/EC) encapsulating food components (B) VA, (C) EMA, and (D) MA.

Figure 31 (A-D) shows DSC measurements of the samples; SA/EC only, and SA/EC with food components (VA, EMA, and MA), heated in range of 20-300 ^OC, and then cooled and reheated.

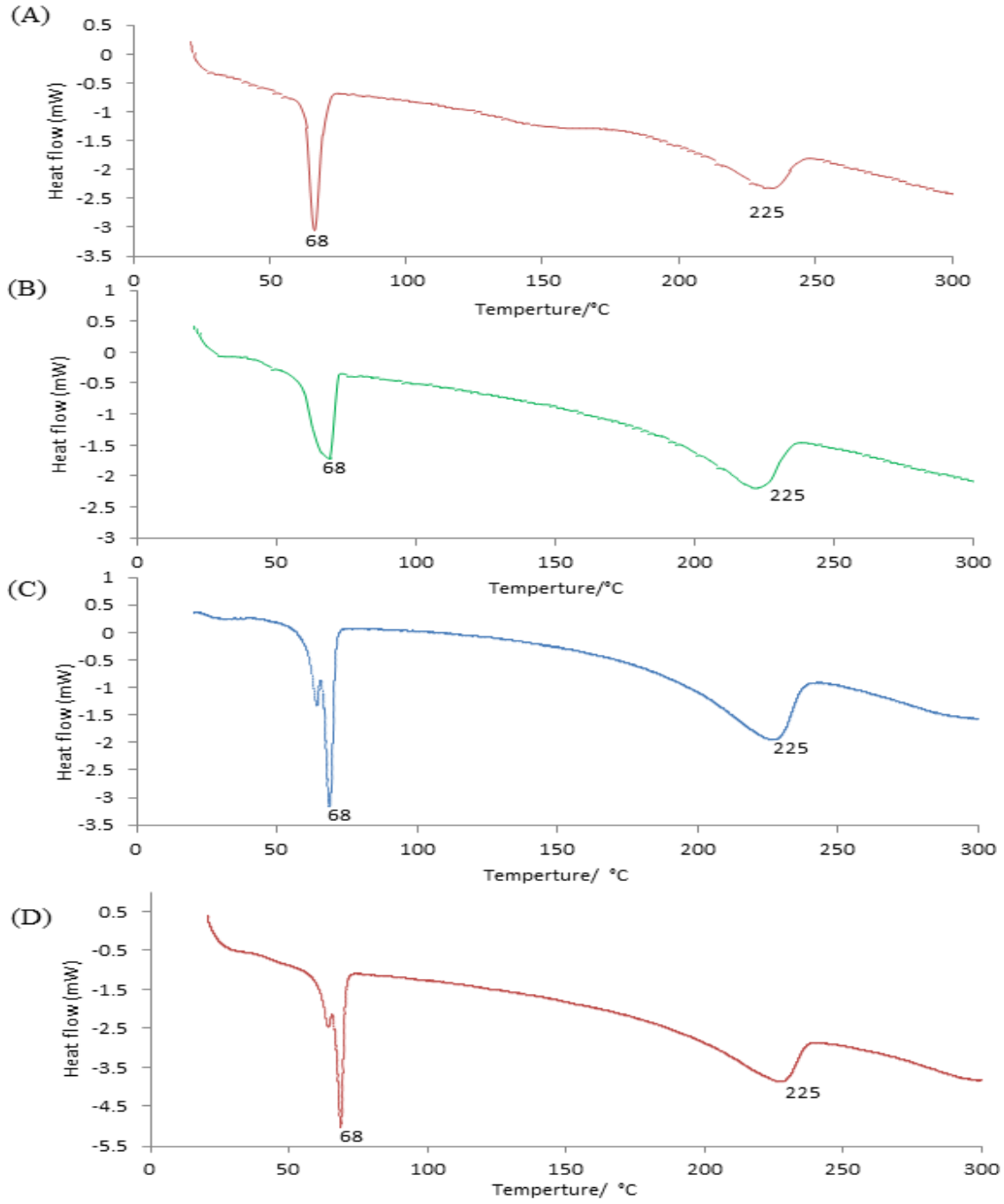

Figure 31: Comparison of the DSC melting curves of; (A) empty nanoparticles (SA/EC) only, and nanoparticles (SA/EC) encapsulating food components (B) VA, (C) EMA, and (D) MA. All curves were recorded with the same temperature calibration

Figure 31 (A) shows the results for the SA/EC nanoparticles indicating crystalline structures. There are two melting peaks 68 ^{O}C and 225 ^{O}C, these two melting peak represent SA and EC respectively. A change of exothermic peak shape was observed with the nanoparticle encapsulated food component VA, EMA, MA in range between 100-250 ^{O}C in Figure 31 (B-D). This was not seen for the polymer-lipid nanoparticle (Figure 31A). The melting point endotherms for food component in food component loaded nanoparticles were disappeared. All in all observations indicate that food component is in an amorphous form in food component loaded nanoparticles and that interactions are present between food component and nanoparticles. Also, it may also be explained by the miscibility of food component in the nanoparticles (Hyvönen et al., 2005), or changed during the EHD spraying process into an amorphous phase (Hanawa et al., 1996). No extra peaks were observed in the DSC of the nanoparticles with or without food component content.

6.7 Summary

This study has demonstrated that core-shell polymer-lipid nanoparticles encapsulating a food component can be prepared by single needle EHD processing. It is clearly evident that the one step single needle EHD has the ability to produce a homogeneous core-shell polymer-lipid structure nanoparticle with good stability. The size and food component content of the nanoparticles could be controlled by varying the EHD parameters and solution properties. The study suggests that the lipid component (e.g. stearic acid) stabilises the nanoparticles against collapse and aggregation and improves encapsulation. Furthermore, it has been demonstrated that EHD processing enables the polymer-lipid nanoparticle size to be tuned in a reproducible manner whilst allowing a narrow size distribution to be achieved.

Chapter 7 Conclusions and Future Work

7.1 Conclusions

With this in mind the influence of different processing parameters on the nanoparticle formation process, nanoparticle characteristic and food component release were investigated. This was done by studying a few different parameters which have previously been shown to have and important influence on nanoparticle characteristic, including flow rate, food component loading and composition of polymer and lipid. The study was focussed on four models of food, and the influence of different materials (e.g. polymer, lipid, mixed polymer and lipid).

7.1.1 Polymer nanoparticles encapsulating food flavour

7.1.1.1 Preparation, characterisation and release kinetics

This study has demonstrated that simple single needle EHD processing can be used to prepare nanoparticles from a food grade polymer (e.g. ethylcellulose) encapsulating a food component (e.g. ethylvanillin) with high encapsulation and loading efficiency. In this study a stable cone-jet was established over a range of liquid flow rates from 15 to 25 µl min^{-1} and applied voltages from 13.6 to 14.5 kV. This was found to be necessary for forming uniform nanoparticles.

The loading and encapsulation efficiency of EV at different concentrations (1, 2.5 and 5 wt%) in the nanoparticles from solutions P3, P4, and P7 were found to be 81, 80, and 75 and 84, 83 and 78%, respectively, e.g. the loading and encapsulation efficiency of the nanoparticles decreased as the amount of EV increased. EV (1 wt%, by weight) was encapsulated within nanoparticles (P3) with 84% encapsulation efficiency. The effect of flow rate on food component release rate shows that as flow rate increased the release rate decreased.

Adjusting the EHD processing parameters allowed the nanoparticle size to be controlled in a reproducible manner whilst maintaining a relatively narrow size distribution. This is important because the release of the food ingredient was found to be very sensitive to nanoparticle size. It was shown that the release of the ethylvanillin from the nanoparticles was sustained over 15 h; and that the release period could be controlled, again by varying the processing parameters. It was shown that the release of the ethylvanillin described by a Ritger-Peppas release model and indicating that release occurred through a non-Fickian diffusion mechanism.

7.1.2 Lipid nanoparticles encapsulating food flavour

7.1.2.1 Preparation, characterisation and release kinetics

In summary, it has been demonstrated that lipid nanoparticles encapsulating a model flavour component (ethylvanillin) can be produced by EHD spraying. It found that the diameter and size distribution of the nanoparticles could be controlled by varying the lipid:ethylvanillin concentration ratio in the sprayed solution.

As showed in chapter 5, nanoparticles were successfully prepared using a single step EHD technique at a flow rate of 15 μl min^{-1} with an applied voltage of 14.5 kV and a collection distance of ~100 mm. Uniform nanoparticles with a mean diameter of 65±6 nm were obtained.

The nanoparticles were found to have a core-shell structure, with the thickness (20 ± 10 nm) of the outer lipid layer being dependent up on the concentration of lipid in the processed solution. The encapsulation efficiency and loading capacity were similarly found to be dependent on the lipid: ethylvanillin concentration ratio; although there was found to be a limit above which both started to decrease. It was shown that the release of the ethylvanillin

described by a zero-order release model and was a function of the nanoparticle size, and lipid: ethylvanillin concentration ratio. This technique for preparation of lipid nanoparticles in one step may be useful for production of lipid based nanoparticles with different characteristics for food applications.

7.1.3 Polymer-lipid nanoparticles encapsulating food flavour

7.1.3.1 Preparation, characterisation, encapsulation efficiency and loading capacity

This study has demonstrated that core-shell polymer-lipid nanoparticles encapsulating a food component can be prepared by EHD processing. It is clearly evident that the one step EHD has the ability to produce a homogeneous core-shell polymer-lipid structure nanoparticle with good stability. The size and food component content of the nanoparticles could be controlled by varying the EHD parameters and solution properties. The study suggests that the lipid component (e.g. stearic acid) stabilises the nanoparticles against collapse and aggregation and improves encapsulation. Furthermore, it has been demonstrated that EHD processing enables the polymer-lipid nanoparticle size to be tuned in a reproducible manner whilst allowing a narrow size distribution to be achieved.

Food ingredient component was encapsulated in polymer-lipid nanoparticles with a good entrapment efficiency and a loading capacity. Based on the findings of this study EHD spraying carried out at the ambient temperature with the major process control parameter of applied voltage and flow rate can be exploited as a potentially attractive method to prepare polymer-lipid nanoparticles containing a low solubility food ingredient such as flavour component. This demonstrates the suitability of these polymer-lipid nanoparticles for food component encapsulation and delivery applications.

7.2 Future work

Based on the research done in this project and result obtained, several aspects of future work are recommended as follows:

7.2.1 Further investigation of the nanoparticle formation process

In this thesis, the EHD spraying nanoparticle formation process was investigated by looking at properties of EHD spraying solutions and characteristics and food component release profile of the nanoparticles. Further build on the results of this thesis, droplet formation and the initial droplet drying stage could be looked further into by visualisation using a high speed camera (e.g. high-speed camera at a frame rate of 1/20000s). This high speed camera would be used to capture images of EHD sprayed droplet immediately after detachment from the cone-jet further downstream of the spray. By capturing the images at different distance from the cone jet it would be interesting to study different stage droplet formation as well as mechanism such as Coulomb fission. This study may give interesting and important new information on the nanoparticle formation process with EHD spraying and the result can be compared with similar spray study done by other research.

7.2.2 Physical structure of nanoencapsulates food ingredients

In the present thesis, nanoparticles were prepared from mono layer lipid with/without polymer to study the influence of these parameters (ratios, concentrations) on the food component delivery in the nanoparticles. The study indicated polymer, lipid concentration and/or ratio may have influence on the food component physical structure in EHD spraying nanoparticles and release profile. The influence of polymer, lipid and food component ingredient concentration and/or ratio would be interesting to further investigate by examining model of multilayer lipid. It is believed to decrease the rate of food ingredient component

release from the nanoparticles. In this case, the shell protects the inner core and environment to some extent against mechanical damage and also against environmental conditions.

7.2.3 Control of food component distribution in nanoparticles of food delivery

In the present thesis, nanoparticles were prepared in different concentration and type and materials to study the influence of these parameters on the food component delivery in the nanoparticles.

The study indicated polymer, lipid concentration and/or ratio may have influence on the food component distribution in EHD spraying nanoparticles. The influence of polymer, lipid and food component ingredient concentration and/or ratio would be interesting to further investigate by examining model of multilayer lipid and functional food ingredient.

7.2.4 Release kinetics from nanoparticles loaded with different food component

In extension of the food component release studies performed in this thesis, where the influence of different nanoparticle characteristic on food component release was studied, it would be interesting to examine the influence of food molecular weight and food component water solubility on their food component release kinetics from nanoparticles.

7.2.5 Delivery system design and nanoparticle characteristics

In this work, I developed nanocarriers (polymer, solid lipid nanoparticles and core-shell nanostructure nanocarriers) for food systems. Having small size, high encapsulation efficiency and potential for large scale production, made nanostructure nanocarriers very interesting to the food sectors. However, there were some limitations incorporated with nanocarriers such as rapid release during initial release times (burst release) as well as particle aggregation due to their low surface charges. Bioavailability of nutritional ingredients

may be enhanced when they are protected in gastric medium and delivered in the colon environment. These drawbacks of nanocarrier motivated us to conduct the current work to produce novel nanocarriers using layer by layer coating of nanocarriers by employing lipid and polymers in order to decrease burst release and enhance stability. The aim of section was to develop novel nanocarriers coated with lipids to overcome nanocarrier burst release and low stability and bioavailability.

The incorporation of manufactured nanoparticles into food products has grown exponentially due to its many advantages. Thesis has highlighted the applications of nanoparticles in the food industry. However there have been safety concerns raised regarding the use of nanoparticles in food products, which was the possibility that nanoparticles could exert toxicity. As a result the need to develop standardized traceable methodology along with certified reference materials for the characterisation of nanoparticles in complex matrices has been much needed recently to provide quality assurance for the experimental work.

The characterisation of nanoparticles in complex food matrices has become a major challenge. The issue with complex food matrices are that they contain a wide range of different natural and engineered nano-size structures which are integrated into the matrices this increases the difficulty of separating and detecting the nanoparticle. Furthermore the appropriate methods in separating the nanoparticle from the food matrices either via physical or chemical means must be selected with care. This was because reducing or changing nanoparticles surrounding such as altering the matrices could potentially affect nanoparticles properties and behaviour. What's more during the analysis of the nanoparticles, interactions could potentially occur between the nanoparticles and the food matrices. This was because nanoparticles have unusual properties compared with larger bulk materials such as their larger surface area to volume ratio that causes them to have a tendency to agglomerate. This

certainly adds to the complexity of analyzing nanoparticles in food. In order to tackle the problem of possible aggregation and problem of matrices, a combination of characterisation methods will be required in order to successfully characterise the nanoparticles.

Some of the nanoparticle characteristics that can be designed into a nano-delivery system to address these issues are;

I. Stability
II. Biological properties
III. Nanoparticle size distribution
IV. Nanoparticle permeability
V. Environmental responsiveness

References…

Al-Omran, M. F., Al-Suwayeh, S. A., El-Helw, A. M., & Saleh, S. I. (2002). Taste masking of diclofenac sodium using microencapsulation. Journal of Microencapsulation, 19(1), 45-52.

Almería, B., Deng, W., Fahmy, T. M., & Gomez, A. (2010). Controlling the morphology of electrospray-generated PLGA microparticles for drug delivery. Journal of Colloid and Interface Science, 343(1), 125-133.

Almería, B., Fahmy, T. M., & Gomez, A. (2011). A multiplexed electrospray process for single-step synthesis of stabilized polymer particles for drug delivery. Journal of Controlled Release, 154(2), 203-210.

Amsden, B. G., & Goosen, M. F. A. (1997). An examination of factors affecting the size, distribution and release characteristics of polymer microbeads made using electrostatics. Journal of Controlled Release, 43(2-3), 183-196.

Arya, N., Chakraborty, S., Dube, N., & Katti, D. S. (2009). Electrospraying: A Facile Technique for Synthesis of Chitosan-Based Micro/Nanospheres for Drug Delivery Applications. Journal of Biomedical Materials Research Part B-Applied Biomaterials, 88B(1), 17-31.

Awad, T. S., Helgason, T., Kristbergsson, K., Decker, E. A., Weiss, J., & McClements, D. J. (2008). Effect of cooling and heating rates on polymorphic transformations and gelation of tripalmitin Solid Lipid Nanoparticle (SLN) suspensions. Food Biophysics, 3(2), 155-162.

Bocca, C., Caputo, O., Cavalli, R., Gabriel, L., Miglietta, A., & Gasco, M. R. (1998). Phagocytic uptake of fluorescent stealth and non-stealth solid lipid nanoparticles. International Journal of Pharmaceutics, 175(2), 185-193.

Bock, N., Woodruff, M. A., Hutmacher, D. W., & Dargaville, T. R. (2011). Electrospraying, a reproducible method for production of polymeric microspheres for biomedical applications. Polymers, 3(1), 131-149.

Bonanome, A., Bennett, M., & Grundy, S. M. (1992). Metabolic effects of dietary stearic acid in mice: Changes in the fatty acid composition of triglycerides and phospholipids in various tissues. Atherosclerosis, 94(2-3), 119-127.

Bottger, P. H. M., Bi, Z., Adolph, D., Dick, K. A., Karlsson, L. S., Karlsson, M. N. A., . . . Deppert, K. (2007). Electrospraying of colloidal nanoparticles for seeding of nanostructure growth. Nanotechnology, 18(10).

Brandenberger, H., Nüssli, D., Piëch, V., & Widmer, F. (1999). Monodisperse particle production: A method to prevent drop coalescence using electrostatic forces. Journal of Electrostatics, 45(3), 227-238.

Bruss, M. L. (1997). Chapter 4 - Lipids and Ketones. In J. J. Kaneko, W. H. John & M. L. Bruss (Eds.), Clinical Biochemistry of Domestic Animals (5) (pp. 83-115). San Diego: Academic Press.

Cavalli, R., Bocca, C., Miglietta, A., Caputo, O., & Gasco, M. (1999). Albumin adsorption on stealth and non-stealth solid lipid nanoparticles. STP pharma sciences, 9(2), 183-189.

Cavalli, R., Caputo, O., Carlotti, M. E., Trotta, M., Scarnecchia, C., & Gasco, M. R. (1997). Sterilization and freeze-drying of drug-free and drug-loaded solid lipid nanoparticles. International Journal of Pharmaceutics, 148(1), 47-54.

Cavalli, R., Caputo, O., & Gasco, M. R. (1993). Solid lipospheres of doxorubicin and idarubicin. International Journal of Pharmaceutics, 89(1), R9-R12.

Celebioglu, A., & Uyar, T. (2010). Cyclodextrin nanofibers by electrospinning. Chemical Communications, 46(37), 6903-6905.

Celebioglu, A., & Uyar, T. (2012). Electrospinning of nanofibers from non-polymeric systems: polymer-free nanofibers from cyclodextrin derivatives. Nanoscale, 4(2), 621-631.

Chakraborty, S., Liao, I. C., Adler, A., & Leong, K. W. (2009). Electrohydrodynamics: A facile technique to fabricate drug delivery systems. Advanced Drug Delivery Reviews, 61(12), 1043-1054.

Chang, M. W., Stride, E., & Edirisinghe, M. (2010). Controlling the thickness of hollow polymeric microspheres prepared by electrohydrodynamic atomization. Journal of the Royal Society Interface, 7(SUPPL. 4), S451-S460.

Chen, D.-R., Pui, D. Y., & Kaufman, S. L. (1995). Electrospraying of conducting liquids for monodisperse aerosol generation in the 4 nm to 1.8 μm diameter range. Journal of Aerosol Science, 26(6), 963-977.

Chen, H., Weiss, J., & Shahidi, F. (2006a). Nanotechnology in nutraceuticals and functional foods. Food Technology, 60(3), 30-36.

Chen, H. D., Weiss, J. C., & Shahidi, F. (2006b). Nanotechnology in nutraceuticals and functional foods. Food Technology, 60(3), 30-36.

Chen, L., Remondetto, G. E., & Subirade, M. (2006c). Food protein-based materials as nutraceutical delivery systems. Trends in Food Science and Technology, 17(5), 272-283.

Choi, M.-J., Ruktanonchai, U., Soottitantawat, A., & Min, S.-G. (2009). Morphological characterization of encapsulated fish oil with β-cyclodextrin and polycaprolactone. Food Research International, 42(8), 989-997.

Ciach, T. (2006). Microencapsulation of drugs by electro-hydro-dynamic atomization. International Journal of Pharmaceutics, 324(1), 51-55.

da Silva Malheiros, P., Daroit, D. J., & Brandelli, A. (2010). Food applications of liposome-encapsulated antimicrobial peptides. Trends in Food Science & Technology, 21(6), 284-292.

Dave, B. S., Amin, A. F., & Patel, M. M. (2004). Gastroretentive drug delivery system of ranitidine hydrochloride: formulation and in vitro evaluation. American Association of Pharmaceutical Scientists, 5(2), 77-82.

De Juan, L., & De La Mora, J. F. (1997). Charge and size distributions of electrospray drops. Journal of colloid and interface science, 186(2), 280-293.

De Miguel, I., Imbertie, L., Rieumajou, V., Major, M., Kravtzoff, R., & Betbeder, D. (2000). Proofs of the structure of lipid coated nanoparticles (SMBV (TM)) used as drug carriers. Pharmaceutical Research, 17(7), 817-824.

de Vos, P., Faas, M. M., Spasojevic, M., & Sikkema, J. (2010). Encapsulation for preservation of functionality and targeted delivery of bioactive food components. International Dairy Journal, 20(4), 292-302.

Desai, J., Alexander, K., & Riga, A. (2006). Characterization of polymeric dispersions of dimenhydrinate in ethyl cellulose for controlled release. International Journal of Pharmaceutics, 308(1–2), 115-123.

Ding, L., Lee, T., & Wang, C. H. (2005). Fabrication of monodispersed Taxol-loaded particles using electrohydrodynamic atomization. Journal of Controlled Release, 102(2), 395-413.

Doshi, J., & Reneker, D. H. (1995). Electrospinning process and applications of electrospun fibers. Journal of Electrostatics, 35(2-3), 151-160.

Dziezak, J. D. (1988). Microencapsulation and encapsulated ingredients. Food Technology, 42(4), 136-151.

Eltayeb, M., Bakhshi, P. K., Stride, E., & Edirisinghe, M. (2013a). Preparation of solid lipid nanoparticles containing active compound by electrohydrodynamic spraying. Food Research International, 53(1), 88-95.

Eltayeb, M., Stride, E., & Edirisinghe, M. (2013b). Electrosprayed core-shell polymer-lipid nanoparticles for active component delivery. [Article]. Nanotechnology, 24(46), 465604.

Enayati, M., Ahmad, Z., Stride, E., & Edirisinghe, M. (2010). Size mapping of electric field-assisted production of polycaprolactone particles. Journal of the Royal Society Interface, 7(SUPPL. 4), S393-S402.

Enayati, M., Farook, U., Edirisinghe, M., & Stride, E. (2011). Electrohydrodynamic preparation of polymeric drug-carrier particles: Mapping of the process. International Journal of Pharmaceutics, 404(1-2), 110-115.

Ezhilarasi, P. N., Karthik, P., Chhanwal, N., & Anandharamakrishnan, C. (2013). Nanoencapsulation Techniques for Food Bioactive Components: A Review. Food and Bioprocess Technology, 6(3), 628-647.

Fang, Z., & Bhandari, B. (2010). Encapsulation of polyphenols – a review. Trends in Food Science and Technology, 21(10), 510-523.

Farokhzad, O. C., & Langer, R. (2009). Impact of nanotechnology on drug delivery. ACS Nano, 3(1), 16-20.

Fathi, M., & Mohebbi, M. (2010). Increasing food safety using nanotechnology. *Magazine of Nanotechnology Initative Council, 143,* 16-18.

Fathi, M., Mozafari, M. R., & Mohebbi, M. (2012). Nanoencapsulation of food ingredients using lipid based delivery systems. Trends in Food Science & Technology, 23(1), 13-27.

Fathi, M., & Varshosaz, J. (2013). Novel hesperetin loaded nanocarriers for food fortification: Production and characterization. Journal of Functional Foods, 5(3), 1382-1391.

Fernandez de la Mora, J. F., & Loscertales, I. (1994). The current emitted by highly conducting Taylor cones. [10.1017/S0022112094003472]. J. Fluid Mech., 260, 155-184.

Flanagan, J., & Singh, H. (2006). Microemulsions: a potential delivery system for bioactives in food. Critical reviews in food science and nutrition, 46(3), 221-237.

Freiberg, S., & Zhu, X. X. (2004). Polymer microspheres for controlled drug release. International Journal of Pharmaceutics, 282(1-2), 1-18.

Fukui, Y., Maruyama, T., Iwamatsu, Y., Fujii, A., Tanaka, T., Ohmukai, Y., & Matsuyama, H. (2010). Preparation of monodispersed polyelectrolyte microcapsules with high encapsulation efficiency by an electrospray technique. Colloids and Surfaces A: Physicochemical and Engineering Aspects, 370(1–3), 28-34.

Gallarate, M., Trotta, M., Battaglia, L., & Chirio, D. (2009). Preparation of solid lipid nanoparticles from W/O/W emulsions: Preliminary studies on insulin encapsulation. Journal of Microencapsulation, 26(5), 394-402.

Ganan-Calvo, A. (1997). On the theory of electrohydrodynamically driven capillary jets. Journal of Fluid Mechanics, 335, 165-188.

Ganan-Calvo, A. (1999). The electrohydrodynamic atomization of liquids today. Journal of Aerosol Science, 30, Supplement 1(0), S547-S548.

Ganan-Calvo, A. M., Davila, J., & Barrero, A. (1997). Current and droplet size in the electrospraying of liquids. Scaling laws. [10.1016/S0021-8502(96)00433-8]. J. Aerosol Sci., 28, 249-275.

Gañán-Calvo, A. M., & Montanero, J. M. (2009). Revision of capillary cone-jet physics: Electrospray and flow focusing. Physical Review E - Statistical, Nonlinear, and Soft Matter Physics, 79(6), 066305.

Gasco, M. R., Cavalli, R., & M.E. Carlotti. (1992). timolol lipospheres. Pharmazie, 47, 119–121.

Ghayempour, S., & Mortazavi, S. M. (2013). Fabrication of micro-nanocapsules by a new electrospraying method using coaxial jets and examination of effective parameters on their production. Journal of Electrostatics, 71(4), 717-727.

Ghosh, A., Mandal, A. K., Sarkar, S., Panda, S., & Das, N. (2009). Nanoencapsulation of quercetin enhances its dietary efficacy in combating arsenic-induced oxidative damage in liver and brain of rats. Life sciences, 84(3), 75-80.

Gibbs, B. F., Kermasha, S., Alli, I., & Mulligan, C. N. (1999). Encapsulation in the food industry: A review. International Journal of Food Sciences and Nutrition, 50(3), 213-224.

Given, P. S., Jr. (2009). Encapsulation of Flavors in Emulsions for Beverages. Current Opinion in Colloid & Interface Science, 14(1), 43-47.

Gomez-Estaca, J., Balaguer, M. P., Gavara, R., & Hernandez-Munoz, P. (2012). Formation of zein nanoparticles by electrohydrodynamic atomization: Effect of the main processing variables and suitability for encapsulating the food coloring and active ingredient curcumin. Food Hydrocolloids, 28(1), 82-91.

Gomez, A., Bingham, D., de Juan, L., & Tang, K. (1998). Production of protein nanoparticles by electrospray drying. Journal of Aerosol Science, 29(5-6), 561-574.

González-Baró, A. C., Parajón-Costa, B. S., Franca, C. A., & Pis-Diez, R. (2008). Theoretical and spectroscopic study of vanillic acid. Journal of Molecular Structure, 889(1), 204-210.

Hadinoto, K., Sundaresan, A., & Cheow, W. S. (2013). Lipid–polymer hybrid nanoparticles as a new generation therapeutic delivery platform: A review. European Journal of Pharmaceutics and Biopharmaceutics, 85(3, Part A), 427-443.

Hanawa, T., Ikoma, R., Watanabe, A., Hidaka, M., & Sugihara, M. (1996). Preparation and characterization of sealed heated mixture of ethenzamide and porous calcium silicate. Chemical and Pharmaceutical Bulletin, 44(7), 1367-1371.

Hao, X., Lu, X., Li, Z., Zhao, Y., Shang, T., Yang, Q., . . . Li, J. (2006). Effects of the electrospray ionization parameters on the formation and morphology of colloidal microspheres of polyacrylonitrile. Journal of Applied Polymer Science, 102(3), 2889-2893.

Hartman, R. P. A., Brunner, D. J., Camelot, D. M. A., Marijnissen, J. C. M., & Scarlett, B. (2000). Jet break-up in electrohydrodynamic atomization in the cone-jet mode. Journal of Aerosol Science, 31(1), 65-95.

Hegsted, D. M., McGandy, R. B., Myers, M. L., & Stare, F. J. (1965). Quantitative effects of dietary fat on serum cholesterol in man. American Journal of Clinical Nutrition, 17(5), 281-295.

Heiati, H., Tawashi, R., & Phillips, N. C. (1998). Drug retention and stability of solid lipid nanoparticles containing azidothymidine palmitate after autoclaving, storage and lyophilization. Journal of Microencapsulation, 15(2), 173-184.

Higuchi, T. (1963). Mechanism of sustained-action medication. Theoretical analysis of rate of release of solid drugs dispersed in solid matrices. Journal of Pharmaceutical Sciences, 52(12), 1145-1149.

Hong, Y., Li, Y., Yin, Y., Li, D., & Zou, G. (2008). Electrohydrodynamic atomization of quasi-monodisperse drug-loaded spherical/wrinkled microparticles. Journal of Aerosol Science, 39(6), 525-536.

Humberstone, A. J., & Charman, W. N. (1997). Lipid-based vehicles for the oral delivery of poorly water soluble drugs. Advanced Drug Delivery Reviews, 25(1), 103-128.

Hyvönen, S., Peltonen, L., Karjalainen, M., & Hirvonen, J. (2005). Effect of nanoprecipitation on the physicochemical properties of low molecular weight poly(l-lactic acid) nanoparticles loaded with salbutamol sulphate and beclomethasone dipropionate. International Journal of Pharmaceutics, 295(1–2), 269-281.

Ijsebaert, J. C., Geerse, K. B., Marijnissen, J. C. M., Lammers, J. W. J., & Zanen, P. (2001). Electro-hydrodynamic atomization of drug solutions for inhalation purposes. Journal of Applied Physiology, 91(6), 2735-2741.

Ilyasoglu, H., & El, S. N. (2014). Nanoencapsulation of EPA/DHA with sodium caseinate–gum arabic complex and its usage in the enrichment of fruit juice. LWT - Food Science and Technology, 56(2), 461-468.

Jackson, L. S., & Lee, K. (1991). MICROENCAPSULATION AND THE FOOD-INDUSTRY. Food Science and Technology-Lebensmittel-Wissenschaft & Technologie, 24(4), 289-297.

Jaiswal, J., Gupta, S. K., & Kreuter, J. (2004). Preparation of biodegradable cyclosporine nanoparticles by high-pressure emulsification-solvent evaporation process. Journal of Controlled Release, 96(1), 169-178.

Jaworek, A. (2008). Electrostatic micro- and nanoencapsulation and electroemulsification: A brief review. Journal of Microencapsulation, 25(7), 443-468.

Jaworek, A., & Sobczyk, A. T. (2008). Electrospraying route to nanotechnology: An overview. Journal of Electrostatics, 66(3–4), 197-219.

Jayasinghe, S. N., & Edirisinghe, M. J. (2002). Effect of viscosity on the size of relics produced by electrostatic atomization. Journal of Aerosol Science, 33(10), 1379-1388.

Karathanos, V. T., Mourtzinos, I., Yannakopoulou, K., & Andrikopoulos, N. K. (2007). Study of the solubility, antioxidant activity and structure of inclusion complex of vanillin with β-cyclodextrin. Food Chemistry, 101(2), 652-658.

Keller, B. C. (2001). Liposomes in nutrition. Trends in Food Science & Technology, 12(1), 25-31.

Khayata, N., Abdelwahed, W., Chehna, M. F., Charcosset, C., & Fessi, H. (2012). Preparation of vitamin E loaded nanocapsules by the nanoprecipitation method: From laboratory scale to large scale using a membrane contactor. International Journal of Pharmaceutics, 423(2), 419-427.

Kim, G., Park, J., & Han, H. (2006). Production of microsized PMMA droplets using electrospraying with various auxiliary fields. Journal of Colloid and Interface Science, 299(2), 593-598.

Kriegel, C., Kit, K. M., McClements, D. J., & Weiss, J. (2009). Electrospinning of chitosan-poly(ethylene oxide) blend nanofibers in the presence of micellar surfactant solutions. Polymer, 50(1), 189-200.

Lacatusu, I., Mitrea, E., Badea, N., Stan, R., Oprea, O., & Meghea, A. (2013). Lipid nanoparticles based on omega-3 fatty acids as effective carriers for lutein delivery. Preparation and in vitro characterization studies. Journal of Functional Foods, 5(3), 1260-1269.

Landy, P., Druaux, C., & Voilley, A. (1995). RETENTION OF AROMA COMPOUNDS BY PROTEINS IN AQUEOUS-SOLUTION. Food Chemistry, 54(4), 387-392.

Lassalle, V., & Ferreira, M. L. (2007). PLA nano- and microparticles for drug delivery: An overview of the methods of preparation. Macromolecular Bioscience, 7(6), 767-783.

Li, L., Shan, H., Yue, C., Lam, Y., Tam, K., & Hu, X. (2002). Thermally induced association and dissociation of methylcellulose in aqueous solutions. Langmuir, 18(20), 7291-7298.

Li, X., & Yang, T. (2008). Fabrication of ethyl cellulose microspheres: Chitosan solution as a stabilizer. Korean Journal of Chemical Engineering, 25(5), 1201-1204.

LIU, C., Ye, A., Liu, W., Liu, C., & Singh, H. (2013). Liposomes as food ingredients and nutraceutical delivery systems. Agro Food Industry Hi-Tech, 24(2), 68-71.

Liu, J., Gong, T., Fu, H., Wang, C., Wang, X., Chen, Q., . . . Zhang, Z. (2008). Solid lipid nanoparticles for pulmonary delivery of insulin. International Journal of Pharmaceutics, 356(1-2), 333-344.

Lopez-Rubio, A., & Lagaron, J. M. (2012). Whey protein capsules obtained through electrospraying for the encapsulation of bioactives. Innovative Food Science & Emerging Technologies, 13, 200-206.

Lopez-Rubio, A., Sanchez, E., Wilkanowicz, S., Sanz, Y., & Maria Lagaron, J. (2012). Electrospinning as a useful technique for the encapsulation of living bifidobacteria in food hydrocolloids. Food Hydrocolloids, 28(1), 159-167.

Luo, C. J., Loh, S., Stride, E., & Edirisinghe, M. (2012). Electrospraying and Electrospinning of Chocolate Suspensions. Food and Bioprocess Technology, 5(6), 2285-2300.

Madene, A., Jacquot, M., Scher, J., & Desobry, S. (2006). Flavour encapsulation and controlled release - a review. International Journal of Food Science and Technology, 41(1), 1-21.

Madrigal-Carballo, S., Lim, S., Rodriguez, G., Vila, A. O., Krueger, C. G., Gunasekaran, S., & Reed, J. D. (2010). Biopolymer coating of soybean lecithin liposomes via layer-by-layer self-assembly as novel delivery system for ellagic acid. Journal of Functional Foods, 2(2), 99-106.

Mainardes, R. M., & Evangelista, R. C. (2005). PLGA nanoparticles containing praziquantel: effect of formulation variables on size distribution. International Journal of Pharmaceutics, 290(1-2), 137-144.

Mandal, B., Bhattacharjee, H., Mittal, N., Sah, H., Balabathula, P., Thoma, L. A., & Wood, G. C. (2013). Core–shell-type lipid–polymer hybrid nanoparticles as a drug delivery platform. Nanomedicine: Nanotechnology, Biology and Medicine, 9(4), 474-491.

Manojlovic, V., Rajic, N., Djonlagic, J., Obradovic, B., Nedovic, V., & Bugarski, B. (2008). Application of electrostatic extrusion - Flavour encapsulation and controlled release. Sensors, 8(3), 1488-1496.

Matalanis, A., Jones, O. G., & McClements, D. J. (2011). Structured biopolymer-based delivery systems for encapsulation, protection, and release of lipophilic compounds. Food Hydrocolloids, 25(8), 1865-1880.

McClements, D. J., Decker, E. A., Park, Y., & Weiss, J. (2009). Structural design principles for delivery of bioactive components in nutraceuticals and functional foods. Critical Reviews in Food Science and Nutrition, 49(6), 577-606.

McClements, D. J., & Li, Y. (2010). Structured emulsion-based delivery systems: Controlling the digestion and release of lipophilic food components. Advances in Colloid and Interface Science, 159(2), 213-228.

Mehnert, W., & Mader, K. (2001). Solid lipid nanoparticles - Production, characterization and applications. Advanced Drug Delivery Reviews, 47(2-3), 165-196.

Meng, F., Jiang, Y., Sun, Z., Yin, Y., & Li, Y. (2009). Electrohydrodynamic liquid atomization of biodegradable polymer microparticles: Effect of electrohydrodynamic liquid atomization variables on microparticles. Journal of Applied Polymer Science, 113(1), 526-534.

Miller, K. S., & Krochta, J. M. (1997). Oxygen and aroma barrier properties of edible films: A review. Trends in Food Science and Technology, 8(7), 228-237.

Mozafari, M., Flanagan J, Matia-Merino L, Awati A, O. A., Suntres ZE, & H, S. (2006). Recent trends in the lipid-based nanoencapsulation of antioxidants and their role in foods. Journal of the Science of Food and Agriculture, 86(13), 2038–2045.

Müller, R. H., Mäder, K., & Gohla, S. (2000). Solid lipid nanoparticles (SLN) for controlled drug delivery - A review of the state of the art. European Journal of Pharmaceutics and Biopharmaceutics, 50(1), 161-177.

Müller, R. H., Petersen, R. D., Hommoss, A., & Pardeike, J. (2007). Nanostructured lipid carriers (NLC) in cosmetic dermal products. Advanced Drug Delivery Reviews, 59(6), 522-530.

Muller, R. H., Radtke, M., & Wissing, S. A. (2002). Solid lipid nanoparticles (SLN) and nanostructured lipid carriers (NLC) in cosmetic and dermatological preparations. Advanced Drug Delivery Reviews, 54, S131-S155.

Müller, R. H., Radtke, M., & Wissing, S. A. (2002). Nanostructured lipid matrices for improved microencapsulation of drugs. International Journal of Pharmaceutics, 242(1-2), 121-128.

Neethirajan, S., & Jayas, D. S. (2011). Nanotechnology for the Food and Bioprocessing Industries. Food and Bioprocess Technology, 4(1), 39-47.

Nie, H., Dong, Z., Arifin, D. Y., Hu, Y., & Wang, C. H. (2010a). Core/shell microspheres via coaxial electrohydrodynamic atomization for sequential and parallel release of drugs. Journal of Biomedical Materials Research - Part A, 95(3 A), 709-716.

Nie, H., Fu, Y., & Wang, C. H. (2010b). Paclitaxel and suramin-loaded core/shell microspheres in the treatment of brain tumors. Biomaterials, 31(33), 8732-8740.

Pareta, R., & Edirisinghe, M. J. (2006). A novel method for the preparation of biodegradable microspheres for protein drug delivery. Journal of the Royal Society Interface, 3(9), 573-582.

Park, C. H., & Lee, J. (2009). Electrosprayed polymer particles: Effect of the solvent properties. Journal of Applied Polymer Science, 114(1), 430-437.

Park, S., Hwang, S., & Lee, J. (2011). PH-responsive hydrogels from moldable composite microparticles prepared by coaxial electro-spray drying. Chemical Engineering Journal, 169(1-3), 348-357.

Parnis, J. M., & Oldham, K. B. (2013). Beyond the Beer–Lambert law: The dependence of absorbance on time in photochemistry. Journal of Photochemistry and Photobiology A: Chemistry, 267(0), 6-10.

Peltonen, L., Valo, H., Kolakovic, R., Laaksonen, T., & Hirvonen, J. (2010). Electrospraying, spray drying and related techniques for production and formulation of drug nanoparticles. Expert Opinion on Drug Delivery, 7(6), 705-719.

Peppas, N. A. (1985). Analysis of Fickian and non-Fickian drug release from polymers. Pharmaceutica Acta Helvetiae, 60(4), 110-111.

Peppas, N. A., & Narasimhan, B. (2014). Mathematical models in drug delivery: How modeling has shaped the way we design new drug delivery systems. Journal of Controlled Release, 190, 75-81.

Perez-Masia, R., Lagaron, J. M., & Lopez-Rubio, A. (2014). Surfactant-aided electrospraying of low molecular weight carbohydrate polymers from aqueous solutions. Carbohydrate Polymers, 101, 249-255.

Phadke, D. S., Keeney, M. P., & Norris, D. A. (1994). Evaluation of batch-to-batch and manufacturer-to-manufacturer variability in the physical properties of talc and stearic acid. Drug Development and Industrial Pharmacy, 20(5), 859-871.

Pham, Q. P., Sharma, U., & Mikos, A. G. (2006). Electrospinning of polymeric nanofibers for tissue engineering applications: A review. Tissue Engineering, 12(5), 1197-1211.

Prilutsky, S., Zussman, E., & Cohen, Y. (2008). The effect of embedded carbon nanotubes on the morphological evolution during the carbonization of poly(acrylonitrile) nanofibers. Nanotechnology, 19(16), 165603.

Ramakrishna, S., Fujihara, K., Teo, W. E., Lim, T. C., & Ma, Z. (Eds.). (2005). An Introduction to Electrospinning and Nanofibers: World Scientific.

Rao, B. S., & Murthy, K. V. R. (2002). Studies on rifampicin release from ethylcellulose coated nonpareil beads. International Journal of Pharmaceutics, 231(1), 97-106.

Rao, J. P., & Geckeler, K. E. (2011). Polymer nanoparticles: Preparation techniques and size-control parameters. Progress in Polymer Science, 36(7), 887-913.

Ravindra, R., Rao, A. K., & Khan, A. A. (1999). A qualitative evaluation of water and monomethyl hydrazine in ethylcellulose membrane. Journal of Applied Polymer Science, 72(5), 689-700.

Rayleigh. (1882). On the equilibrium of liquid conducting masses charged with electricity. Philos Mag Series, 5(14), 184-186.

Rezvanpour, A., Attia, A. B. E., & Wang, C. H. (2010). Enhancement of particle collection efficiency in electrohydrodynamic atomization process for pharmaceutical particle fabrication. Industrial and Engineering Chemistry Research, 49(24), 12620-12631.

Risch, S. J., & Reineccius, G. A. (1995). Encapsulation and Controlled Release of Food Ingredients ACS Symposium Series (Vol. 590, pp. pp 2-7). Washington, DC: American Chemical Society.

Ritger, P., & Peppas, N. A. (1987). A simple equation for description of solute release I. Fickian and non-Fickian release from non-swellable devices in the form of slabs, spheres, cylinders or discs. Journal of Controlled Release, 5, 23-36.

Rizvi, S. S. H., Moraru, C. I., Bouwmeester, H., & Kampers, F. W. H. (2010). Nanotechnology and Food Safety. In E. B. Christine, S. Aleksandra, O. Sangsuk & H. L. M. Lelieveld (Eds.), Ensuring Global Food Safety (pp. 263-280). San Diego: Academic Press.

Rohner, T. C., Lion, N., & Girault, H. H. (2004). Electrochemical and theoretical aspects of electrospray ionisation. Physical Chemistry Chemical Physics, 6(12), 3056-3068.

Sagalowicz, L., & Leser, M. E. (2010). Delivery systems for liquid food products. Current Opinion in Colloid & Interface Science, 15(1–2), 61-72.

Sagalowicz, L., Leser, M. E., Watzke, H. J., & Michel, M. (2006). Monoglyceride self-assembly structures as delivery vehicles. Trends in Food Science and Technology, 17(5), 204-214.

Sáiz-Abajo, M.-J., González-Ferrero, C., Moreno-Ruiz, A., Romo-Hualde, A., & González-Navarro, C. J. (2013). Thermal protection of β-carotene in re-assembled casein micelles during different processing technologies applied in food industry. Food Chemistry, 138(2–3), 1581-1587.

Sanguansri, P., & Augustin, M. A. (2006). Nanoscale materials development – a food industry perspective. Trends in Food Science and Technology, 17(10), 547-556.

Schwarz, C., Mehnert, W., Lucks, J., & Müller, R. (1994). Solid lipid nanoparticles (SLN) for controlled drug delivery. I. Production, characterization and sterilization. Journal of Controlled Release, 30(1), 83-96.

Sezer, A. D., Kazak, H., Oner, E. T., & Akbuga, J. (2011). Levan-based nanocarrier system for peptide and protein drug delivery: Optimization and influence of experimental parameters on the nanoparticle characteristics. Carbohydrate Polymers, 84(1), 358-363.

Shah, R. B., Zidan, A. S., Funck, T., Tawakkul, M. A., Nguyenpho, A., & Khan, M. A. (2007). Quality by design: Characterization of self-nano-emulsified drug delivery systems (SNEDDs) using ultrasonic resonator technology. International Journal of Pharmaceutics, 341(1-2), 189-194.

Shahidi, F., & Han, X. Q. (1993). ENCAPSULATION OF FOOD INGREDIENTS. Critical Reviews in Food Science and Nutrition, 33(6), 501-547.

Shenoy, S. L., Bates, W. D., Frisch, H. L., & Wnek, G. E. (2005). Role of chain entanglements on fiber formation during electrospinning of polymer solutions: Good solvent, non-specific polymer-polymer interaction limit. Polymer, 46(10), 3372-3384.

Shimoni, E. (2009). Nanotechnology for Foods: Delivery Systems. In B.-C. Gustavo, M. Alan, L. David, S. Walter, B. Ken & C. Paul (Eds.), Global Issues in Food Science and Technology (pp. 411-424). San Diego: Academic Press.

Shimoni, E., Edited, B., & Gustavo, B. C. (2009). Nanotechnology for foods: Delivery Systems. Global Issues in Food Science and Technology, 411-424.

Silva, H. D., Cerqueira, M. A., & Vicente, A. A. (2012). Nanoemulsions for Food Applications: Development and Characterization. Food and Bioprocess Technology, 5(3), 854-867.

Smith, A., & Hunneyball, I. M. (1986). Evaluation of poly(lactic acid) as a biodegradable drug delivery system for parenteral administration. Int. J. Pharm., 30, 215–220.

Sokolsky-Papkov, M., Agashi, K., Olaye, A., Shakesheff, K., & Domb, A. J. (2007). Polymer carriers for drug delivery in tissue engineering. Advanced Drug Delivery Reviews, 59(4-5), 187-206.

Souto, E. B., Wissing, S. A., Barbosa, C. M., & Müller, R. H. (2004). Development of a controlled release formulation based on SLN and NLC for topical clotrimazole delivery. International Journal of Pharmaceutics, 278(1), 71-77.

Stratulat, I., Britten, M., Salmieri, S., Fustier, P., St-Gelais, D., Champagne, C. P., & Lacroix, M. (2014). Enrichment of cheese with bioactive lipophilic compounds. Journal of Functional Foods, 6, 48-59.

Tang, K., & Gomez, A. (1996). Monodisperse Electrosprays of Low Electric Conductivity Liquids in the Cone-Jet Mode. Journal of Colloid and Interface Science, 184(2), 500-511.

Teixeira, A. P. C., Purceno, A. D., Barros, A. S., Lemos, B. R. S., Ardisson, J. D., Macedo, W. A. A., . . . Lago, R. M. (2012). Amphiphilic magnetic composites based on layered vermiculite and fibrous chrysotile with carbon nanostructures: Application in catalysis. Catalysis Today, 190(1), 133-143.

Teo, W. E., & Ramakrishna, S. (2006). A review on electrospinning design and nanofibre assemblies. Nanotechnology, 17(14), R89-R106.

Thevenot, J., Troutier, A.-L., David, L., Delair, T., & Ladaviere, C. (2007). Steric stabilization of lipid/polymer particle assemblies by poly(ethylene glycol)-lipids. Biomacromolecules, 8(11), 3651-3660.

Ting, Y., Jiang, Y., Ho, C.-T., & Huang, Q. (2014). Common delivery systems for enhancing in vivo bioavailability and biological efficacy of nutraceuticals. Journal of Functional Foods, 7, 112-128.

Torres-Giner, S., Martinez-Abad, A., Ocio, M. J., & Lagaron, J. M. (2010). Stabilization of a Nutraceutical Omega-3 Fatty Acid by Encapsulation in Ultrathin Electrosprayed Zein Prolamine. Journal of Food Science, 75(6), N69-N79.

Trotta, M., Cavalli, R., Trotta, C., Bussano, R., & Costa, L. (2010). Electrospray technique for solid lipid-based particle production. Drug Development and Industrial Pharmacy, 36(4), 431-438.

Valo, H., Peltonen, L., Vehviläinen, S., Karjalainen, M., Kostiainen, R., Laaksonen, T., & Hirvonen, J. (2009). Electrospray Encapsulation of Hydrophilic and Hydrophobic Drugs in Poly(L-lactic acid) Nanoparticles. Small, 5(15), 1791-1798.

Varshosaz, J., Ghaffari, S., Khoshayand, M. R., Atyabi, F., Azarmi, S., & Kobarfard, F. (2010a). Development and optimization of solid lipid nanoparticles of amikacin by central composite design. Journal of Liposome Research, 20(2), 97-104.

Varshosaz, J., Minayian, M., & Moazen, E. (2010b). Enhancement of oral bioavailability of pentoxifylline by solid lipid nanoparticles. Journal of Liposome Research, 20(2), 115-123.

Varshosaz, J., Tabbakhian, M., & Mohammadi, M. Y. (2009). Formulation and optimization of solid lipid nanoparticles of buspirone HCl for enhancement of its oral bioavailability. J Liposome Res, 3, 1-11.

Velikov, K. P., & Pelan, E. (2008). Colloidal delivery systems for micronutrients and nutraceuticals. Soft Matter, 4(10), 1964-1980.

Vieira, E. F., Cestari, A. R., de Santos, E. B., & Rezende, C. X. (2006). Measurement of cation binding to immobilized vanillin by isothermal calorimetry. Journal of Colloid and Interface Science, 298(1), 74-78.

Vyas, S., Rai, S., Paliwal, R., Gupta, P. N., Khatri, K., Goyal, A. K., & Vaidya, B. (2008). Solid lipid nanoparticles (SLNs) as a rising tool in drug delivery science: One step up in nanotechnology. Current Nanoscience, 4(1), 30-44.

Wang, Y., Xia, T. D., Zheng, H., & Feng, H. X. (2011). Stearic acid/silica fume composite as form-stable phase change material for thermal energy storage. Energy and Buildings, 43(9), 2365-2370.

Weiss, J., Decker, E. A., McClements, D. J., Kristbergsson, K., Helgason, T., & Awad, T. (2008). Solid lipid nanoparticles as delivery systems for bioactive food components. Food Biophysics, 3(2), 146-154.

Wu, J., Liu, H., Ge, S., Wang, S., Qin, Z., Chen, L., . . . Zhang, Q. (2015). The preparation, characterization, antimicrobial stability and in vitro release evaluation of fish gelatin films incorporated with cinnamon essential oil nanoliposomes. Food Hydrocolloids, 43, 427-435.

Wu, Y., & Clark, R. L. (2008). Electrohydrodynamic atomization: A versatile process for preparing materials for biomedical applications. Journal of Biomaterials Science, Polymer Edition, 19(5), 573-601.

Wu, Y., Kennedy, S. J., & Clark, R. L. (2009a). Polymeric particle formation through electrospraying at low atmospheric pressure. Journal of Biomedical Materials Research - Part B Applied Biomaterials, 90(1), 381-387.

Wu, Y., MacKay, J. A., McDaniel, J. R., Chilkoti, A., & Clark, R. L. (2009b). Fabrication of Elastin-Like polypeptide Nanoparticles for Drug Delivery by Electrospraying. Biomacromolecules, 10(1), 19-24.

Xie, J., Lim, L. K., Phua, Y., Hua, J., & Wang, C. H. (2006a). Electrohydrodynamic atomization for biodegradable polymeric particle production. Journal of Colloid and Interface Science, 302(1), 103-112.

Xie, J., Lim, L. K., Phua, Y., Hua, J., & Wang, C.-H. (2006b). Electrohydrodynamic atomization for biodegradable polymeric particle production. Journal of Colloid and Interface Science, 302(1), 103-112.

Xie, J., Marijnissen, J. C. M., & Wang, C. H. (2006c). Microparticles developed by electrohydrodynamic atomization for the local delivery of anticancer drug to treat C6 glioma in vitro. Biomaterials, 27(17), 3321-3332.

Xie, J., Ng, W. J., Lee, L. Y., & Wang, C.-H. (2008a). Encapsulation of protein drugs in biodegradable microparticles by co-axial electrospray. Journal of Colloid and Interface Science, 317(2), 469-476.

Xie, J., Ng, W. J., Lee, L. Y., & Wang, C. H. (2008b). Encapsulation of protein drugs in biodegradable microparticles by co-axial electrospray. Journal of Colloid and Interface Science, 317(2), 469-476.

Xie, J., Tan, J. C., & Wang, C.-H. (2008c). Biodegradable films developed by electrospray deposition for sustained drug delivery. Journal of Pharmaceutical Sciences, 97(8), 3109-3122.

Xie, J., & Wang, C.-H. (2007a). Encapsulation of proteins in biodegradable polymeric microparticles using electrospray in the Taylor Cone-Jet mode. Biotechnology and Bioengineering, 97(5), 1278-1290.

Xie, J., & Wang, C. H. (2007b). Encapsulation of proteins in biodegradable polymeric microparticles using electrospray in the Taylor cone-jet mode. Biotechnology and Bioengineering, 97(5), 1278-1290.

Xie, J. W., Marijnissen, J. C. M., & Wang, C. H. (2006d). Microparticles developed by electrohyd ro dynamic atomization for the local delivery of anticancer drug to treat C6 glioma in vitro. Biomaterials, 27(17), 3321-3332.

Xu, Y., & Hanna, M. A. (2006). Electrospray encapsulation of water-soluble protein with polylactide - Effects of formulations on morphology, encapsulation efficiency and release profile of particles. International Journal of Pharmaceutics, 320(1-2), 30-36.

Xu, Y., & Hanna, M. A. (2007). Electrosprayed bovine serum albumin-loaded tripolyphosphate cross-linked chitosan capsules: Synthesis and characterization. Journal of Microencapsulation, 24(2), 143-151.

Xu, Y., & Hanna, M. A. (2008). Morphological and structural properties of two-phase coaxial jet electrosprayed BSA-PLA capsules. Journal of Microencapsulation, 25(7), 469-477.

Yao, J., Lim, L. K., Xie, J., Hua, J., & Wang, C.-H. (2008). Characterization of electrospraying process for polymeric particle fabrication. Journal of Aerosol Science, 39(11), 987-1002.

Yoon, K. H., Unyong, J., & Eun, C. C. (2008). Production of uniform-sized polymer core-shell microcapsules by coaxial electrospraying. Langmuir, 24(6), 2446-2451.

Yoshii, H., Soottitantawat, A., Liu, X. D., Atarashi, T., Furuta, T., Aishima, S., . . . Linko, P. (2001). Flavor release from spray-dried maltodextrin/gum arabic or soy matrices as a function of storage relative humidity. Innovative Food Science and Emerging Technologies, 2(1), 55-61.

Yu, D.-G., Lu, P., Branford-White, C., Yang, J.-H., & Wang, X. (2011). Polyacrylonitrile nanofibers prepared using coaxial electrospinning with LiCl solution as sheath fluid. Nanotechnology, 22(43), 435301.

Yu, D.-G., Shen, X.-X., Branford-White, C., White, K., Zhu, L.-M., & Bligh, S. W. A. (2009). Oral fast-dissolving drug delivery membranes prepared from electrospun polyvinylpyrrolidone ultrafine fibers. Nanotechnology, 20(5), 055104.

Yu, D. G., Yang, J. H., Wang, X., & Tian, F. (2012). Liposomes self-assembled from electrosprayed composite microparticles. [Article]. Nanotechnology, 23(10), 105606.

Zhang, Q., Yie, G., Li, Y., Yang, Q., & Nagai, T. (2000). Studies on the cyclosporin A loaded stearic acid nanoparticles. International Journal of Pharmaceutics, 200(2), 153-159.

Zhang, S., & Kawakami, K. (2010). One-step preparation of chitosan solid nanoparticles by electrospray deposition. International Journal of Pharmaceutics, 397(1-2), 211-217.

Zheng, D., Hu, C., Peng, Y., & Hu, S. (2009). A carbon nanotube/polyvanillin composite film as an electrocatalyst for the electrochemical oxidation of nitrite and its application as a nitrite sensor. Electrochimica Acta, 54(21), 4910-4915.

Zheng, P., Li, L., Hu, X., & Zhao, X. (2004). Sol–gel transition of methylcellulose in phosphate buffer saline solutions. Journal of Polymer Science Part B: Polymer Physics, 42(10), 1849-1860.

Zimet, P., & Livney, Y. D. (2009). Beta-lactoglobulin and its nanocomplexes with pectin as vehicles for ω-3 polyunsaturated fatty acids. Food Hydrocolloids, 23(4), 1120-1126.

Zuidam, N. J., & Heinrich, J. (2009). Encapsulation of aroma. N. J. Zuidam, Nedovic, V.A. (Ed.) Encapsulation Technologies for Food Active Ingredients and Food Processing. (pp. 127-160).

Zúñiga, R. N., & Aguilera, J. M. (2008). Aerated food gels: fabrication and potential applications. Trends in Food Science and Technology, 19(4), 176-187.

zur Mühlen, A., Schwarz, C., & Mehnert, W. (1998). Solid lipid nanoparticles (SLN) for controlled drug delivery - Drug release and release mechanism. European Journal of Pharmaceutics and Biopharmaceutics, 45(2), 149-155.